STEADY STATE RESPONSE OF A SECOND ORDER SERVOMECHANISM WITH BACKLASH AND RESILIENCE IN THE GEARS BETWEEN MOTOR AND LOAD

NORRIS O. ANDERSON, JR.
and
THOMAS W. LUCKETT

Released by Committee 3/19/68

12/10

STEADY STATE RESPONSE

OF A

SECOND ORDER SERVOMECHANISM

WITH

BACKLASH AND RESILIENCE IN THE

GEARS BETWEEN MOTOR AND LOAD

* * * * *

Norris O. Anderson, Jr.

and

Thomas W. Luckett

STEADY STATE RESPONSE

OF A

SECOND ORDER SERVOMECHANISM

WITH

BACKLASH AND RESILIENCE IN THE

GEARS BETWEEN MOTOR AND LOAD

by

Norris O. Anderson, Jr.

Lieutenant, United States Navy

and

Thomas W. Luckett

Lieutenant, United States Navy

Submitted in partial fulfillment of
the requirements for the degree of

MASTER OF SCIENCE
IN
ELECTRICAL ENGINEERING

United States Naval Postgraduate School
Monterey, California

1961

STEADY STATE RESPONSE

OF A

SECOND ORDER SERVOMECHANISM

WITH

BACKLASH AND RESILIENCE IN THE

GEARS BETWEEN MOTOR AND LOAD

by

Norris O. Anderson, Jr.

and

Thomas W. Luckett

This work is accepted as fulfilling

the thesis requirements for the degree of

MASTER OF SCIENCE

IN

ELECTRICAL ENGINEERING

from the

United States Naval Postgraduate School

ABSTRACT

This thesis is concerned with the steady state response to a step input of a non-linear servomechanism having viscous friction and a load position unity feedback loop. A gear train with backlash between resilient gear teeth was located between the motor and load.

The physical equations describing the system are presented and adapted to a form for the Control Data Corporation 1604 digital computer. The computer program used in this analysis is presented along with its flow diagram and description of its operation.

The results of this thesis are presented in several forms using the parameters of system damping coefficient, distribution of friction and inertia, backlash angle and coefficient of restitution. The results are applied to sample problems in illustration of their use for design and analysis.

The authors wish to express their appreciation to Dr. George J. Thaler of the Department of Electrical Engineering, and to Dr. William Wainwright and Mr. Edward N. Ward of the Department of Mathematics for their assistance and encouragement in completing this work.

TABLE OF CONTENTS

TABLE OF SYMBOLS

Θ_R	(ONE)*	Angular step input (radians). Desired load displacement at steady state
Θ_C	(THETAL)	Output displacement of load (radians).
$\dot{\Theta}_C$	(THETADL)	Output velocity of load $\left(\frac{\text{radians}}{\text{sec}}\right)$
E		Error in radians. $E = \Theta_R - \Theta_C$
K	(KMOTCONST)	Constant of proportionality relating position error to torque developed by the motor.
T_m		Developed torque of motor.
T_L		Torque of load.
T_{Lm}		Torque of load referred to motor.
ρ	(RHO)	$\frac{\text{Number of teeth on gear 1}}{\text{Number of teeth on gear 2}}$
J_m	(MOINERT)	Inertia of motor measured at motor.
J_L	(JLOADVAL)	Inertia of load measured at load.
J		Total inertial measured at motor $J = Jm + \rho^2 J_L$
F_m	(FMOTOR)	Friction of motor measured at motor.
F_L	(FLOAD)	Friction of load measured at load.
Δ	(DELTA)	Backlash of gearbox measured in radians at the output.
N_S		Slope of phase trajectory (combined system). $N_S \triangleq \frac{d\dot{\theta}_c}{d\theta_c} = \frac{\ddot{\theta}_c}{\dot{\theta}_c}$
N_L		Slope of phase trajectory (load floating free). $N_L \triangleq \frac{d\dot{\theta}_c}{d\theta_c} = \frac{\ddot{\theta}_c}{\dot{\theta}_c}$
$\dot{\theta}_m', \dot{\theta}_c'$		Velocities of motor and load after impact.

*( ) Terms indicate computer mnemonics referred to in Sec. 3, Computer Program Development.

e	(RESTITUT)	Coefficient of restitution.
ζ	(ZETA)	System damping coefficient.
ω_n	(OMEGAN)	System natural frequency.
ω_n^2	(OMEGANSQ)	System natural frequency, squared.
$\frac{F_L}{F_T}$	(FLFTPRIN)	Load friction ratio with respect to friction of the system.
$\frac{J_m}{J_L}$	(INERTRAT)	Inertia ratio.
Θ_m	(THETAM)	Displacement of motor (radians).
$\dot{\Theta}_m$	(THETADM)	Velocity of motor $\left(\frac{\text{radians}}{\text{sec}}\right)$

1. Introduction and Background

The problem under investigation was the response to a unit step input of a nonlinear servomechanism having viscous friction and load-position unity feedback loop. A gear train with backlash between the resilient gear teeth was located between the motor and load. A determination of the possible existence of a limit cycle with variation of several parameters was made. The variable parameters considered were motor, load, and system time constants, backlash and the coefficient of restitution of the gear teeth. If a limit cycle existed, a further investigation was made into the change of the size of the limit cycle with variation of the above parameters.

If a gear train is required between the motor and load in a servomechanism, the gear train may be treated as ideal with perfect meshing of the gears. In this case the components of the system are joined at all times and the system may be described by a single linear differential equation. The classical linear solution in either the frequency or time domain is the result.

Present production methods cannot meet the requirements of an ideal gear train, having perfect engagement of the teeth, nor is the ideal gear train desirable from the standpoint of wear on the gear faces. The result is that the practical gear train has separation of the gear teeth when the velocities of the motor and load are different. The response of a servomechanism with backlash is in effect discontinuous or nonlinear. The net system acts as three individual but dependent systems with the boundary conditions of each being specified by certain physical laws.

Two accepted methods of analysis are available for solution of the

[illegible]

[illegible]

[illegible]

[illegible]

[illegible]

problem. The first is the solution by describing function methods while the second is by analytical methods. Describing function methods are primarily frequency response techniques and depend upon the assumption that the nonlinear element may be considered as linear over the range of consideration. A further assumption is made that the input to the nonlinear element is a pure sinusoid with no harmonic frequencies. The describing function method is primarily concerned with steady state results.

The analytical solution, which is the second method of considering the problem is primarily a transient response technique concerned with solution in the time domain. This approach also requires certain assumptions concerning the behavior of the system. The assumptions used in several investigations are pointed out in the following paragraphs, while the assumptions of this investigation are outlined in Section 3, Development of Equations. The validity of the analysis by any method depends on the accuracy with which the real system has been defined.

Chestnut and Mayer, Ref. a, have considered the backlash problem using describing functions and supported the findings by analog computer studies. The main difference between this cited work and previous describing function analyses was the simulation of backlash by a dead zone between the motor and load and springiness in the interconnecting shaft.

Various analytical approaches have been made to the problem of backlash, Lutkenhouse, Ref. b, used graphical methods in the phase plane to solve several cases of plastic impact between the gear teeth of a second order servomechanism. Pastel and Thaler, Ref. c, developed

[illegible]

[illegible]

[illegible]

[illegible]

analytical equations for the existence of limit cycles using phase plane equations for the case of plastic impact and no load inertia. Knoll and Narud, Ref. d, investigated limit cycles in the phase plane using an analog computer. The investigation of Knoll and Narud covered a wide range of parameters for the case of plastic contact between the gear teeth.

To analytically describe the total system response of a second order servo with backlash, three differential equations and one or more algebraic equations are required. The system as a whole may be treated as being piece wise linear. One differential equation is used to describe the entire system when the gear teeth are in contact and the motor is driving or braking. When the gear teeth are not in contact, two more differential equations are required, one for the motor alone and one for the load alone. The boundary conditions of the differential equations are determined from the solution of one or more algebraic equations, expressing the laws of conservation of momentum and energy. For plastic impact with no bounce of the gear teeth, the law of conservation of momentum must be satisfied. For perfect elastic contact between the gear teeth the law of conservation of momentum and the law of conservation of energy must be satisfied simultaniously. Intermediate cases between perfect elastic and perfect plastic contact can fulfill only the law of conservation of momentum. However, total energy accounting may be made in the intermediate and perfect plastic impact cases.

New, Ref. e, adapted the differential equations of system motion and the law of conservation of momentum (plastic contact) to a digital computer analysis of a second order servomechanism with backlash. The

digital computer was chosen as the method of solution for this investigation primarily because of the flexibility of data presentation and the ease with which cyclic parameter variation could be obtained.

In later sections of this thesis, the differential equations for the system and the algebraic equations for the impact boundary conditions are developed. The computer program and its flow diagram and modes of operation are pointed out. The results of the solutions of problems are presented in several forms and observations are made in Section 5, Results and Discussion. Sample applications of the results to mechanical systems are presented in Section 6, Application of Results.

At this writing, associated work in the area of transient response, primarily peak overshoot and settling time, of a second order servomechanism with backlash and plastic and elastic impact is being prepared as a thesis by C. E. Andrews and R. A. Kelley at the U. S. Naval Postgraduate School.

2. Development of Equations

The equations developed were those of a phase plane analysis. Prior to defining the net system equations, the assumptions under which the analysis was made will be stated. When necessary these assumptions will be amplified and referred to later in this work.

It was assumed that:

1. The gear teeth were initially in contact and the initial conditions of the system were all equal to zero. This was later proved to be an unnecessary limitation for the study of steady state response.
2. Plastic deformation of the gear teeth during steady contact and impact and any torsional deformations of driving shafts are negligible.
3. The inertias of the gears and drive shafts are considered as part of the load or motor inertia depending on their attachment in the system.
4. The law of conservation of energy was completely satisfied in only the perfect elastic case by maintaining the total mechanical rotational energy of the system constant at the instant prior to and after impact. The law of conservation of momentum is satisfied in plastic, elastic, and intermediate cases. When the law of conservation of momentum is the only equation required to be satisfied, the energy lost from the system is dissipated in the heat of infinitesimal deformations of the gear teeth.
5. The gear teeth are in contact only instantaneously during impact for the elastic and intermediate cases (excluding

plastic) and that the impulse torques of drive, friction and bearing supports, etc., are zero during impact, e.g.

$$\int_{dt \to 0} T_m \, dt = 0 \qquad \text{and} \qquad \theta = \theta'$$

6. The coefficient of restitution of the two opposing gear teeth is the same or is described by an equivalent coefficient if the two gear teeth are of unequal coefficients.
7. Backlash is assumed to be equal at all points on the gear circumference. Backlash is measured at the output shaft.

A block diagram of the system considered is presented below.

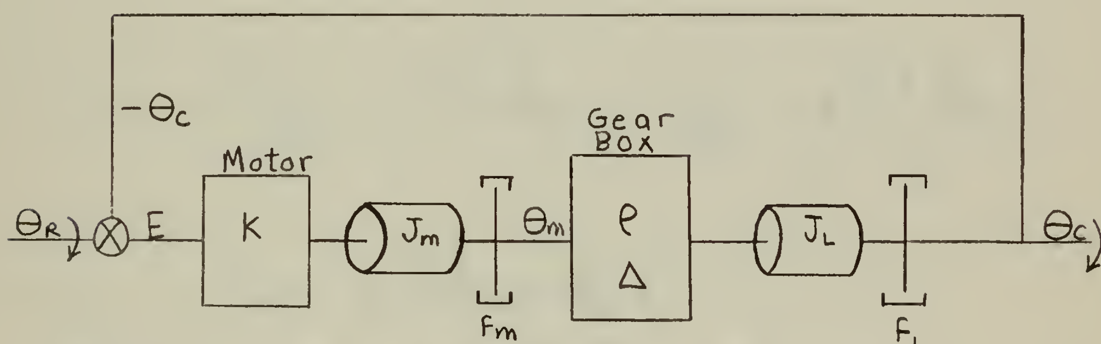

The equations for the motor and load in contact are:

$$E = \theta_R - \theta_c$$

$$T_m = KE = K(\theta_R - \theta_c)$$

$$T_L = J_L \ddot{\theta}_c + f_L \dot{\theta}_c$$

$$T_{Lm} = \rho T_L = \rho (J_L \ddot{\theta}_c + f_L \dot{\theta}_c)$$

$$\theta_c = \rho \theta_m \ \text{forward drive} \qquad \theta_c = \rho \theta_m + \Delta \ \text{backward drive}$$

$\dot{\theta}_c = \rho \dot{\theta}_m$ forward and backward drive

hence $T_{Lm} = \rho (J_L \rho \ddot{\theta}_m + f_L \rho \dot{\theta}_m)$

$$= \rho^2 (J_L \ddot{\theta}_m + f_L \dot{\theta}_m)$$

$$T_m = J_m \ddot{\theta}_m + f_m \dot{\theta}_m + T_{Lm}$$

$$= J_m \frac{\ddot{\theta}_c}{\rho} + f_m \frac{\dot{\theta}_c}{\rho} + \rho^2 \left(J_L \frac{\ddot{\theta}_c}{\rho} + f_L \frac{\dot{\theta}_c}{\rho} \right)$$

$$= \left(\frac{J_m}{\rho} + \rho J_L \right) \ddot{\theta}_c + \left(\frac{f_m}{\rho} + \rho f_L \right) \dot{\theta}_c$$

$$T_m = K (\theta_R - \theta_c)$$

$$K \theta_R = \left(\frac{J_m}{\rho} + \rho J_L \right) \ddot{\theta}_c + \left(\frac{f_m}{\rho} + \rho f_L \right) \dot{\theta}_c + K \theta_c$$

$$\ddot{\theta}_c + \frac{\left(\frac{f_m}{\rho} + \rho f_L \right) \dot{\theta}_c}{\left(\frac{J_m}{\rho} + \rho J_L \right)} + \frac{K \theta_c}{\left(\frac{J_m}{\rho} + \rho J_L \right)} = \frac{K \theta_R}{\left(\frac{J_m}{\rho} + \rho J_L \right)}$$

$$\ddot{\theta}_c + 2\zeta\omega_n\dot{\theta}_c + \omega_n^2\theta_c = \omega_n^2\theta_R$$

$$\text{where} \quad \omega_n^2 = \frac{\rho k}{J_m + \rho^2 J_L}$$

$$2\zeta\omega_n = \frac{f_m + \rho^2 f_L}{J_m + \rho^2 J_L}$$

The equation for load alone with gears not in contact is:

$$J_L\ddot{\theta}_c + f_L\dot{\theta}_c = 0$$

$$\text{or} \quad \ddot{\theta}_c + \frac{f_L}{J_L}\dot{\theta}_c = 0$$

The equation for the motor alone with the gears not in contact is.

$$J_m\ddot{\theta}_m + f_m\dot{\theta}_m = k(\theta_R - \theta_c)$$

The method of analysis used by New, Ref. e, is used in order to be able to examine the system independently of its ω_n

Defining first $\quad \omega_n t \triangleq t^*$

and differentiating $\quad \omega_n dt = dt^*$

$$\omega_n = \frac{dt^*}{dt} \quad \text{and} \quad \omega_n^2 = \left(\frac{dt^*}{dt}\right)^2$$

$$\dot{\theta}_c = \frac{d\theta_c}{dt} = \frac{d\theta_c}{dt^*}\frac{dt^*}{dt}, \quad \frac{d\theta_c}{dt^*} = \dot{\theta}_c^*$$

$$\text{hence} \quad \dot{\theta}_c = \dot{\theta}_c^*\,\omega_n$$

similarly

$$\ddot{\theta}_c = \frac{d^2\theta_c}{dt^2} = \frac{d^2\theta_c}{(dt^*)^2}\left(\frac{dt^*}{dt}\right)^2 = \frac{d^2\theta_c}{(dt^*)^2}\,\omega_n^2$$

$$\frac{d^2\theta_c}{(dt^*)^2} = \ddot{\theta}_c^* \quad \text{and} \quad \ddot{\theta}_c = \ddot{\theta}_c^*\,\omega_n^2$$

$$\text{finally} \quad \dot{\theta}_c = \dot{\theta}_c^*\,\omega_n = \dot{\theta}_c^*\,\frac{dt^*}{dt}$$

$$\int \dot{\theta}_c\,dt = \int \dot{\theta}_c^*\,dt^* \quad \text{or} \quad \theta_c = \theta_c^*$$

Using the equations of the combined system and the load alone,

$$\ddot{\theta}_c + 2\zeta\omega_n\dot{\theta}_c + \omega_n^2\theta_c = \omega_n^2\theta_r \qquad \text{combined system}$$

$$\ddot{\theta}_c + \frac{f_L}{J_L}\dot{\theta}_c = 0 \qquad \text{load alone}$$

and making the indicated substitution to a transformed (*) coordinate system for the system equation

$$\omega_n^2\ddot{\theta}_c^* + 2\zeta\omega_n^2\dot{\theta}_c^* + \omega_n^2\theta_c^* = \omega_n^2\theta_R$$

$$\ddot{\theta}_c^* + 2\zeta\dot{\theta}_c^* + \theta_c^* = \theta_R$$

and introducting the slope equations of the phase plane

$$N_s\,\dot{\theta}_c^* + 2\zeta\dot{\theta}_c^* + \theta_c^* = \theta_R \quad \text{results.}$$

If the load equation is first put in the form for the phase plane

$$N_L\,\dot{\theta}_c + \frac{f_L}{J_L}\dot{\theta}_c = 0$$

and then transformed to the (*) coordinate system where $\dot{\theta}_c^* \neq 0$

$$N_L\,\dot{\theta}_c^* + \frac{f_L}{J_L}\dot{\theta}_c^* = 0 \qquad \text{results.}$$

The same result may be obtained by setting $\omega_n = 1$. The results of such a transformation require inverse scaling for practical application, examples of which given in Section 6. It is noted that the slope of the load-free equation is mathematically the same whether in the phase plane or in the transformed phase plane. It is pointed out at this time that the equations later developed to satisfay the laws of conservation of momentum and energy are independent of the system natural frequency.

To establish equations for the law of the conservation of momentum and a relationship satisfying the law of the conservation of energy, the following schematic is used.

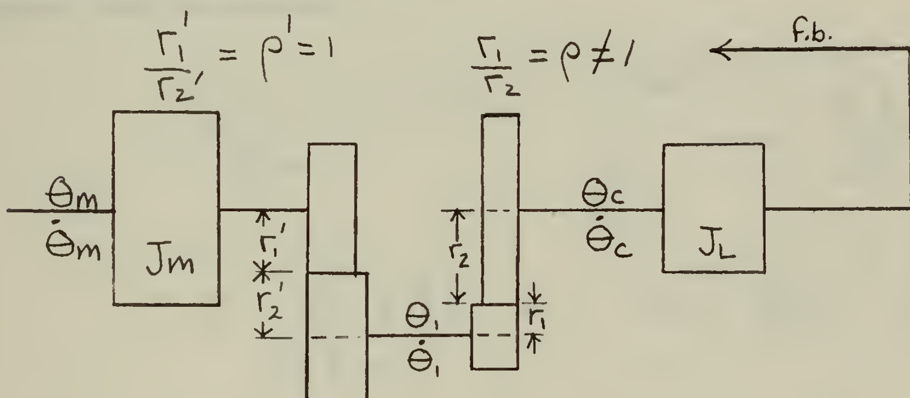

It is seen that $\theta_c = -\rho\,\theta_1 \quad , \quad \dot{\theta}_c = -\rho\,\dot{\theta}_1$

and since $\rho' = 1$ an equivalent schematic results

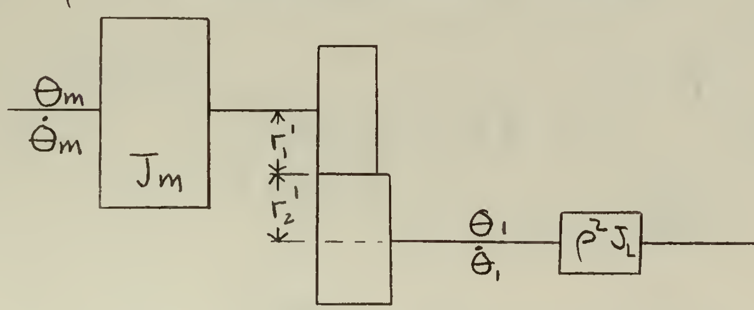

By representing the inertia of the load and motor as inertia of the gears the following figure is obtained at the instant of impact.

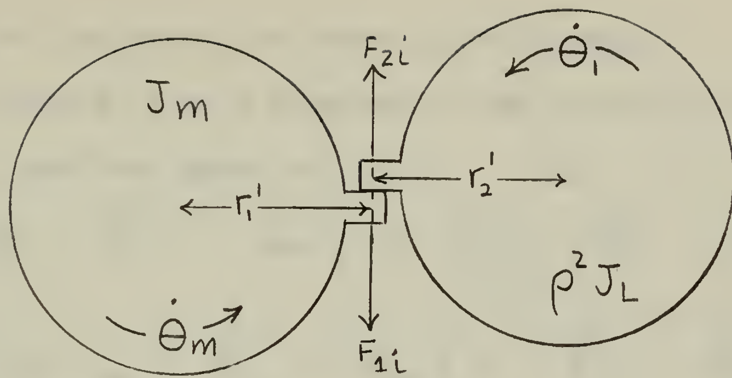

$r_1' = r_2'$

The torque equation may be expressed $T = J\ddot{\theta} = J\frac{d\dot{\theta}}{dt}$

Impulse is equal to the time rate of change of momentum. The expressions for the rates of change of momentum of the gears treated separately may be written:

$$-\int_{dt\to 0} |F_{1i}|\, r_1'\, dt = \int_{\dot{\theta}_m}^{\dot{\theta}_m'} J_m \frac{d\dot{\theta}_m}{dt}\, dt$$

$$-r_1' \int_{dt\to 0} |F_{1i}|\, dt = J_m(\dot{\theta}_m' - \dot{\theta}_m)$$

$$-\int_{dt\to 0} |F_{1i}|\, dt = \frac{J_m}{r_1'}(\dot{\theta}_m' - \dot{\theta}_m)$$

for the motor

and

$$\int_{dt\to 0} |F_{2i}|\, r_2'\, dt = \int_{\dot{\theta}_1}^{\dot{\theta}_1'} \rho^2 J_L \frac{d\dot{\theta}_1}{dt}\, dt$$

$$\int_{dt\to 0} |F_{2i}|\, dt = \rho^2 \frac{J_L}{r_2'}(\dot{\theta}_1' - \dot{\theta}_1)$$

where the primed velocities are those following impact.

If the momentum is to be conserved in the system the impulse functions are equal and opposite.

$$\frac{J_m}{r_1'}\left(\dot{\theta}_m' - \dot{\theta}_m\right) = \frac{\rho^2 J_L}{r_2'}\left(\dot{\theta}_1' - \dot{\theta}_1\right)$$

and
$$\frac{J_m}{J_L}\,\frac{1}{\rho}\left(\dot{\theta}_m' - \dot{\theta}_m\right) = \left(\dot{\theta}_c - \dot{\theta}_c'\right)$$

from substitution of the equations

$$r_1' = r_2' \quad , \qquad \dot{\theta}_c = -\rho\,\dot{\theta}_1$$

The assumption that all other impulse functions are zero at the instant of impact is restated at this point.

A definition of the coefficient of restitution will be made for purposes of this work:

$$e \triangleq -\frac{\left(\dot{\theta}_m' + \dot{\theta}_1'\right)}{\left(\dot{\theta}_m + \dot{\theta}_1\right)} = -\frac{\left(\rho\,\dot{\theta}_m' - \dot{\theta}_c'\right)}{\left(\rho\,\dot{\theta}_m - \dot{\theta}_c\right)}$$

It will be shown that this definition of e will satisfy the law of conservation of energy. Consider the case of e=0,

$$0 = -\left(\rho\,\dot{\theta}_m' - \dot{\theta}_c'\right), \qquad \rho\,\dot{\theta}' = \dot{\theta}_c$$

in which case for plastic impact (e=0) the gears are moving at the same velocity following impact.

The expression for the coefficient of restitution is examined for the case of perfect elastic contact, e=1, for which the law of conservation of energy is satisfied.

Solution of the restitution equation for e=1 yields

$$\rho\,\dot\theta_m - \dot\theta_c = -\rho\,\dot\theta_m' + \dot\theta_c'$$

$$\rho(\dot\theta_m + \dot\theta_m') = \dot\theta_c' + \dot\theta_c$$

For conservation of energy

$$\frac{1}{2}\left(J_m\dot\theta_m^2 + J_L\dot\theta_c^2\right) = \frac{1}{2}\left(J_m\dot\theta_m'^2 + J_L\dot\theta_c'^2\right)$$

or

$$\frac{J_m}{J_L}\left(\dot\theta_m^2 - \dot\theta_m'^2\right) = \left(\dot\theta_c'^2 - \dot\theta_c^2\right)$$

and factoring

$$\frac{J_m}{J_L}\left(\dot\theta_m + \dot\theta_m'\right)\left(\dot\theta_m - \dot\theta_m'\right) = \left(\dot\theta_c' + \dot\theta_c\right)\left(\dot\theta_c' - \dot\theta_c\right)$$

The momentum equation which is independent of e is:

$$\frac{J_m}{\rho J_L}\left(\dot\theta_m' - \dot\theta_m\right) = \left(\dot\theta_c - \dot\theta_c'\right)$$

or rearranging

$$\frac{J_m}{\rho J_L}\left(\dot\theta_m - \dot\theta_m'\right) = \left(\dot\theta_c' - \dot\theta_c\right)$$

The factored energy equation is now divided by the momentum equation to yield

$$\rho\left(\dot\theta_m + \dot\theta_m'\right) = \left(\dot\theta_c' + \dot\theta_c\right)$$

which checks with the definition of the coefficient of restitution for e=1.

The momentum equation implied from the impulse approach that $dt \to 0$ hence $\theta_c = \theta_c'$ and $\theta_m = \theta_m'$. The definition of the coefficient of restitution is independent of position. It may be noted that the equations for energy and momentum depend only on the inertia distribution, gear ratio and angular velocities.

In manipulation of these equations it is seen that load inertia may be transferred to the θ_1, shaft by multiplication ρ^2, the same transfer may be accomplished with load friction. Since θ_1, and $\dot\theta_1$, are related to θ_L and $\dot\theta_L$ it may be reasoned that the results

for $\rho = 1$ may be extrapolated to physical systems where $\rho \neq 1$.

Since a total energy accounting may be made for the system with the equations used, the rotational energy lost is attributed to the heat of deformation of the gear teeth. This transfer of energy could in fact be determined from the equations used. Thus the conservation of rotational energy e=1 is a special case of a broad interpretation of the law of conservation of energy.

3. Computer Program Development

The physical equations of the net systems were programmed for solution using the Control Data Corporation 1604 high speed digital computer utilizing paper tape program input and magnetic tape output. An IBM 717 line printer was used to extract data from the magnetic tape. The Control Data Corporation machine library and the U. S. Naval Postgraduate School computer subroutine library were used for assembly, Runge-Kutta-Gill numerical integration, and decimal output.

Several changes were made in the forms of the physical equations of the net system in order to eliminate duplicate computing operations and to fit the equations to a form suited to the variable parameters. In the table of symbols, computer mnemonic (m) terms which are used in the assembly subroutine have been indicated by parenthises and will be defined when encountered.

The equation of the system with motor and load combined

$$\ddot{\theta}_C = \omega_n^2 \theta_R - \omega_n^2 \theta_C - 2\zeta\omega_n \dot{\theta}_C$$

was put in the form

$$\ddot{\theta}_C = \omega_n^2 \theta_R - \omega_n^2 \theta_C - \underline{A}\, \dot{\theta}_C \quad \text{where}$$

$$\underline{A} = 2\zeta\omega_n \quad \text{and}$$

THETAL	=	θ_C	ONE	=	θ_R
THETALD	=	$\underline{U} = \dot{\theta}_C$	ZETA	=	ζ
UDOT	=	$\ddot{\theta}_C$	OMEGANSQ	=	ω_n^2

were the computer m terms used. Underlining will be used in this section to denote the transition to the m terms of the computer equations.

The differential equations were solved using the Runge-Kutta-Gill,

(RUNGE), numerical integration method. The RUNGE subroutine required the definition of synonymous terms for the four iterative cycles used to produce one extrapolated set of variables. The increment of the independent time variable chosen was 0.01 sec. for all $\zeta > 0.1$ and 0.004 sec. for all $\zeta \leq 0.1$.

The load free equation

$$\ddot{\theta}_c + \frac{f_L}{J_L} \dot{\theta}_c = 0 \qquad \text{was put in the form}$$

$$\ddot{\theta}_c + \underline{B} \, \dot{\theta}_c = 0 \qquad \text{for the computer.}$$

A separate set of RUNGE synonyms was used for the load free equation in order not to destroy the previous computations before they were determined of no further value in computing and also in the making of program decisions.

$\dot{\theta}_c$ was designated V and $\ddot{\theta}_c$ was designated VDOT for the computer program.

The equation for the motor alone

$$\ddot{\theta}_m + \frac{f_m}{J_m} \dot{\theta}_m + \frac{K}{J_m} \theta_c = \frac{K}{J_m} \theta_R$$

was put in the form

$$\ddot{\theta}_m = - \frac{f_m}{J_m} \dot{\theta}_m + \frac{K}{J_m} (\theta_R - \theta_c)$$

$$\ddot{\theta}_m = - \underline{D} \, \dot{\theta}_m + \underline{C} \, (\theta_R - \theta_c)$$

and for RUNGE, the terms

θ_m = THETAM $\qquad \dot{\theta}_m$ = THETADM = W

and $\ddot{\theta}_m$ = WDOT were used.

The equation representing the law of conservation of momentum and the definition of coefficient of restitution were combined to the forms

[illegible]

$$[illegible]$$

[illegible]

[illegible]

$$[illegible]$$

[illegible]

$$[illegible]$$

[illegible]

$$[illegible]$$

[illegible]

$$\dot{\theta}_c' = \frac{J_m}{J_m + \rho^2 J_L}\left[\rho\,\dot{\theta}_m(1+e) + \dot{\theta}_c\left(\rho^2\frac{J_L}{J_m} - e\right)\right]$$

$$\dot{\theta}_m' = \frac{\dot{\theta}_c' - e\rho\dot{\theta}_m + e\,\dot{\theta}_c}{\rho}$$

for the computer program. No provision for additional m terms was made to denote the primed values. The additional terms:

$$e = \underline{\text{RESTITUT}} \quad \rho = \underline{\text{RHO}} \quad \text{and} \quad \rho^2 = \underline{\text{RHOSQ}}$$

were used.

Two equations were used to define the boundaries of operation of the load and motor when they were acting separately,

$$\theta_c = \rho\,\theta_m \quad \text{and} \quad \theta_c = \rho\,\theta_m + \Delta$$

Two major decisions of the computing cycle were the determination of the point where the motor and load would float free, <u>FLOATEST</u>, and the response of the system to impact of the load and motor gears when the boundary conditions on position were met, <u>COMBTEST</u>.

The first decision, the point of float free, is made on the equality or inequality of slopes in the phase plane, i.e., at separation $N_L = N_S$. Equating the slopes:

$$\frac{\omega_n^2}{\dot{\theta}_c}(\theta_R - \theta_c) - \underline{A} + \underline{B} = 0$$

The above equation is solved after computing each point in the combined phase trajectory. If $N_S + N_L > 0$ the system remains combined. If $N_S + N_L \leq 0$ the system separates, having the response motor alone and load alone immediately thereafter.

The second major decision, that of whether after impact the

$$[illegible]$$

$$[illegible]$$

[illegible]

$$[illegible]$$

[illegible]

$$[illegible]$$

[illegible]

[illegible]

$$[illegible]$$

[illegible]

response should be that of the combined system or the response of the load and motor acting separately, is made on the basis of the resultant velocities after impact and upon which side of the backlash the motor and load positions are found.

The computer program, its flow diagram, a description of the program operation, and an explanation of the readout of information with examples are presented in the Appendix.

4. Methods and Scope of Examination

Two modes of operation of the computer program were used. The first mode considered was the phase trajectory. This mode was used to check the operation of the computing cycle. Time, velocity and position of the load were printed when the system was combined. When the system was separated, the values of motor velocity and motor position were also printed. Although the time increment used for computations was either 0.01 sec. or 0.004 sec., printed outputs for the first mode were taken only every 0.1 sec. Additional printed outputs were taken at the time of contact of the gears just prior to and immediately following the solution of the momentum and restitution equations. A typical printout of the phase trajectory mode of operation is shown in Appendix C.

The second mode of operation was used for printing only the maximum computed positive load overshoot position for each cycle, the associated load velocity and the exact problem time of the computation. A sufficient number of print-outs for each problem was obtained to prove limit cycle existence and average size. Since this investigation was concerned primarily with the steady state response, the second mode of operation was the one utilized to obtain the majority of the data. This read-out method markedly decreased the data reduction time for the problem analysis, as opposed to the analysis of steady state conditions provided by a full phase trajectory print-out. Since the time required for computer read-out was several magnitudes greater than the computing time, valuable computer time was saved by this mode of operation. An example of the printed output obtained when only maximum load position overshoot was of interest is given in Appendix D. Approximately 1400

phase trajectories were solved using this mode of operation. Each solution required an average of three minutes of computer time.

For the purpose of general examination of the problem it was assumed that $\rho = 1$, $K = 1$, $\omega_n = 1$, $J_m + \rho^2 J_L = 1$. Specific solutions were made with $\rho \neq 1$, $\omega_n \neq 1$ to determine scaling effects. The results of these solutions are presented in Section 6, Application of Results.

The program can also be made to solve linear systems by setting $\Delta = 0$.

The major variable parameters used in this investigation were:

ζ = 0.1, 0.2, 0.3, 0.4, 0.5, 0.6, 0.8, 1.0

$\frac{\rho^2 f_L}{F_T}$ = 0, 0.2, 0.4, 0.6, 0.8, 1.0

$\frac{\rho^2 J_L}{J_m} = \frac{0.1}{0.9}, \frac{0.2}{0.8}, \frac{0.5}{0.5}, \frac{0.8}{0.2}, \frac{0.9}{0.1}$

Δ = 0.3 radians

e = 0, 0.6, 0.8, 1.0

Additional parameters of

$\frac{\rho^2 f_L}{F_T}$ = 0.04, 0.1, 0.9; and Δ = 0.01, 0.03, 0.01, 0.15 radians

were used in certain instances to examine particular characteristics of the response.

The program was limited somewhat in that the value of $\frac{\rho^2 J_L}{J_m} = \infty$ and zero were exluded due to generation of undefined mathematical quantities.

The value of backlash was made abnormally large, Δ = 0.3 radians, to allow an easier interpretation of the non-linear response. Since the influence of Δ was linear, this caused no inaccuracies. All

graphs for limit cycle size were plotted with Δ = 0.3 radians. The effect of values for Δ other than 0.3 is also shown in graphical form.

5. Results and Discussion

Two types of system response were observed. The first type was a convergence to zero error, which was a case of static and dynamic equilibrium of the system. This is a characteristic of a linear second order servomechanism. The second type of system response observed was the divergence or convergence to a state of dynamic equilibrium. This second type of response is termed a limit cycle and is characterized by cyclic travel of the load through the same points of the phase trajectory. When the second mode of computer operation was used, both the maximum load position per cycle and the period of the recorded position were analyzed to determine if the characteristic response was a limit cycle. Exact repetition of cyclic values was impossible due to the numerical methods used and the computer round-off error for the output routine. Typical examples of the limit cycle and no limit cycle response are given in Appendices D 1 and D 2.

No case of dynamic instability or divergence of the system without bound was observed in the investigation. Intuition might lead to this same conclusion when the following unique characteristics of this system are pointed out: (a) As a maximum limit, energy was conserved at the instant of impact. (b) Energy was supplied to the system only in finite amounts and at a finite rate by the error detector. (c) Energy sinks were present in the system frictional elements while energy storage units were present in both the motor and load. (d) No undefined limits appeared in the applied physical equations,

$\rho^2 \frac{J_L}{J_m} = 0$ and ∞ excluded.

[illegible]

[illegible]

[illegible]

The results of the investigation are offered in the form of charts for parameter areas of limit cycle existence and nonexistence in Fig. 1 for e = 0., 0.6, 0.8 and Fig. 2 for e = 1.0. The parameters $\rho^2 \frac{f_L}{F_T}$ and $\rho^2 \frac{J_L}{J_m}$ are designated abscissa and ordinate respectively. The parameter points of examination for which solutions were obtained are circled. The zone enclosed by a particular δ line is largely an interpretation by the authors of the results of the investigation, and shows the area in which no limit cycle existed. Due to the large change of the variable parameter values between solutions, the charts are <u>not exact</u>. All circled intersections interior to the δ line indicate parameters which resulted in no limit cycles, e.g., Fig. 1 for e = 0, 0.6, 0.8 at a $\delta = 0.4$, the values of $\rho^2 \frac{f_L}{F_T} =$ 0.6, 0.8 at a $\rho^2 \frac{J_L}{J_m} = 9.0$ and the value of $\rho^2 \frac{f_L}{F_T} = 0.6$ at a $\rho^2 \frac{J_L}{J_m} = 4.0$ resulted in no limit cycle. Similarly, for $\delta = 0.5$, the values of $\rho^2 \frac{f_L}{F_T} = 0.4$, 0.6, and a $\rho^2 \frac{J_L}{J_m} = 1.0$ as well as all other parameter intersections interior to the $\delta = 0.5$ curves, resulted in no limit cycles.

All circled parameter intersections exterior to particular δ lines define paramters which were examined and resulted in a steady state limit cycle. The area to the right of the single $\delta = 1.0$ line designates the parameters for which no limit cycles were observed. Limit cycles were observed for all $\delta \leq 0.3$ for the parameters examined.

The investigation was made with $\Delta = 0.3$ radians; however, results of the investigation of variation of limit cycle size indicate

that existence of the limit cycle is independent of the size of backlash in a nonlinear system for a Δ greater than zero. Variation of Δ had the effect of a linear variation of limit cycle size only.

The zones depicted on the existence charts are approximately represented by straight lines; however there is reason to believe that a complete examination would show a curvature in the lines. This observation will be elaborated upon later when the relationship between the existence charts and the figures of limit cycle size is discussed.

From Fig. 1 it is seen that there is only a very small difference in the limit cycle existence zones for plastic impact (e = 0) and the intermediate values of the coefficient of restitution, e = 0.6 and 0.8. When comparing the elastic impact (e = 1) in Fig. 2 to the plastic and intermediate cases in Fig. 1, the most obvious point of comparison is the drastic reduction of the areas in which limit cycles did not result for e = 1.0. However, it may be generally observed that with any e held constant, the area in which a limit cycle could not be obtained increased with the increase of system $\int$.

For all values of e, there is an apparent common enclosed zone centroid which is described by the system parameters $\rho^2 f_L/F_T = 0.5$ and $\rho^2 J_L/J_m = 1.0$. These parameters result in the system time constants $f_L/J_L = f_m/Jm$, since $\omega_n = 1$ and $\rho = 1$ were chosen for the investigation. There is also an apparent symmetry about the centroid of opposite quadrants which can be related to the fact that since $\omega_n = 1$ and $\rho = 1$, the points diametrically opposite across the centroid of the figure (using the decimal values of the parameter intersection) represent an exact exchange of component time constants. (See Fig. 2 for example). Two diametrically opposite points may have

exactly the same motor and load time constants; however, they are descriptive of two different systems since the friction and inertia distributions are different for the two points.

Figs. 3 through 26 present the maximum positive error in radians of the limit cycle for a unit step input and with backlash equal to 0.3 radians. The use of the charts is explained in Section 6, Application of Results. Each figure is presented with $\rho^2 f_L/F_T$ and e constant. The independent parameter $\rho^2 J_L/J_m$ is indicated as abscissa and curves of constant ζ are plotted with limit cycle error as the ordinate. The results were presented on a log log plot since the observed limit cycle errors encompassed a range from 0.01 to 1.0 radians, and the appearance and disappearance of limit cycles and the change of limit cycle error was more readily apparent on the log log form.

In general as e increases, the size of limit cycle decreases, all other parameters remaining constant. However this is not without a few exceptions; the generalization is most accurate for large size limit cycles. It may be noted that when viewing the individual charts, if a limit cycle exists at very low $\rho^2 J_L/J_M$ ratio there is a tendency for the same system to have a smaller limit cycle for higher $\rho^2 J_L/J_m$ ratio. In addition, for these same conditions, if limit cycles exist for several values of ζ, there is a convergence toward the same size of limit cycles for each ζ as $\rho^2 J_L/J_m$ increases. At the value $\rho^2 f_L/F_T = 0$, a limit cycle will always occur for any value of e or ζ.

Viewing the charts in sequence, with either e constant or $\rho^2 f_L/F_T$ constant, it is noted that there is continuity of pattern flow between

adjacent charts. This continuity between charts appears to form a symmetrical pattern of constant ζ lines which can be interpolated for intermediate values. When the figures for $\rho^2 f_L/F_T = 0.4$ and 0.6 are analyzed, this symmetrical pattern is observed in each chart about $\rho^2 J_L/J_m = 1$. The limit cycle decreases and disappears at the opposite extremes of $\rho^2 J_L/J_m$. The charts of $\rho^2 f_L/F_T = 0.4$ and 0.6 are symmetrical to each other, while $\rho^2 f_L/F_T = 0.2$ and 0.8 are similar. At the extreme values of $\rho^2 f_L/F_T = 0$ and 1.0, no symmetrical comparison can be made. An additional point of symmetry about $\rho^2 f_L/F_T = 0.5$ can be visualized for all values of e. These parameters for symmetry are noted in the discussion of the existence charts. The irregularities in the curves of medium values of ζ can not be explained by the authors; however, it may be mentioned again that the points of symmetry are characterized by exact exchange of component time constants.

The noted symmetry of the limit cycle size charts shows a direct relationship to the symmetry found in the existence charts. Since the existence charts show contours of constant ζ for a surface of zero limit cycle size, one is led to the possibility of a three dimensional presentation to show a variation of limit cycle size for the same parameters used in the existence charts. Such a three dimensional figure for constant e using $\rho^2 f_L/F_T$, $\rho^2 J_L/J_m$ and ζ as the axes is shown in Fig. 27. Other surfaces could be added above this zero limit cycle "floor" to show the variation of a given limit cycle size by contours of ζ. The ultimate result of this line of investigation would be the evaluation of the poles and zeros for a conformal mapping presentation. Unfortunately, time did not permit the authors to investigate

this avenue further.

The results of the investigation of the dependence of limit cycle size on the amount of backlash are presented in Figs. 28 and 29 using coefficients of restitution of 0 and 1.0 at a $\zeta = 0.6$. A thorough investigation was made at this ζ since it is an average system parameter often used in design work. The limit cycle size was found to vary directly with backlash size without exception between the values of 0.3 and 0.01 radians. When limit cycles existed at $\Delta = 0.3$, there was no disappearance of limit cycle with decreasing magnitude of Δ. Where no limit cycle existed, at $\Delta = 0.3$, limit cycles continued to be non-existent throughout the range of Δ examined. Several solutions of problems with $\zeta = 0.6$ and $e = 0.6$ & 0.8 and $\zeta = 0.1$ & $e = 1.0$ & 0 with various Δ values, proved the linear variation of limit cycle size with backlash size for all values of e.

When a servomechanism under steady state conditions is disturbed by a small perturbation, it will return to the original steady state conditions. However, the transient response due to the perturbation may be quite different from the transient response which occured due to the original signal input. The concepts of energy and static and dynamic equilibrium mentioned in Section 1 may be better understood as a result of the perturbation technique if the usual initial conditions of $\dot{\theta}_c(0) = \theta_c(0) = 0$ are considered as a disturbance from the stability conditions predetermined by selection of system parameters and signal input.

This same small perturbation technique was simulated mathematically using the digital computer to obtain several solutions. The cases examined and their initial conditions were:

[illegible]

a) $\zeta = 0.6, \quad \rho^2 J_L/J_m = 0.8/0.2, \quad \rho^2 f_L/F_T = 0, \ e = 0, \ \Delta = 0.3$

$\dot{\theta}_c(0) = 0, \ \theta_c(0) = 1.2$

$\dot{\theta}_m(0) = 0, \ \theta_m(0) = 1.0$

system separated.

b) $\zeta = 0.6, \quad \rho^2 J_L/J_m = 0.1/0.9, \quad \rho^2 f_L/F_T = 1.0, \ e = 1.0, \ \Delta = 0.3$

$\dot{\theta}_c(0) = 1.0, \ \theta_c(0) = 1.0$

$\dot{\theta}_m(0) = 1.0, \ \theta_m(0) = 1.0$

system combined

c) $\zeta = 0.4, \quad \rho^2 J_L/J_m = 0.5/0.5, \quad \rho^2 f_L/F_T = 0.4, \ e = 0.6, \ \Delta = 0.3$

$\dot{\theta}_c(0) = 0, \ \theta_c(0) = 1.005$

$\dot{\theta}_m(0) = 0, \ \theta_m = 1.00$

system separated

In the three cases examined, the same limit cycle was obtained, both in size and period, as that resulting from the normally used initial conditions, $\dot{\theta}_c(0) = \theta_c(0) = 0$. The maximum difference between the perturbation response and the original limit cycle size for the three cases was 18×10^{-5} radians. Two types of transient response were observed. These were convergence to limit cycle in the first two cases and divergence to limit cycle in the last case.

The results obtained by the small perturbation technique supported the validity of the analysis of the problem by digital methods. This result also concurs with the findings for the case of e = 0 by Knoll and Narud, Ref. d, in that the steady state limit cycle size is completely specified by the choice of system parameters and independent of system initial conditions.

Mention is made here that the computer program could not be run normally for the perturbation method. The computer was stopped after

$$[illegible]$$

[illegible]

[illegible]

[illegible]

the print out of system constants, then the initial conditions of the servo system were inserted manually. The program was then restarted at the desired point for computing, either as a combined system or with the motor and load separated. The program was then allowed to operate to the normal completion of the solution.

The work of Ref. d reported that the system transient response for the case e = 0 arrived at a steady state limit cycle by two possible phase trajectories. One of these phase trajectories was smooth convergence to the limit cycle, while the second was a converging overshoot toward the inside of the limit cycle followed by a divergence to the limit cycle. From the results of this investigation for the cases e = 0, 0.6, 0.8 and 1.0, similar transient indications were obtained.

Several computer solutions were accomplished for the cases $\Delta = 0.3$ radians, e = 0, 1.0, $\rho = 1.0$, $\omega n = 1.0$, $K = J \neq 1.0$. In addition various combinations of $\rho \neq 1.0$ and $\omega n \neq 1.0$ were obtained. The purpose of these solutions were:

1. To determine the general applicability of the computer program.
2. To verify the scaling developed in Section 2, Development of Equations.
3. To determine the applicability of the results of this thesis.

The following results were determined:

A. Two solutions were obtained (e = 0 & 1.0) for the case $\zeta = 0.4$, $\rho = 1.0$ $\omega n = 1.0$, $J = 2.0$, $K = 2.0$, $\rho^2 \frac{f_L}{F_T} = 0.4$, $\rho^2 \frac{J_L}{J_m} = 4.0$. The results of these solutions were the same (time, load velocity, load position, and limit cycle size) as the solutions obtained for $\rho^2 \frac{f_L}{F_T} = 0.4$, $\rho^2 \frac{J_L}{J_m} = 4.0$, $\zeta = 0.4$ using the nondimensional parameters $\omega n = 1.0$, $\rho = 1.0$, $J = 1.0$, $K = 1.0$.

B. Solutions were obtained for e = 0 & 1.0 for the case $\zeta = 0.4$, $\rho = 1.0$, $\omega_n = 2.0$, J = 1.0, K = 4.0, $\rho^2 \frac{f_L}{F_T} = 0.4$, $\rho^2 \frac{J_L}{J_m} = 4.0$. The results of these solutions yielded the same size maximum overshoots and limit cycle size as the nondimensional solutions for $\zeta = 0.4$, $\rho^2 \frac{f_L}{F_T} = 0.4$, $\rho^2 \frac{J_L}{J_m} = 4.0$. The times of maximum overshoots in this case were one-half the times of occurence of the same overshoots for the nondimensional solution. The velocity at a maximum overshoot was twice the value of velocity obtained for the same overshoot in the nondimensional solution. This same comparison can be made for Cases A and B. The results of these and other solutions prove the validity formulae used in Section 2, Development of Equations, concerning the transformation to the coordinate system. (*)

C. Solutions were obtained for the case e = 0 & 1.0, $\zeta = 0.4$, $\rho = 0.5$, $\omega_n = 1.0$, $\frac{f_L}{F_T} = 0.8$, $\frac{J_L}{J_m} = 4.0$, $\rho^2 \frac{f_L}{F_T} = 0.2$, $\rho^2 \frac{J_L}{J_m} = 1.0$. The results of these solutions were the same (time, load velocity, maximum overshoots and limit cycle size) as for the nondimensional solutions $\zeta = 0.4$, $\rho = 1.0$, $\omega_n = 1.0$, $\rho^2 \frac{f_L}{F_T} = 0.2$, $\rho^2 \frac{J_L}{J_m} = 1.0$.

D. Solutions were obtained for the case e = 0 & 1.0, $\zeta = 0.4$, $\rho = 0.5$, $\omega_n = 2.0$, $\frac{f_L}{F_T} = 0.8$, $\frac{J_L}{J_m} = 4.0$, $\rho^2 \frac{f_L}{F_T} = 0.2$, $\rho^2 \frac{J_L}{J_m} = 1.0$. The results of these solutions yielded the same size maximum overshoots and limit cycle size as the nondimensional solutions for $\zeta = 0.4$, $\rho^2 \frac{f_L}{F_T} = 0.2$, $\rho^2 \frac{J_L}{J_m} = 1.0$. The times and velocities in this case were scaled by ω_n as in Case B.

Several phase trajectories using e = 0 were compared with those obtained by New, Ref. e. Generally good correlation was obtained on the value of limit cycle error and in the transient response. Small disagreements were expected, resulting primarily from differences in the

programming procedures and analysis of results by read-out methods.

Sample phase trajectories for the cases of e = 0 & 1.0 are presented in Figs. 30 and 31. Although the transient analysis of the system is beyond the scope of this work, these figures may aid in understanding the physical problem.

Of academic interest was the accidental operation of the computer program for several solutions using $\zeta = 0$. Several responses were observed. One was a nearly pure oscillatory system from the first overshoot and thereafter another was a very slow convergence or slow divergence of the oscillations after the first overshoot. The convergence or divergence probably resulted from errors generated in numerical iterations and approximations.

6. Application of Results

In this section, the results of this thesis will be applied to hypothetical physical systems. Methods will be indicated by which physical systems may be analyzed or designed. Attention is called to the assumptions stated in Section 2 under which this study was made.

It is desirable to find an equation relating certain system variables, therefore the equations:

$$\text{(1)} \qquad \omega_n^2 = \frac{\rho k}{J_m + \rho^2 J_L} = \frac{\rho k}{J_m}\left[\frac{1}{1 + \rho^2 \frac{J_L}{J_m}}\right]$$

and

$$\text{(2)} \qquad 2\zeta\omega_n = \frac{f_m + \rho^2 f_L}{J_m + \rho^2 J_L} = \frac{\rho^2 f_L\left[\frac{f_m}{\rho^2 f_L} + 1\right]}{J_m\left[1 + \rho^2 \frac{J_L}{J_m}\right]}$$

will be manipulated to the form

$$\text{(3)} \qquad \zeta = \frac{1}{2}\rho^2 \frac{f_L}{J_m} \frac{\left[\frac{f_m}{\rho^2 f_L} + 1\right]}{\left[1 + \rho^2 \frac{J_L}{J_m}\right]} \frac{\sqrt{J_m}}{\sqrt{\rho}\sqrt{K}} \sqrt{1 + \rho^2 \frac{J_L}{J_m}}$$

or

$$\text{(4)} \qquad \zeta = \frac{1}{2} f_L\left[\frac{f_m}{\rho^2 f_L} + 1\right]\left[\frac{\rho^3}{J_m K\left(1 + \rho^2 \frac{J_L}{J_m}\right)}\right]^{1/2}$$

In view of the form of Equation (4) for ζ and recalling that the variable parameters used on the figures were $\rho^2 \frac{J_L}{J_m}$ and $\rho^2 \frac{f_L}{F_T} = \frac{\rho^2 f_L}{f_m + \rho^2 f_L} = \frac{1}{\frac{f_m}{\rho^2 f_L} + 1}$ it is seen that the expression for ζ in fact includes the other two variable parameters.

[illegible]

[illegible]

$$[illegible]$$

[illegible]

$$[illegible]$$

[illegible]

$$[illegible]$$

$$[illegible]$$

[illegible]

From discussion concerning the effects system natural frequency, it will be recalled that the value of overshoot and hence limit cycle are not affected by ω_n; however, the time and velocity are scaled for $\omega_n \neq 1.0$. Thus the transient response characteristics may be related to the same parameters used in these applications.

If a motor and load are selected for a system and the limitation is imposed that system operation shall not result in a limit cycle, Equation (4) and the limit cycle existence charts may be used to determine the unspecified system parameters ζ, K and ρ. The coefficient of restitution for the proposed gear train material may be determined by the use of the equation in Section 2.

To proceed, select a value of K and ρ, then determine the value of ζ from Equation (4). Enter the limit cycle existence chart for the value of e, system ζ and the parameters $\rho^2 \frac{J_L}{J_m}$ and $\frac{1}{\frac{f_m}{\rho^2 f_L} + 1}$. Determine if the selected parameters describe a point of no limit cycle. Since limit cycle existence is independent of backlash ($\Delta \neq 0$ excluded), backlash is not a variable parameter. Successive trial values of the unspecified parameters may be required to meet the limitation of no limit cycle. If it is also required that certain transient response characteristics be met, these conditions could be examined by a similar method.

In the event that no acceptable parameters are found to satisfy the system requirements for no limit cycle, the figures for limit cycle size may be examined to obtain a minimum size limit cycle. The method of solution is similar to that previously described.

Example: The material intended for use in the gears has an e = 0.6.

[illegible]

[illegible]

[illegible]

[illegible]

The motor and load have the parameters fm = 0.64, Jm = 0.25, f_L = 0.64, J_L = 1.0 and it desired that the system operate with no limit cycle. If the values are selected K = 4.0, ρ = 0.5, the values $\rho^2 \frac{J_L}{J_m}$ = 1.0 and $\frac{f_m}{\rho^2 f_L}$ = 4.0, $\frac{1}{\frac{f_m}{\rho^2 f_L}+1}$ = 0.2 result.

Solve Equation (4) for ζ = .5(.64)(5+1) $\frac{.5^{3/2}}{[.25(4)(1+1)]^{1/2}}$, thus ζ = 0.4. Enter the chart for limit cycle existence, Fig. 1, e = 0.6, ζ = 0.4, $\frac{1}{\frac{f_m}{\rho^2 f_L}+1}$ = 0.2, $\rho^2 \frac{J_L}{J_m}$ = 1.0

It can be seen that limit cycle will exist for these parameters.

Since K is most easily varied in equation (4), a new K is selected at 1.0 in an effort to find parameters for no limit cycle. It is seen that

$$\zeta_{K=1.0} = \zeta_{K=4.0}\sqrt{\frac{4}{1}} = 0.4(2)$$

with all other parameters constant, thus ζ = 0.8 Enter Fig. 1 with e = 0.6 , $\zeta = 0.8$ $\rho^2 \frac{J_L}{J_m} = 1.0$, $\frac{1}{\frac{f_m}{\rho^2 f_L}+1} = 0.2$

These parameters describe system operation with no limit cycle and are well within the area limits. The transient response of this system may be undesirable and various combinations of ρ and K would have to be tested to satisfy the additional requirements of the problem. It will be restated that the existence areas of Figs. 1 and 2 are not exact.

The figures of limit cycle size may be used in the same manner as the existence charts. The same parameters of the first case are assumed: K = 4.0, ρ = 0.5, $\rho^2 \frac{J_L}{J_m}$ = 1.0, $\frac{1}{\frac{f_m}{\rho^2 f_L}+1}$ = 0.2 ζ = 0.4

$e = 0.6$, $\Delta = 0.1$ radians. Enter Fig. 10 with the parameters given. The ordinate, Limit Cycle Error $\left(\frac{0.3}{\Delta}\right) = 0.13$ radians, is obtained. The maximum positive error in the limit cycle $= 0.13 \frac{(0.1)}{(0.3)} = 0.0434$ radians. Enter the same figure for $e = 0.6$, $\zeta = 0.8$, $\rho^2 \frac{J_L}{J_m} = 1.0$, $\frac{1}{\frac{f_m}{\rho^2 f_L} + 1} = 0.2$, $\Delta = 0.5$ radians; this is the second case of examination for existence. No $\zeta = 0.8$ curve exists; hence no limit cycle exists for this choice of parameters for any nominal value of backlash.

7. Conclusions

Within the limitations of the assumptions made and the scope of this thesis, it is concluded that:

A. Two types of system steady state response result. The type of response is independent of backlash size, system natural frequency and initial conditions. The types of response are convergence to signaled input position and convergence to a limit cycle.

B. If a limit cycle exists in the steady state response of a system, the size of the limit cycle varies directly with the size of backlash, all other parameters constant.

C. The greatest change in system steady state response occurred for the case when system rotational energy is conserved (e = 1.0).

D. A point of symmetry for the type of system steady state response exists with equal motor and load time constants. For medium to high values of system damping coefficient, symmetry with respect to limit cycle size exists for an exchange of motor and load time constants.

E. The results of this thesis are presented in a form which may aid in system design or analysis.

8. Recommendations

From the results of this thesis it can be seen that there remain many fertile areas for further investigation. For studies of this type it is strongly recommended that the digital computer be used because of its speed and versatility. The limits of investigation depend to a great extent on the ingenuity of the programmer. Some recommended areas of future investigation are:

a) More precise definition of the limit cycle existence zones and a more thorough coverage of the limit cycle size of similar systems having the same type of parameters. A three-dimensional presentation as mentioned in the discussion could be obtained.

b) Include torsion and other deformations of the mechanical system in the physical equations of the system to determine their affect on the system response.

c) An analysis of the limit cycle existence zone and transient response of a system to determine if there is a relationship between the two. An analytical expression for the possibility of limit cycle existence might be developed in terms of system parameters.

d) Examine the transient and frequency response of the system due to various θ_R input functions. This would require minor modifications to the computation section of the existing computer program.

e) Since the physically realizable quantities of position, velocity and acceleration of both the motor and load are available as computed quantities, the study of the compensation problem and its optimization are obvious areas for further consideration.

f) The general study of other higher order nonlinear systems is suitable for digital computer programming since most numerical inte-

gration methods will handle systems having equations of any order.

9. REFERENCES

a. Chestnut, H. and Mayer, R.W., Servomechanisms and Regulating System Design, John Wiley & Sons, Inc., New York, N. Y., 1955.

b. Lutkenhouse, W.J., "Dividing Lines for Backlash in the Phaseplane", Unpublished Master's Thesis, United States Naval Postgraduate School, 1959.

c. Pastel, M.P. and Thaler, G.J., "Instrument Servomechanisms with Backlash, Couloumb Friction, and Stiction", Trans. A.I.E.E. (Applications and Industry) July 1960.

d. Knoll, A.L. and Narud, J.A., "Phase Plane Investigation of a Servomechanism with Backlash between Motor and Load", Technical Report 309 for Office of Naval Research, NR-375-017, Cruft Laboratory, Harvard University, Cambridge, Massachusetts, July 30, 1959.

e. New, N.C., "Effects of Backlash in the Second Order Servo", Unpublished Master's Thesis, United States Naval Postgraduate School, 1960.

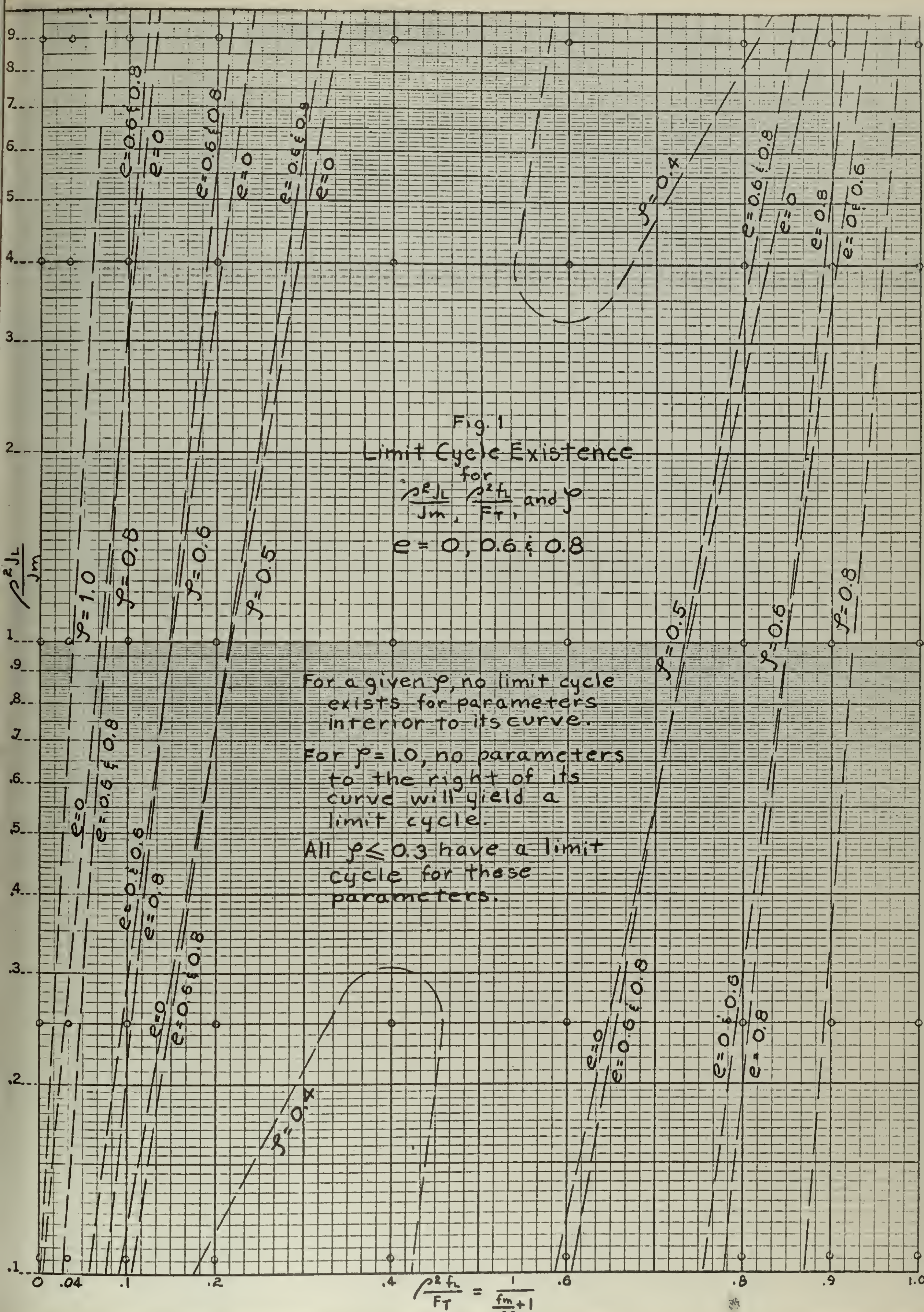

Fig. 1
Limit Cycle Existence
for
$\frac{\rho^2 J_L}{J_m}$, $\frac{\rho^2 f_L}{F_T}$, and ρ
$e = 0,\ 0.6\ \&\ 0.8$

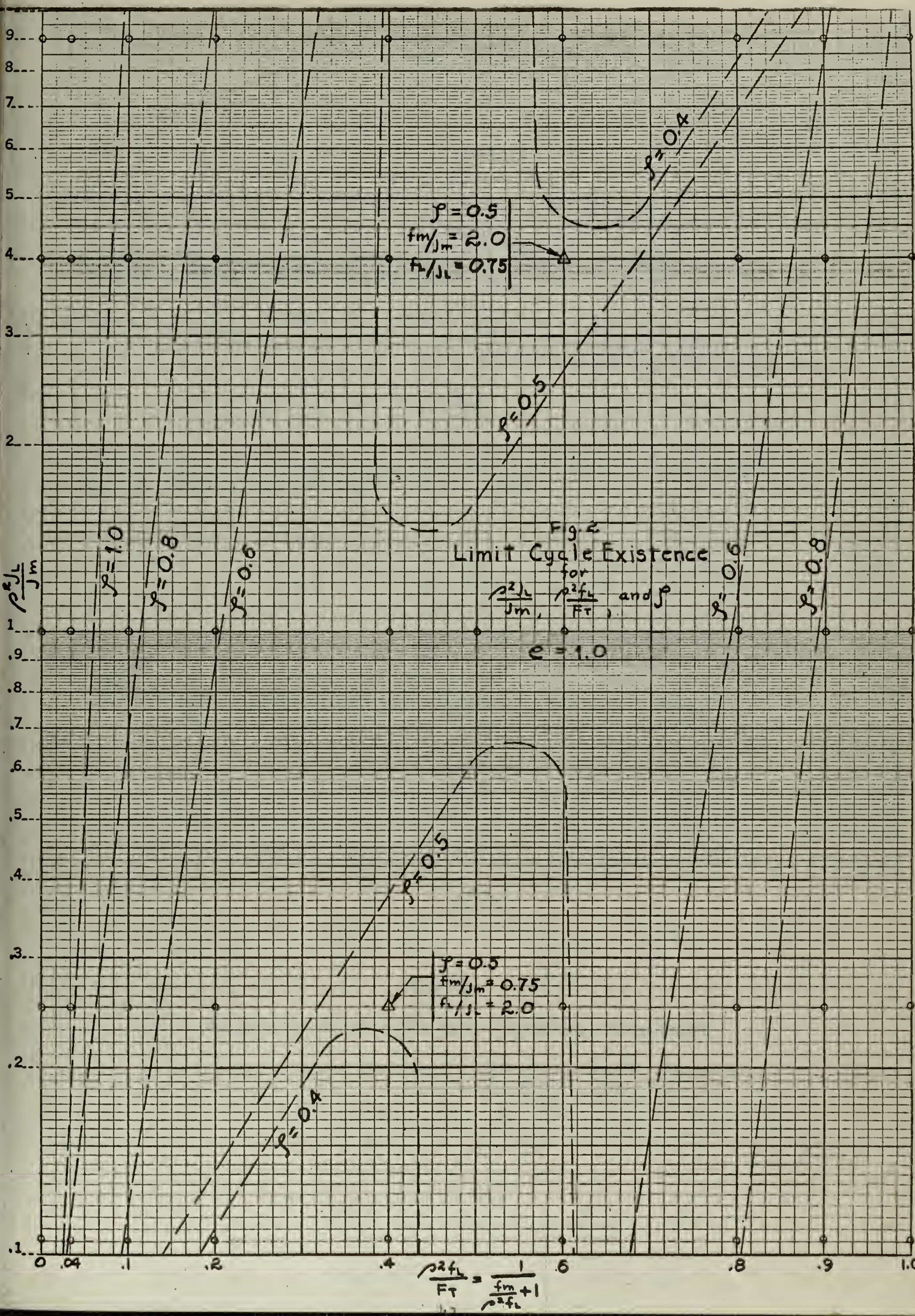

Fig. 2
Limit Cycle Existence
for
$\frac{\rho^2 J_L}{J_m}$, $\frac{\rho^2 f_L}{F_T}$, and ρ
$e = 1.0$
$\rho = 0.5$
$f_m/J_m = 2.0$
$f_L/J_L = 0.75$
$\rho = 0.5$
$f_m/J_m = 0.75$
$f_L/J_L = 2.0$
$\rho = 1.0$
$\rho = 0.8$
$\rho = 0.6$
$\rho = 0.5$
$\rho = 0.4$
$\frac{\rho^2 J_L}{J_m}$
$\frac{\rho^2 f_L}{F_T} = \frac{1}{\frac{f_m}{\rho^2 f_L}+1}$

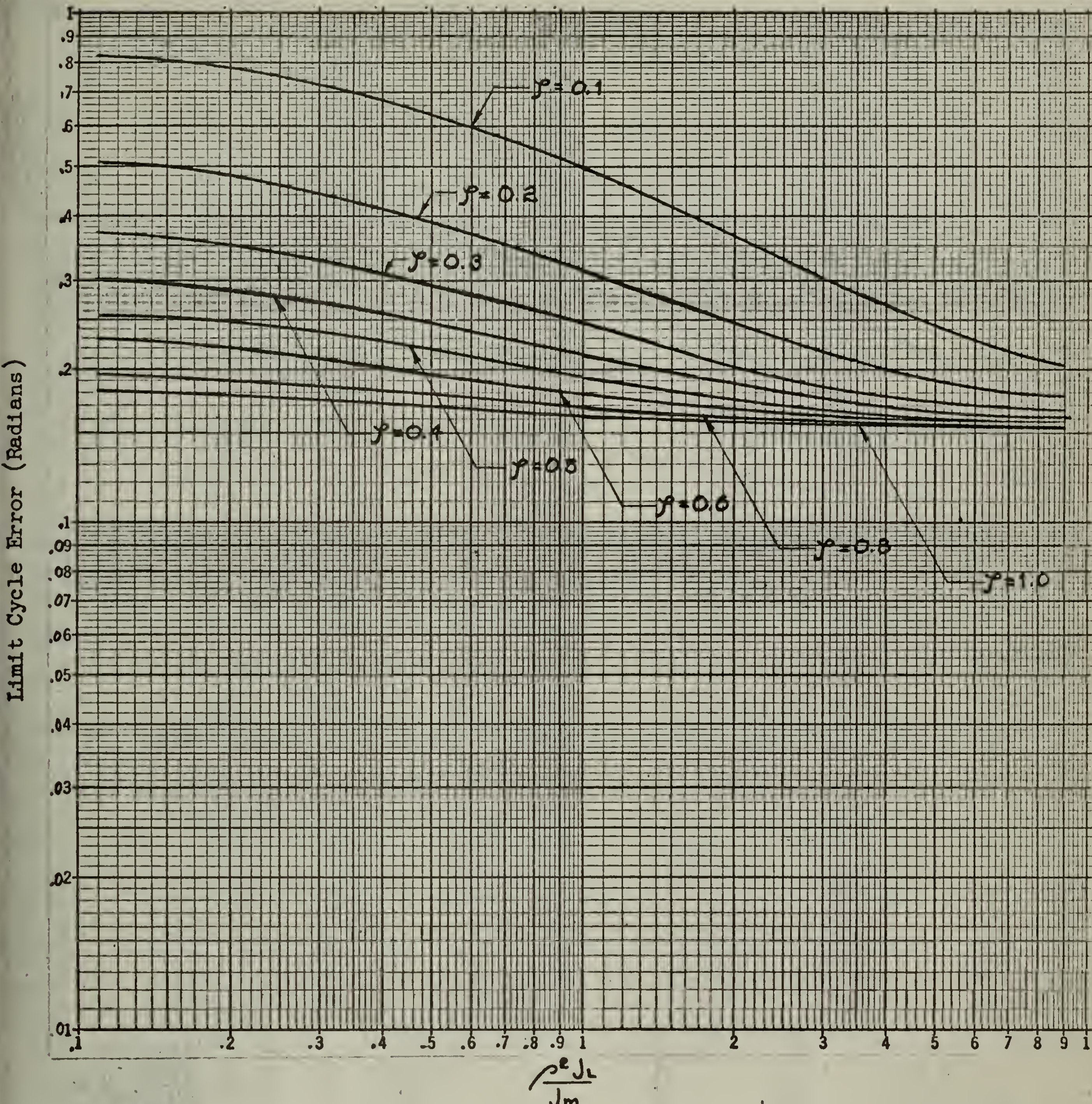

Fig. 3

Maximum Error of Limit Cycle from Unit Step Input

Limit Cycle Error (Radians) $\left(\frac{0.3}{\Delta}\right)$ for $\frac{\rho^2 J_L}{J_m}$ Variable

$$\frac{\rho^2 f_L}{F_T} = \frac{1}{\frac{f_m}{\rho^2 f_L} + 1} = 0$$

$$e = 0$$

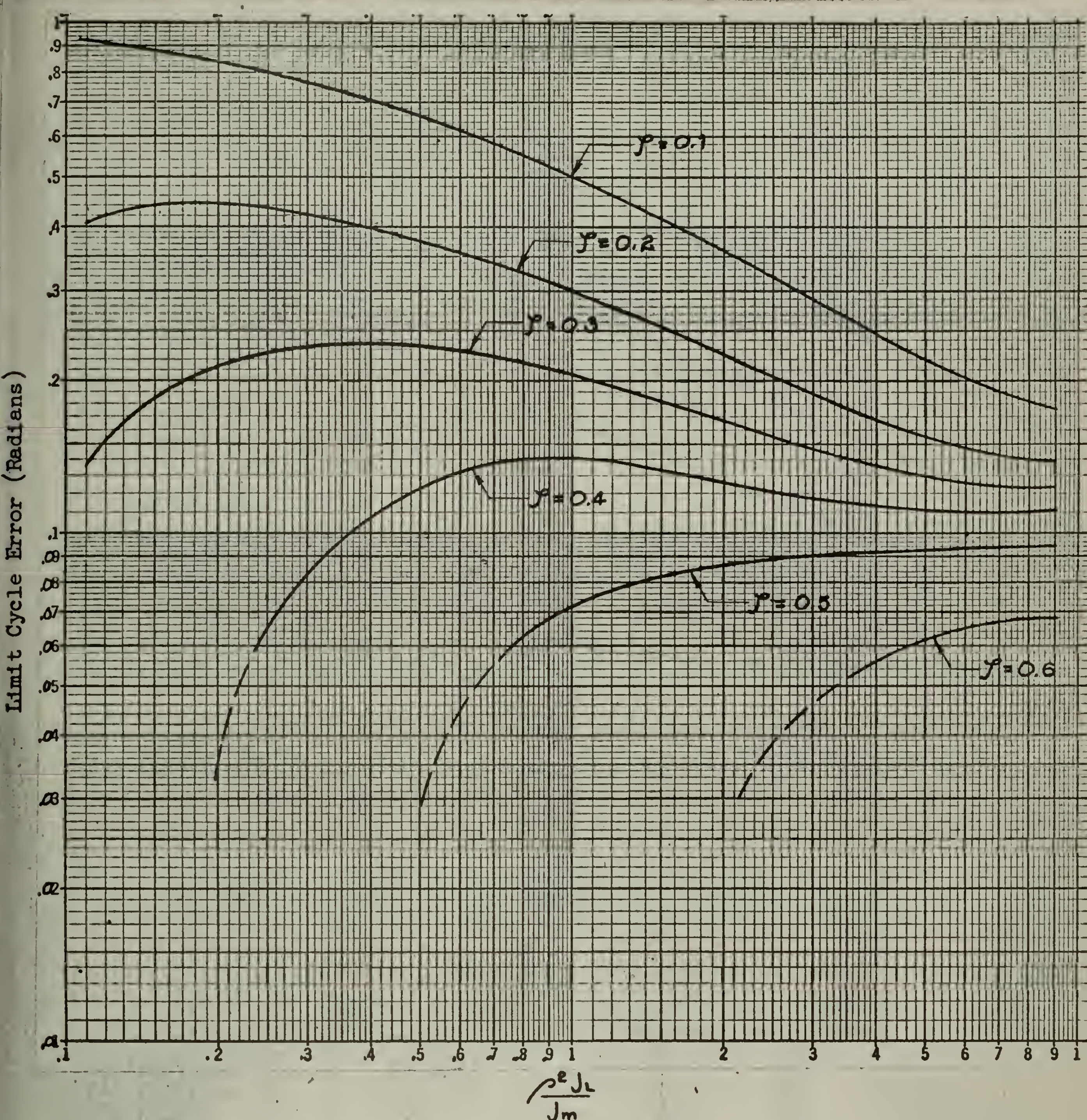

Fig. 4

Maximum Error of Limit Cycle from Unit Step Input

Limit Cycle Error (Radians) $\left(\frac{0.3}{\Delta}\right)$ for $\frac{\rho^2 J_L}{J_m}$ Variable

$$\frac{\rho^2 f_L}{F_T} = \frac{1}{\frac{f_m}{\rho^2 f_L} + 1} = 0.2$$

$$e = 0$$

No limit cycle exists for $\rho \geq 0.8$

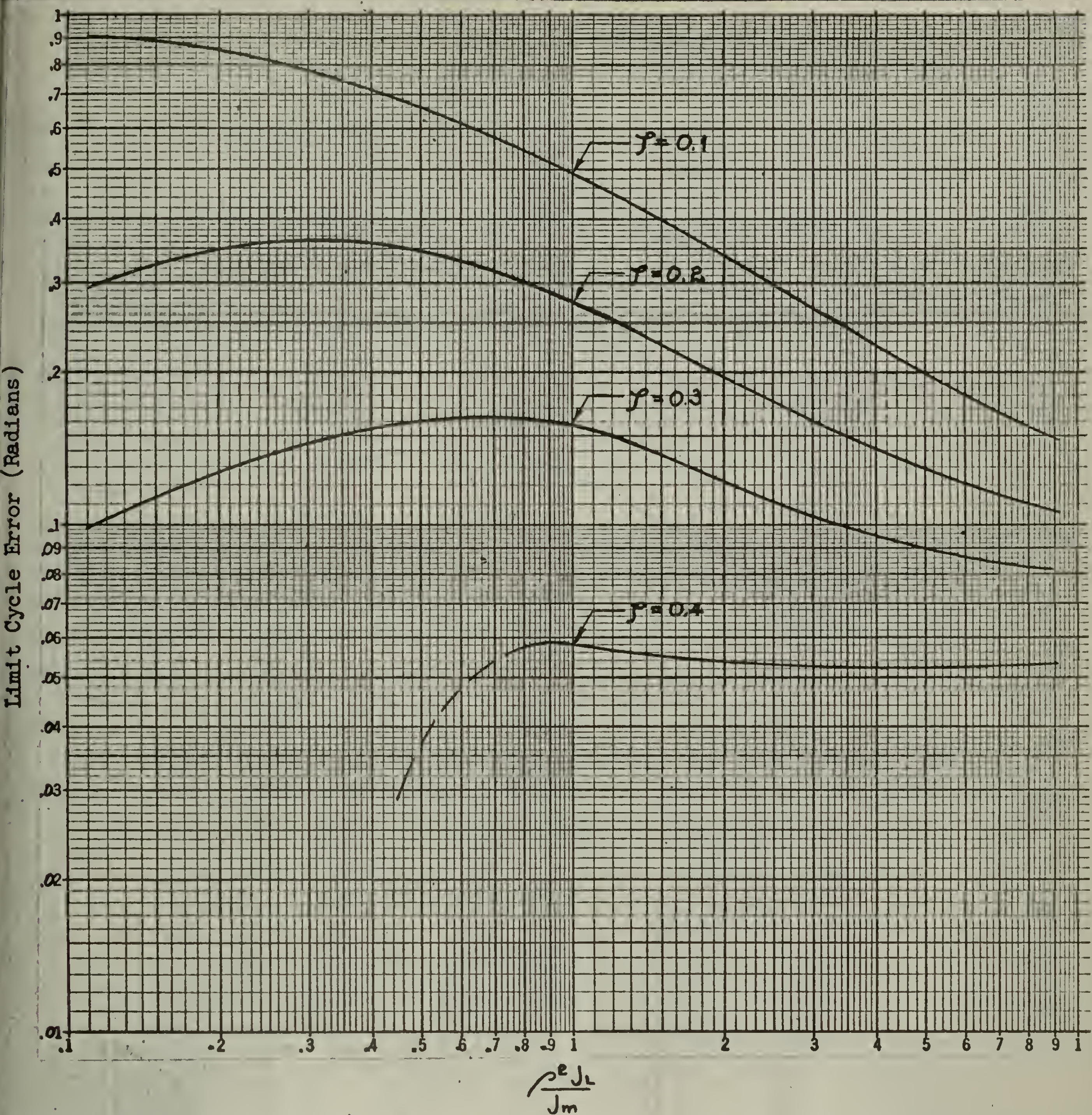

Fig. 5

Maximum Error of Limit Cycle from Unit Step Input

Limit Cycle Error (Radians) $\left(\frac{0.3}{\Delta}\right)$ for $\frac{\rho^2 J_L}{J_m}$ Variable

$$\frac{\rho^2 f_L}{F_T} = \frac{1}{\frac{f_m}{\rho^2 f_L} + 1} = 0.4$$

$$e = 0$$

No limit cycle exists for $\rho \geqslant 0.5$

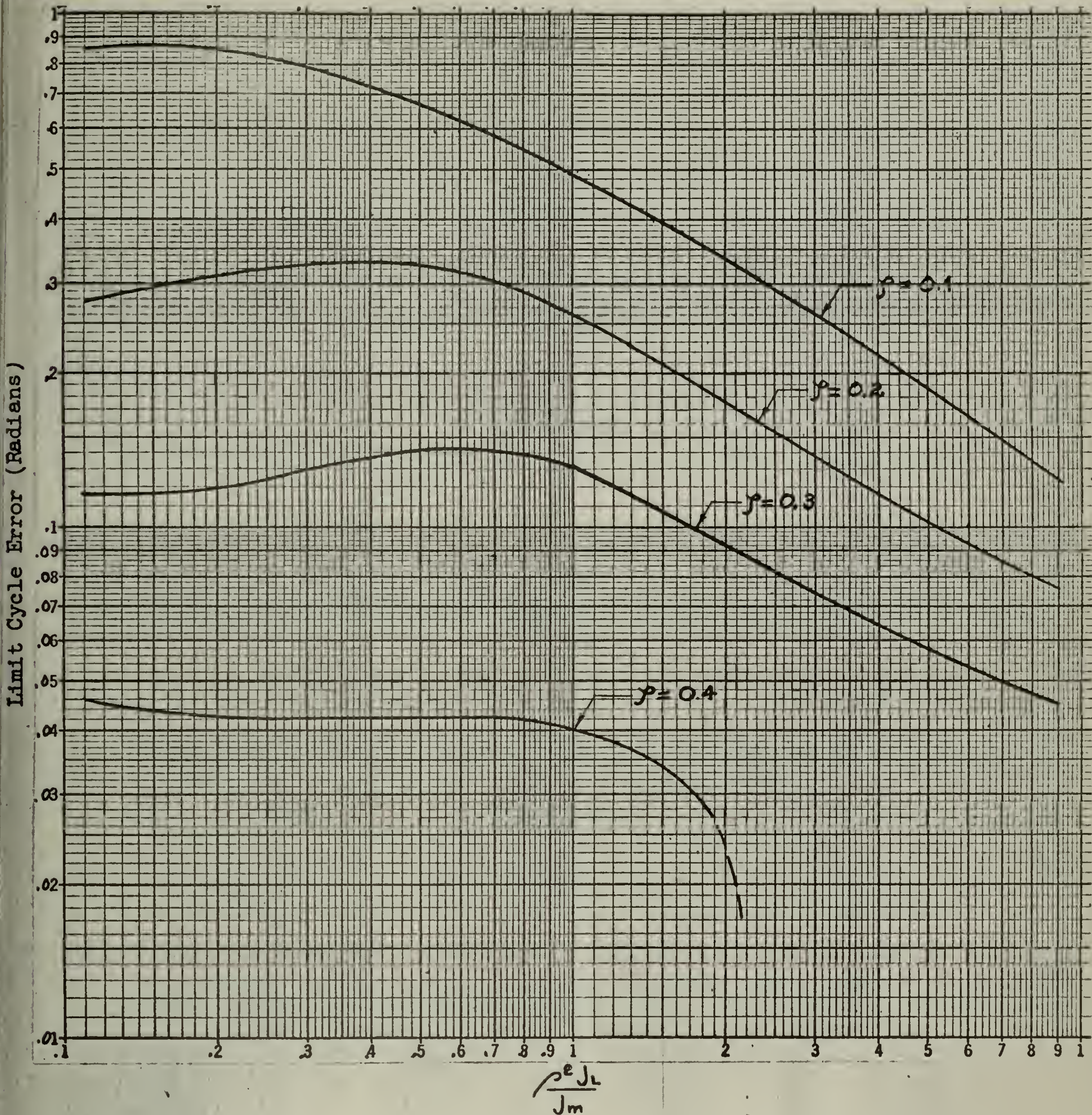

Fig. 6

Maximum Error of Limit Cycle from Unit Step Input

Limit Cycle Error (Radians) $\left(\frac{0.3}{\Delta}\right)$ for $\frac{\rho^2 J_L}{J_m}$ Variable

$$\frac{\rho^2 f_L}{F_T} = \frac{1}{\frac{f_m}{\rho^2 f_L} + 1} = 0.6$$

$$e = 0$$

No limit cycle exists for $\rho \geq 0.5$

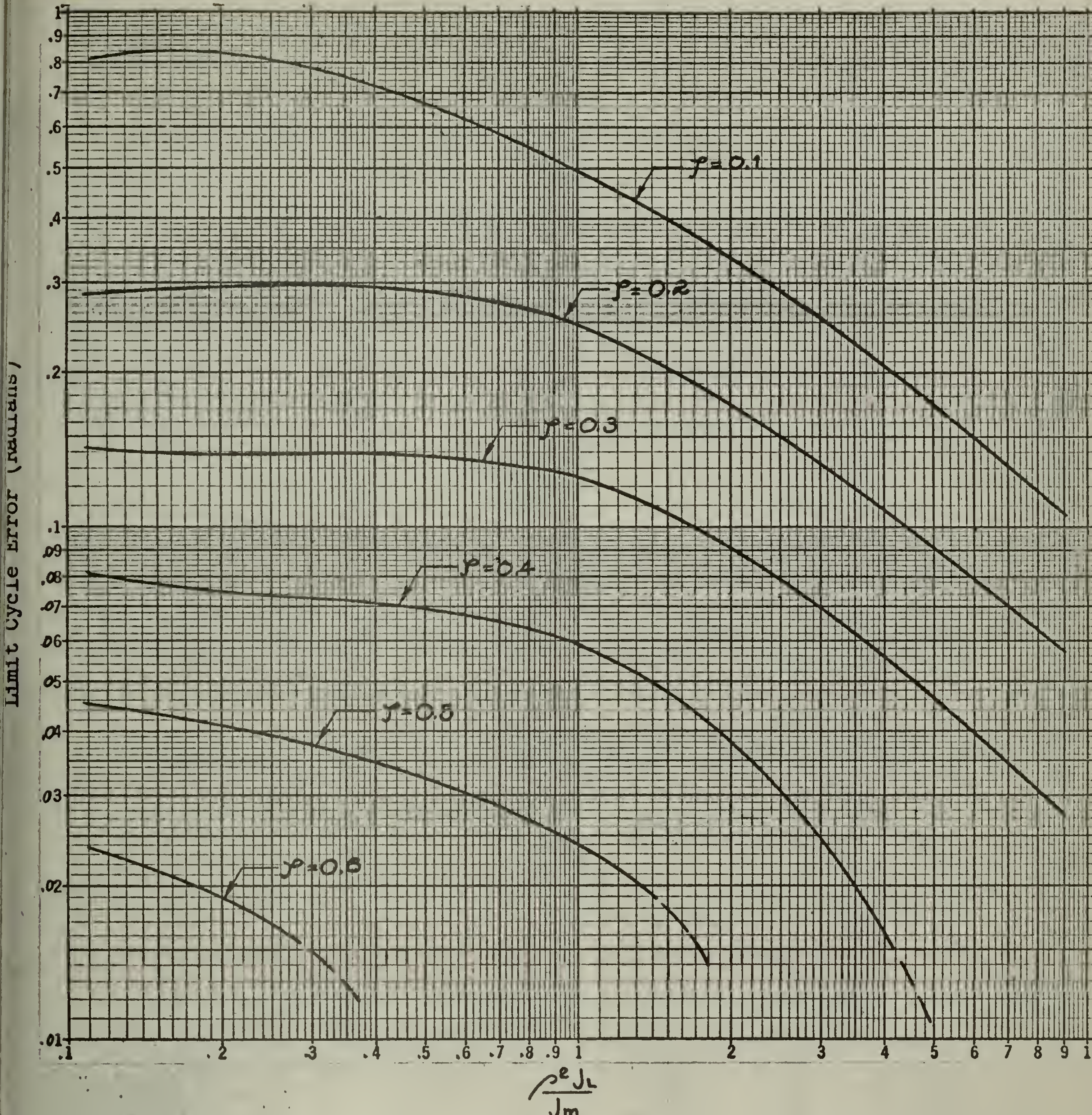

Fig. 7

Maximum Error of Limit Cycle from Unit Step Input

Limit Cycle Error (Radians) $\left(\frac{0.3}{\Delta}\right)$ for $\frac{\rho^2 J_L}{J_m}$ Variable

$$\frac{\rho^2 f_L}{F_T} = \frac{1}{\frac{f_m}{\rho^2 f_L} + 1} = 0.8$$

$$e = 0$$

No limit cycle exists for $\rho \geq 0.8$

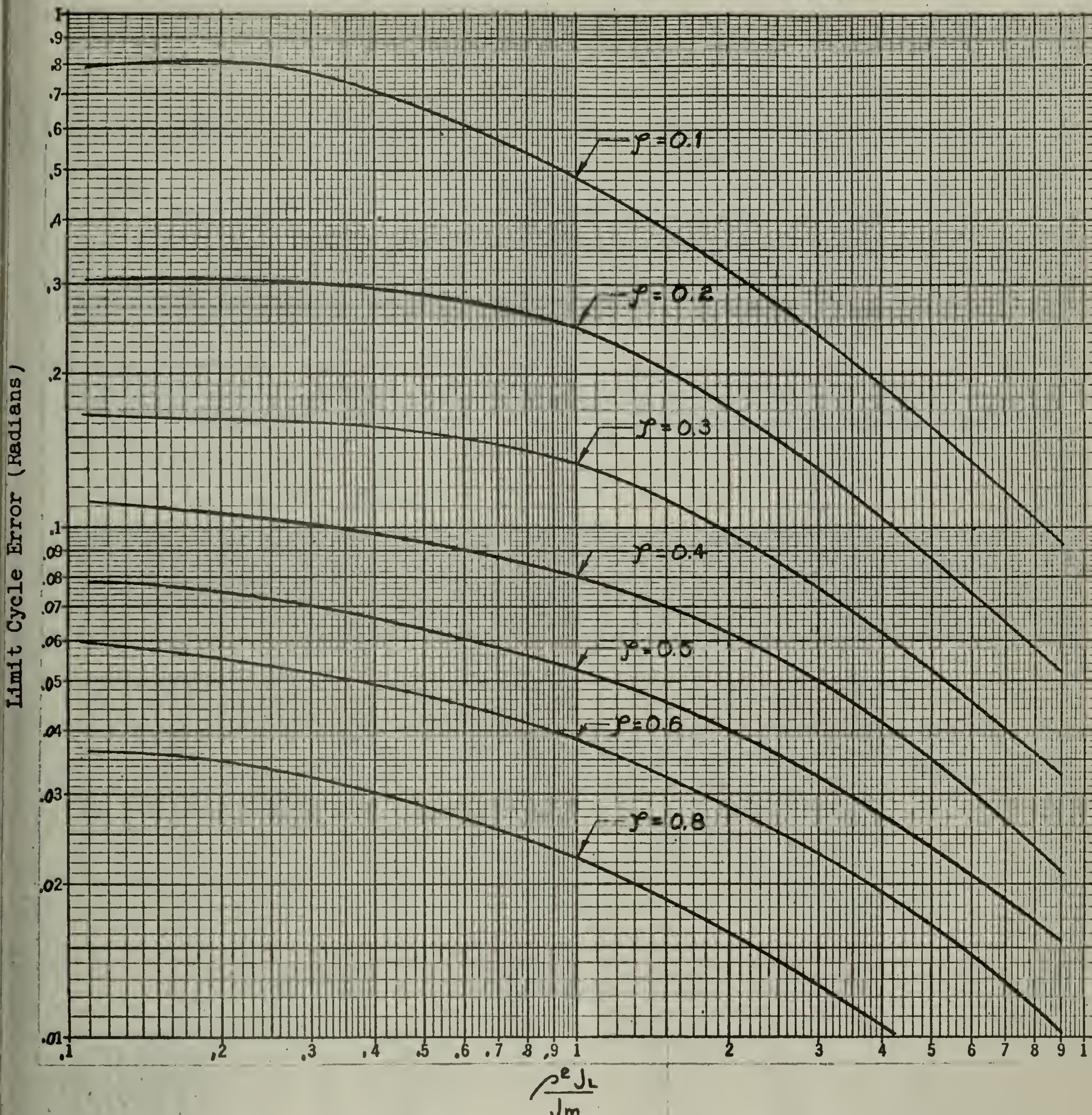

Fig. 8

Maximum Error of Limit Cycle from Unit Step Input

Limit Cycle Error (Radians) $\left(\frac{0.3}{\Delta}\right)$ for $\frac{\rho^2 J_L}{J_m}$ Variable

$$\frac{\rho^2 f_L}{F_T} = \frac{1}{\frac{f_m}{\rho^2 f_L} + 1} = 1.0$$

$e = 0$

No limit cycle exists for $\rho \geq 1.0$

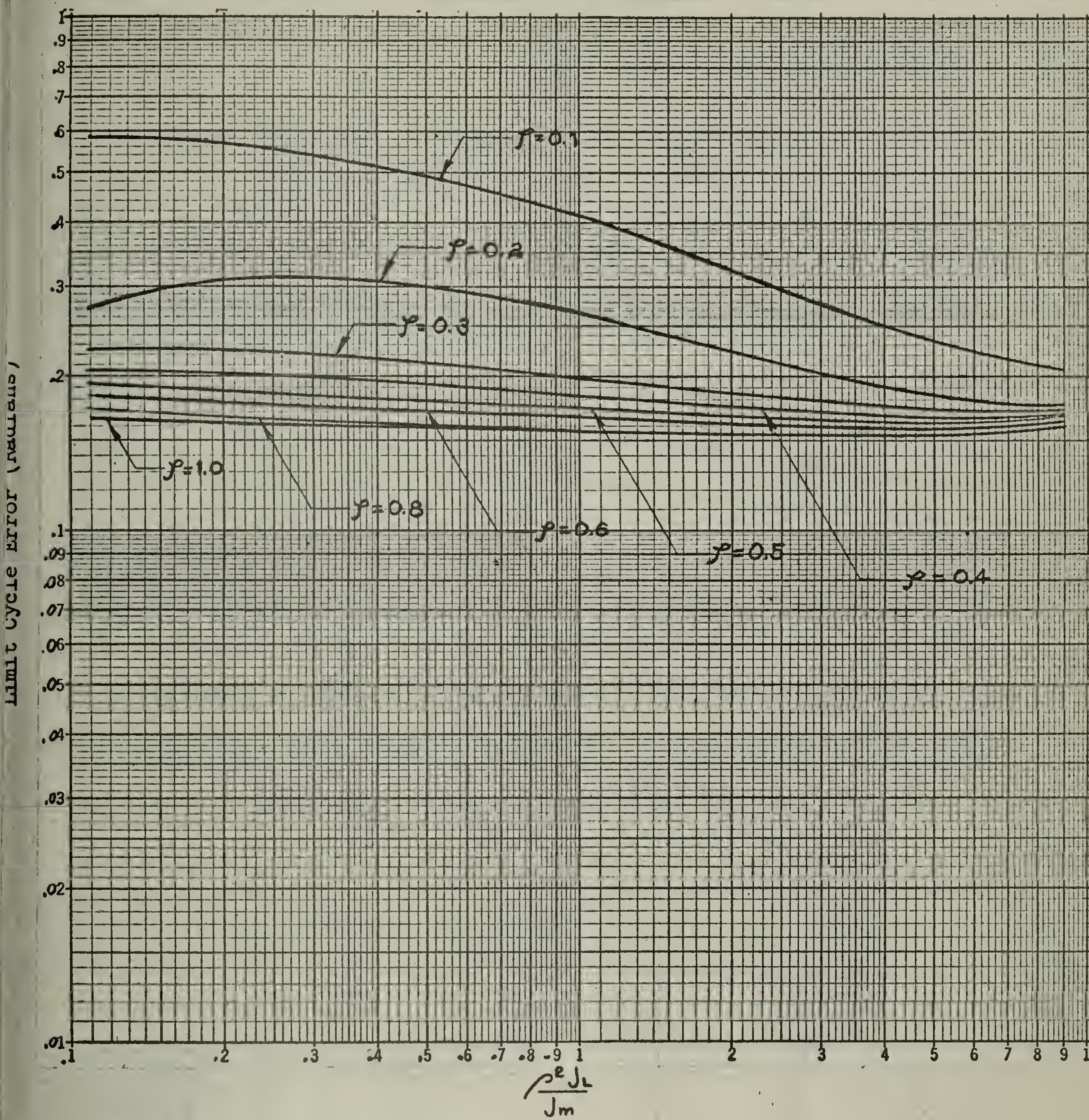

Fig. 9

Maximum Error of Limit Cycle from Unit Step Input

Limit Cycle Error (Radians) $\left(\frac{0.3}{\Delta}\right)$ for $\frac{\rho^2 J_L}{J_m}$ Variable

$$\frac{\rho^2 f_L}{F_T} = \frac{1}{\frac{f_m}{\rho^2 f_L} + 1} = 0$$

$$e = 0.6$$

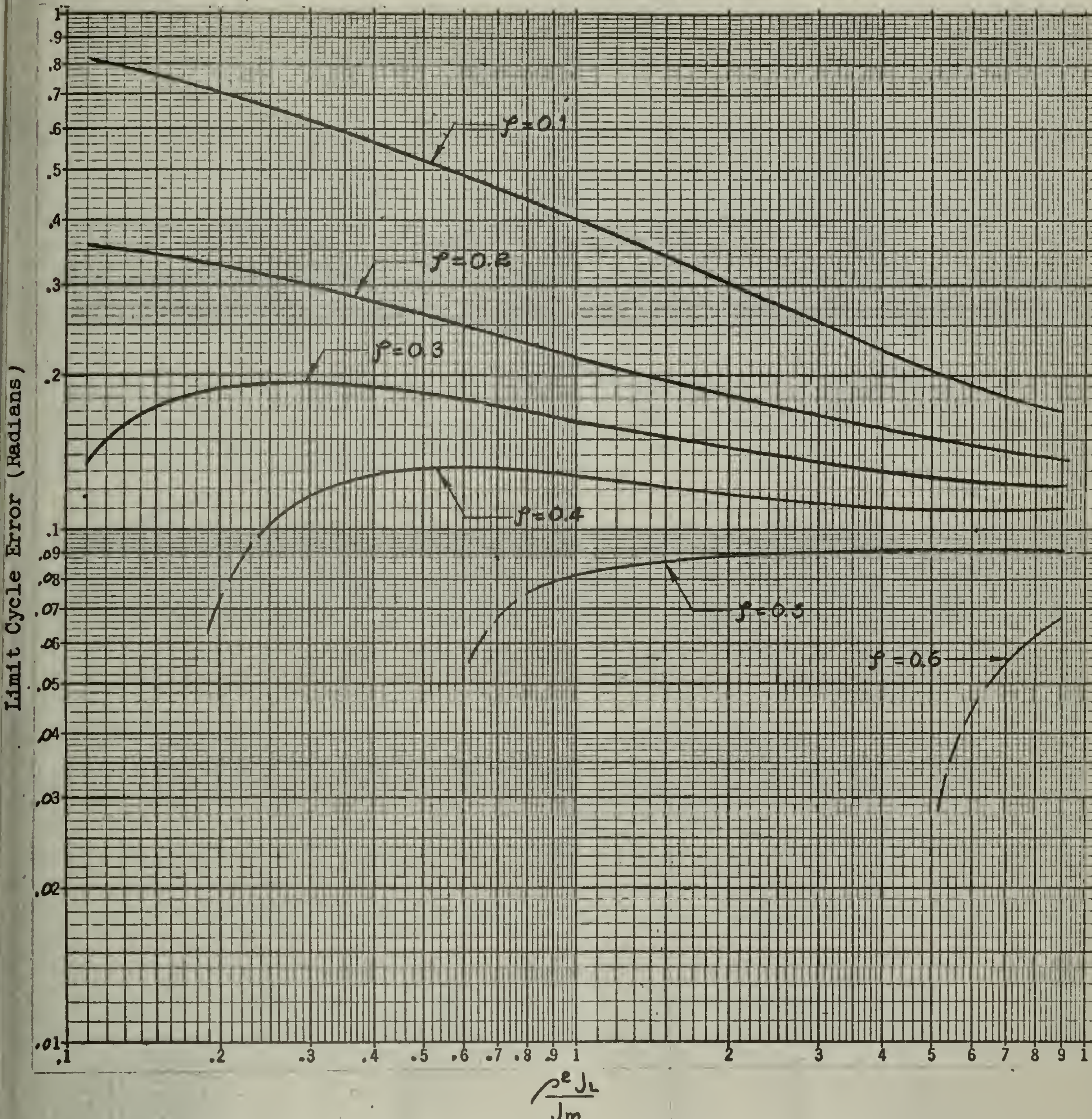

Fig. 10

Maximum Error of Limit Cycle from Unit Step Input

Limit Cycle Error (Radians) $\left(\frac{0.3}{\Delta}\right)$ for $\frac{\rho^2 J_L}{J_m}$ Variable

$$\frac{\rho^2 f_L}{F_T} = \frac{1}{\frac{f_m}{\rho^2 f_L} + 1} = 0.2$$

$$e = 0.6$$

No limit cycle exists for $\rho \geq 0.8$

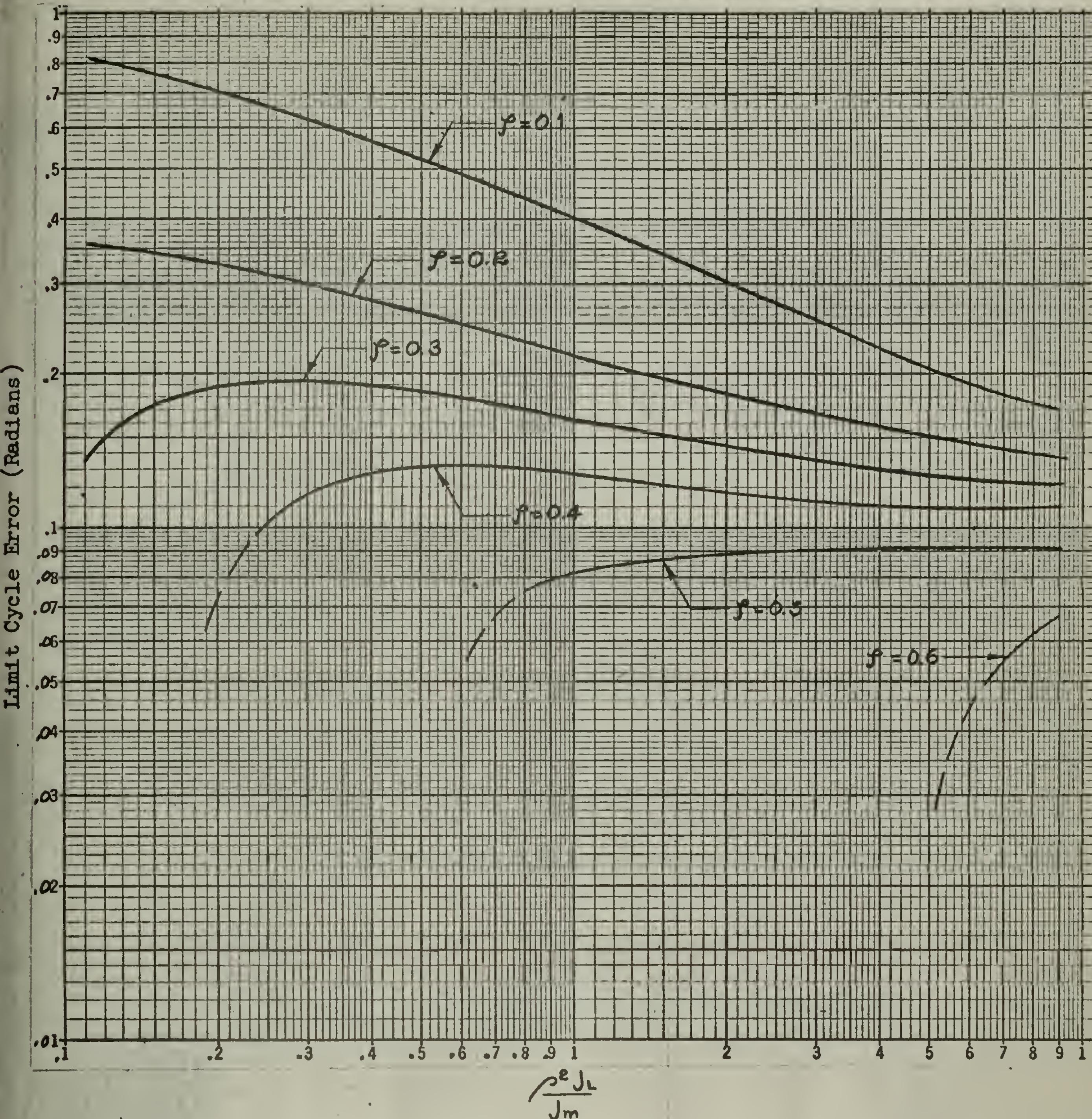

Fig. 10

Maximum Error of Limit Cycle from Unit Step Input

Limit Cycle Error (Radians) $\left(\frac{0.3}{\Delta}\right)$ for $\frac{\rho^2 J_L}{J_m}$ Variable

$$\frac{\rho^2 f_L}{F_T} = \frac{1}{\frac{f_m}{\rho^2 f_L} + 1} = 0.2$$

$$e = 0.6$$

No limit cycle exists for $\rho \geq 0.8$

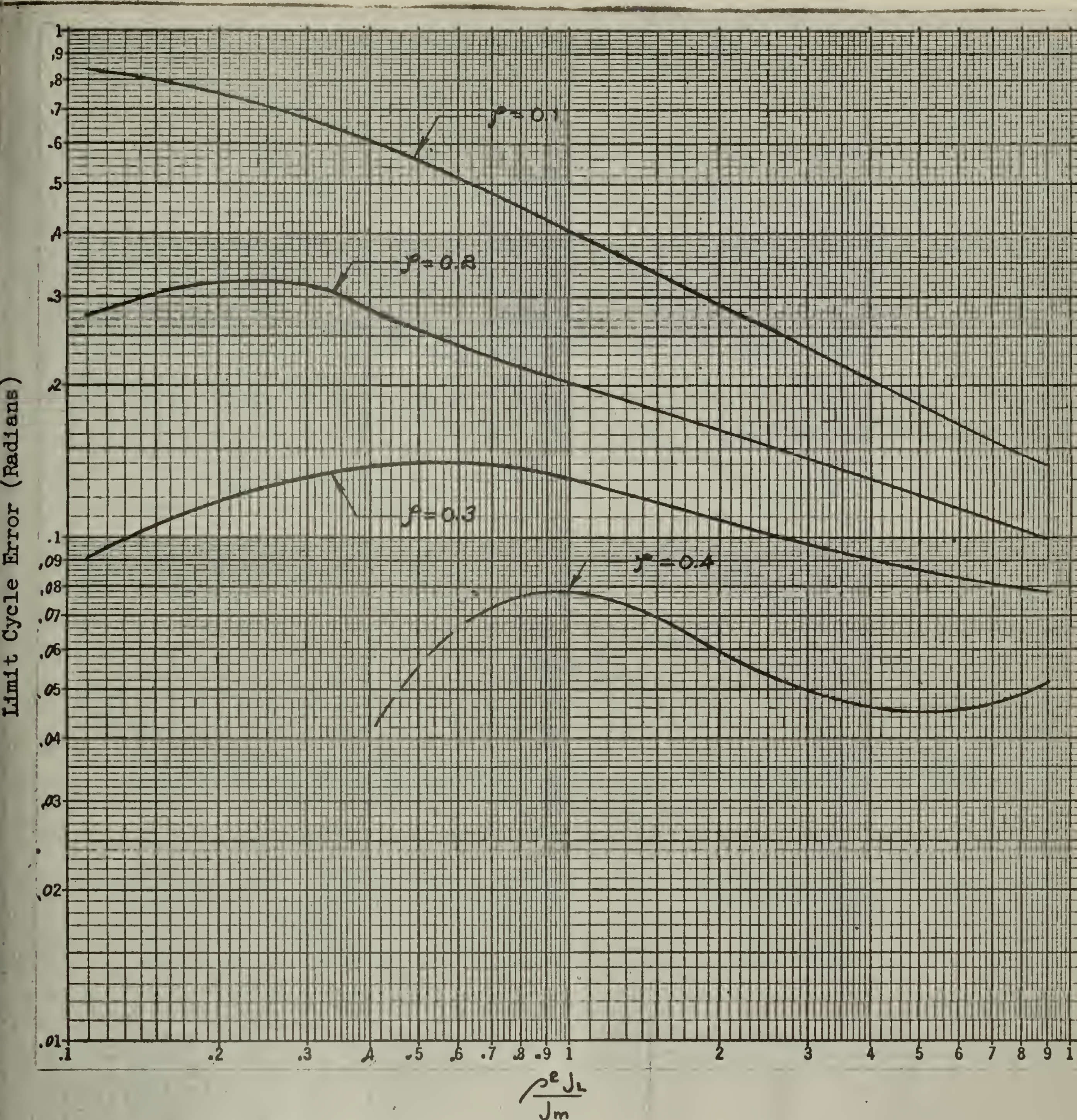

Fig. 11

Maximum Error of Limit Cycle from Unit Step Input

Limit Cycle Error (Radians) $\left(\frac{0.3}{\Delta}\right)$ for $\frac{\rho^2 J_L}{J_m}$ Variable

$$\frac{\rho^2 f_L}{F_T} = \frac{1}{\frac{f_m}{\rho^2 f_L} + 1} = 0.4$$

$$e = 0.6$$

No limit cycle exists for $\rho \geq 0.5$

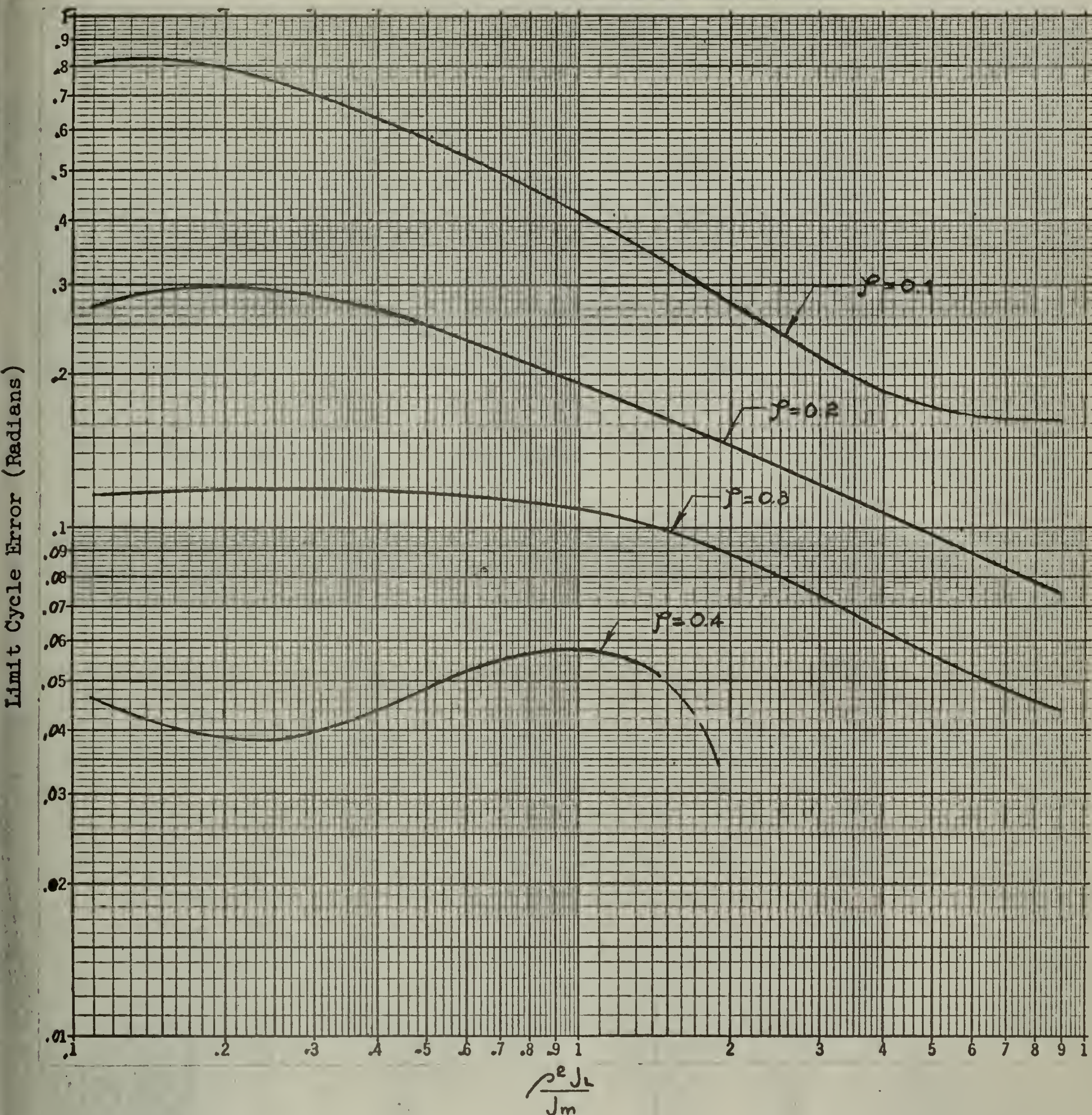

Fig. 12

Maximum Error of Limit Cycle from Unit Step Input

Limit Cycle Error (Radians) $\left(\frac{0.3}{\Delta}\right)$ for $\frac{\rho^2 J_L}{J_m}$ Variable

$$\frac{\rho^2 f_L}{F_T} = \frac{1}{\frac{f_m}{\rho^2 f_L}+1} = 0.6$$

$e = 0.6$

No limit cycle exists for $\rho \geq 0.5$

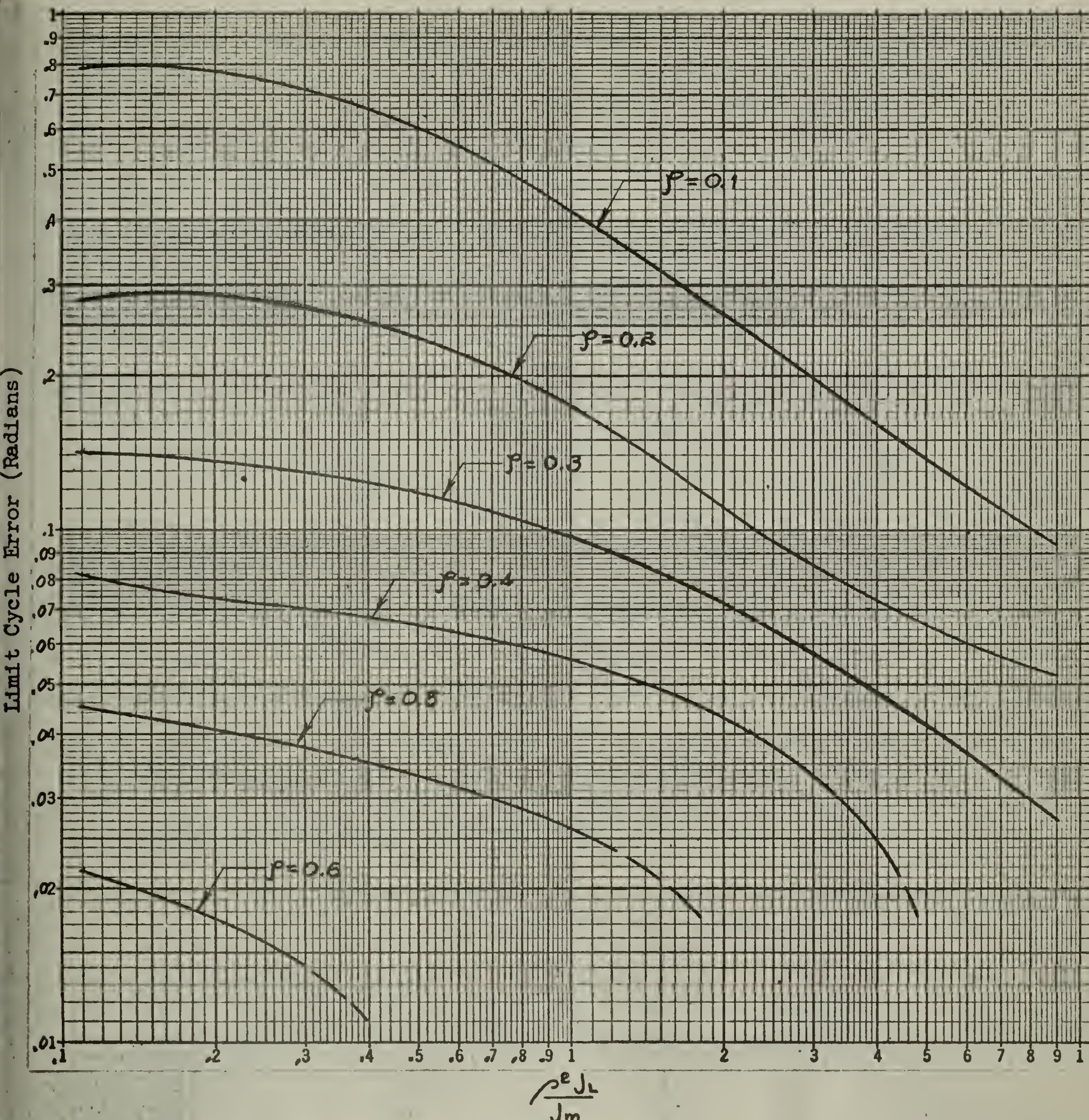

Fig. 13

Maximum Error of Limit Cycle from Unit Step Input

Limit Cycle Error (Radians) $\left(\frac{0.3}{\Delta}\right)$ for $\frac{\rho^2 J_L}{J_m}$ Variable

$$\frac{\rho^2 f_L}{F_T} = \frac{1}{\frac{f_m}{\rho^2 f_L} + 1} = 0.8$$

$$e = 0.6$$

No limit cycle exists for $\rho \geq 0.8$

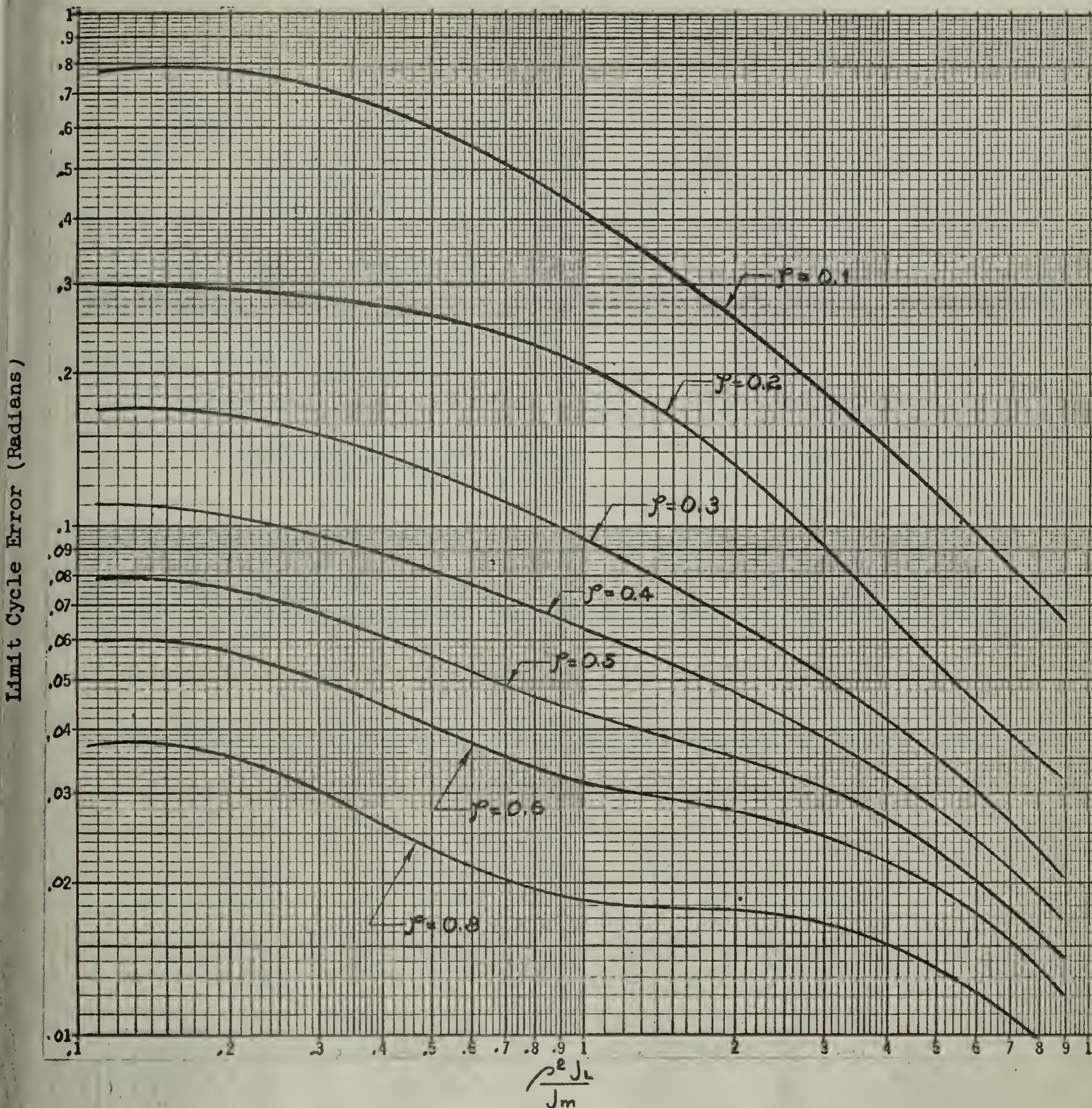

Fig. 14

Maximum Error of Limit Cycle from Unit Step Input

Limit Cycle Error (Radians) $\left(\frac{0.3}{\Delta}\right)$ for $\frac{\rho^2 J_L}{J_m}$ Variable

$$\frac{\rho^2 f_L}{F_T} = \frac{1}{\frac{f_m}{\rho^2 f_L} + 1} = 1.0$$

$$e = 0.6$$

No limit cycle exists for $\rho \geq 1.0$

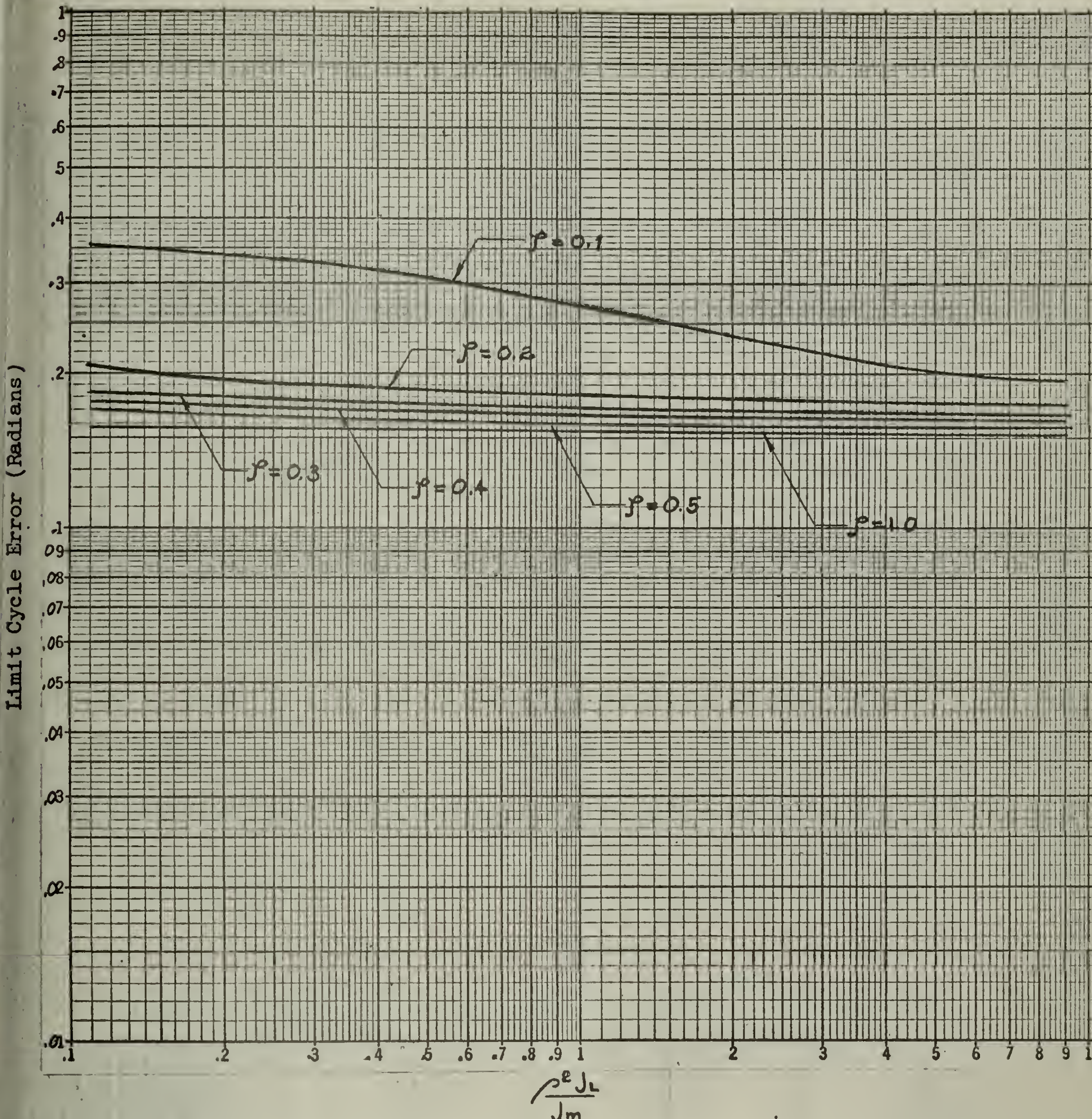

Fig. 15

Maximum Error of Limit Cycle from Unit Step Input

Limit Cycle Error (Radians) $\left(\frac{0.3}{\Delta}\right)$ for $\frac{\rho^2 J_L}{J_m}$ Variable

$$\frac{\rho^2 f_L}{F_T} = \frac{1}{\frac{f_m}{\rho^2 f_L} + 1} = 0$$

$$e = 0.8$$

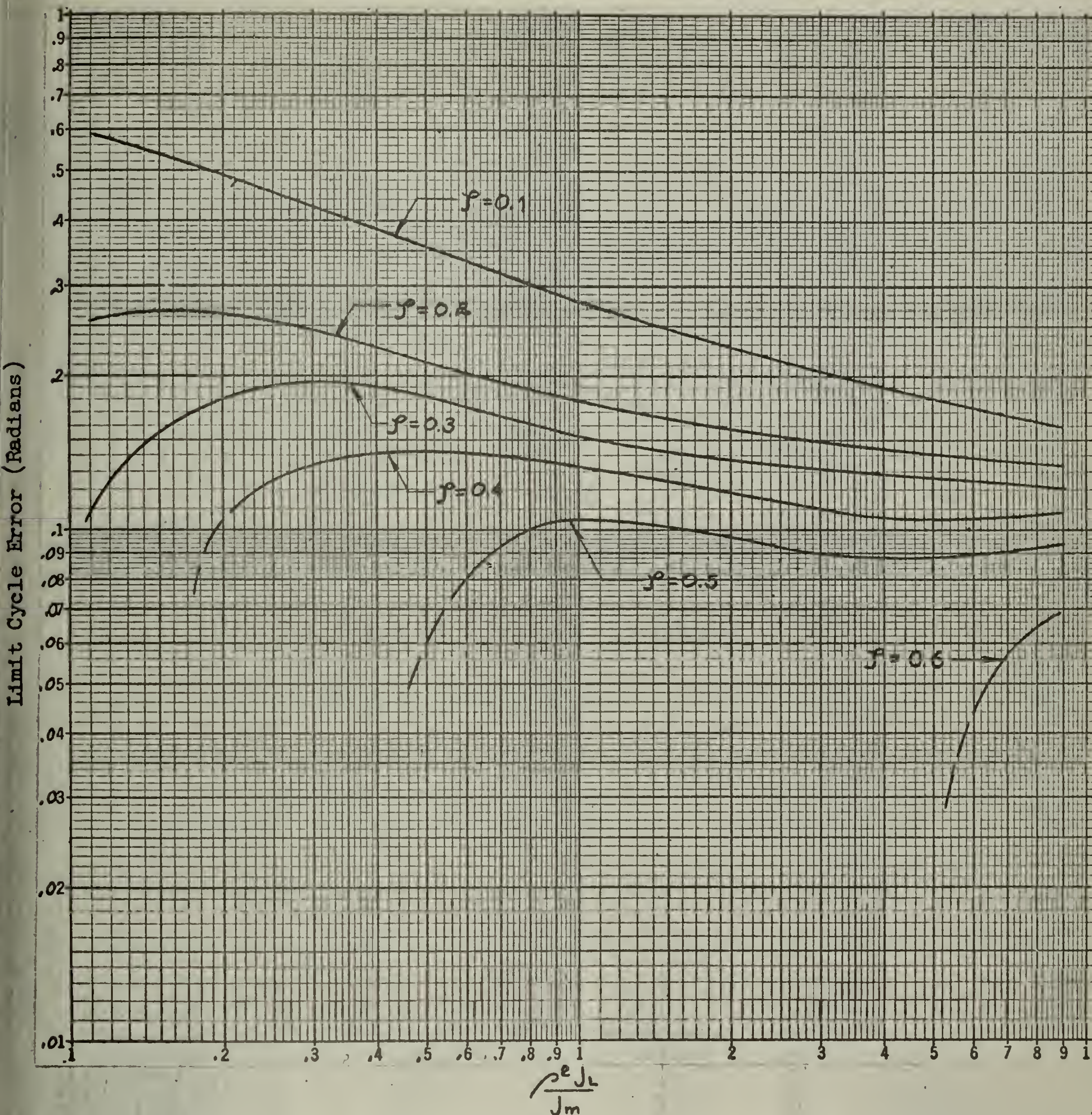

Fig. 16

Maximum Error of Limit Cycle from Unit Step Input

Limit Cycle Error (Radians) $\left(\frac{0.3}{\Delta}\right)$ for $\frac{\rho^2 J_L}{J_m}$ Variable

$$\frac{\rho^2 f_L}{F_T} = \frac{1}{\frac{f_m}{\rho^2 f_L} + 1} = 0.2$$

$$e = 0.8$$

No limit cycle exists for $\rho \geq 0.8$

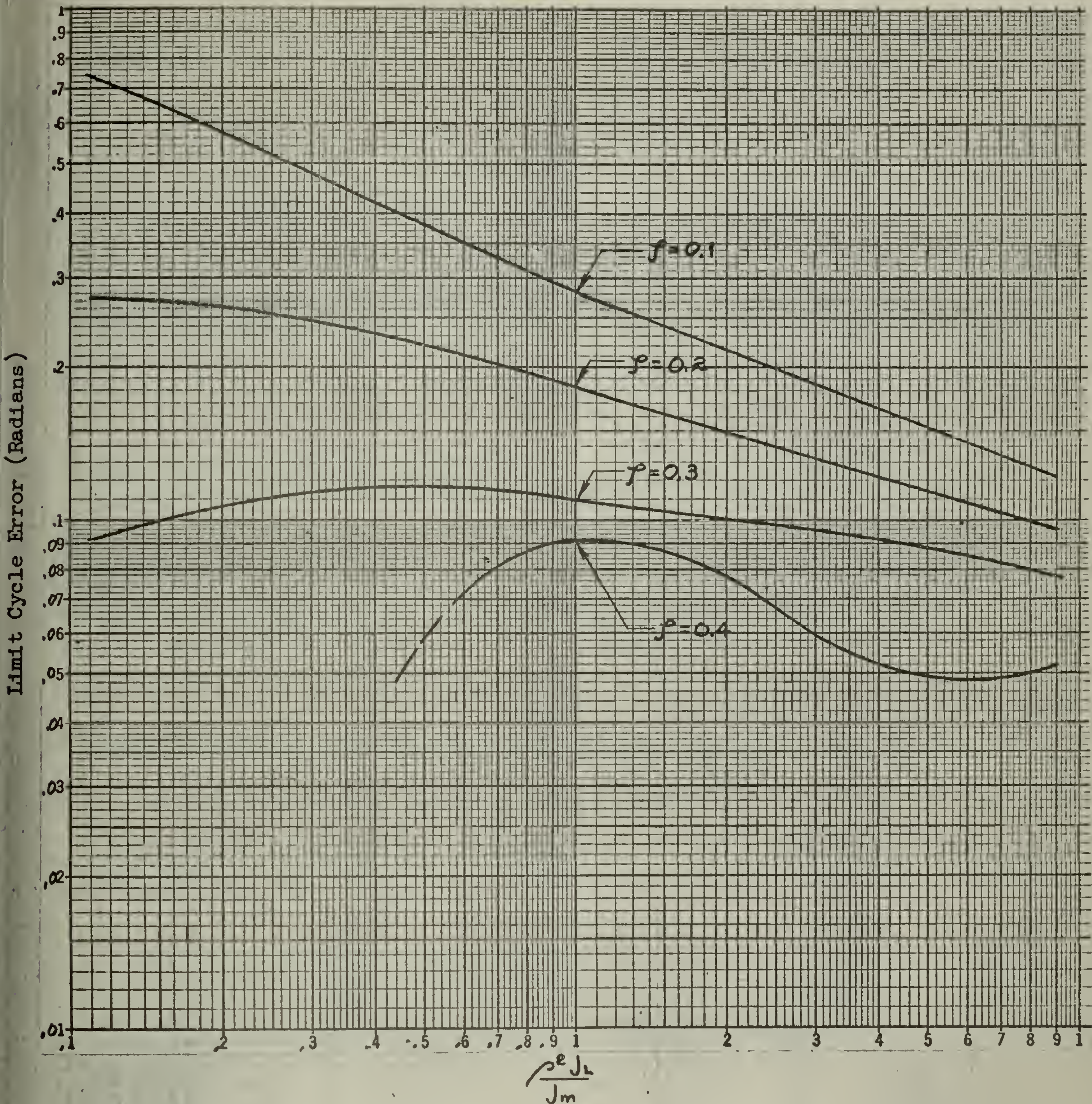

Fig. 17

Maximum Error of Limit Cycle from Unit Step Input

Limit Cycle Error (Radians) $\left(\frac{0.3}{\Delta}\right)$ for $\frac{\rho^2 J_L}{J_m}$ Variable

$$\frac{\rho^2 f_L}{F_T} = \frac{1}{\frac{f_m}{\rho^2 f_L} + 1} = 0.4$$

$$e = 0.8$$

No limit cycle exists for $\rho \geq 0.5$

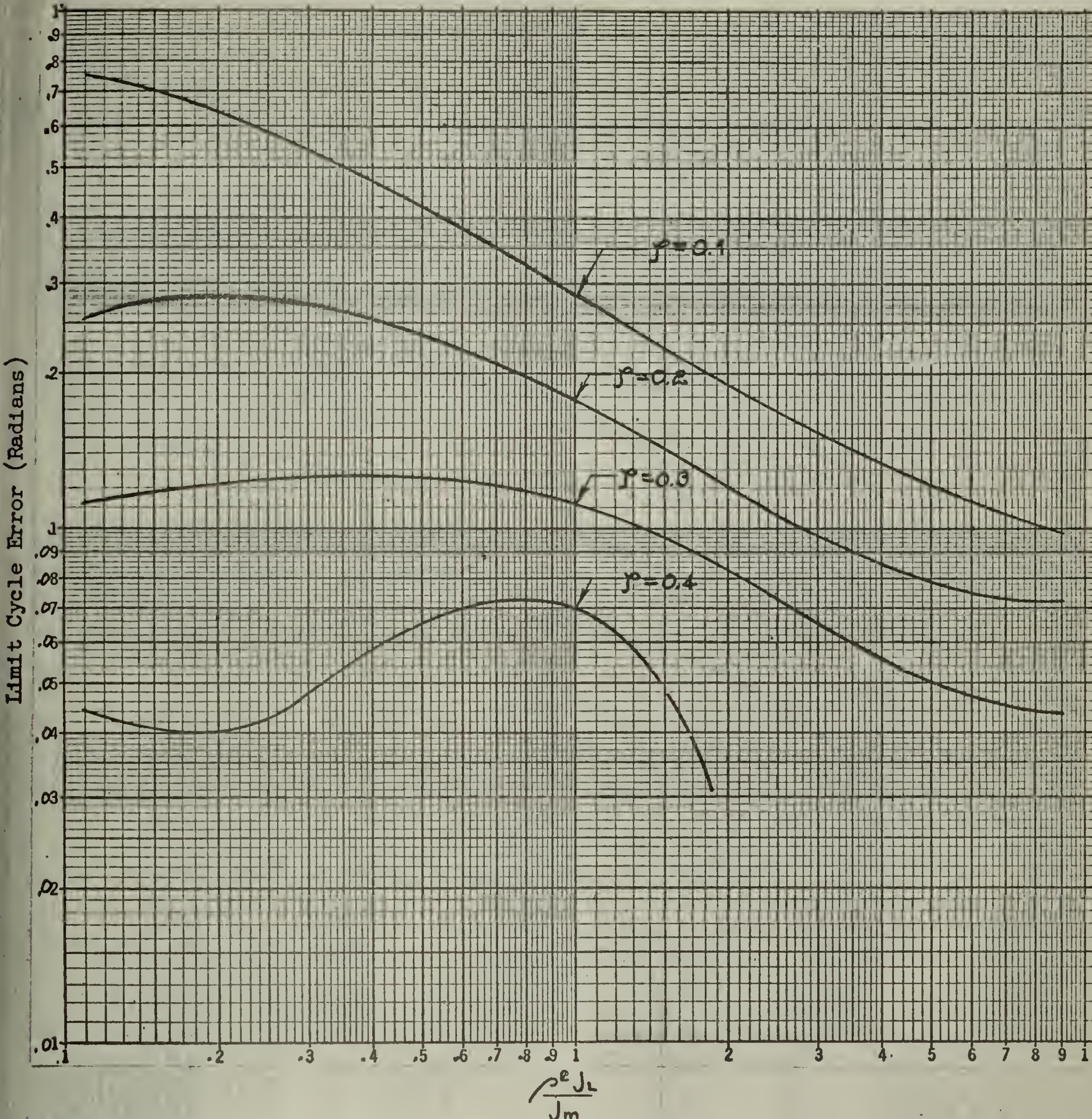

Fig. 18

Maximum Error of Limit Cycle from Unit Step Input

Limit Cycle Error (Radians) $\left(\frac{0.3}{\Delta}\right)$ for $\frac{\rho^2 J_L}{J_m}$ Variable

$$\frac{\rho^2 f_L}{F_T} = \frac{1}{\frac{f_m}{\rho^2 f_L} + 1} = 0.6$$

$$e = 0.8$$

No limit cycle exists for $\gamma \geq 0.5$

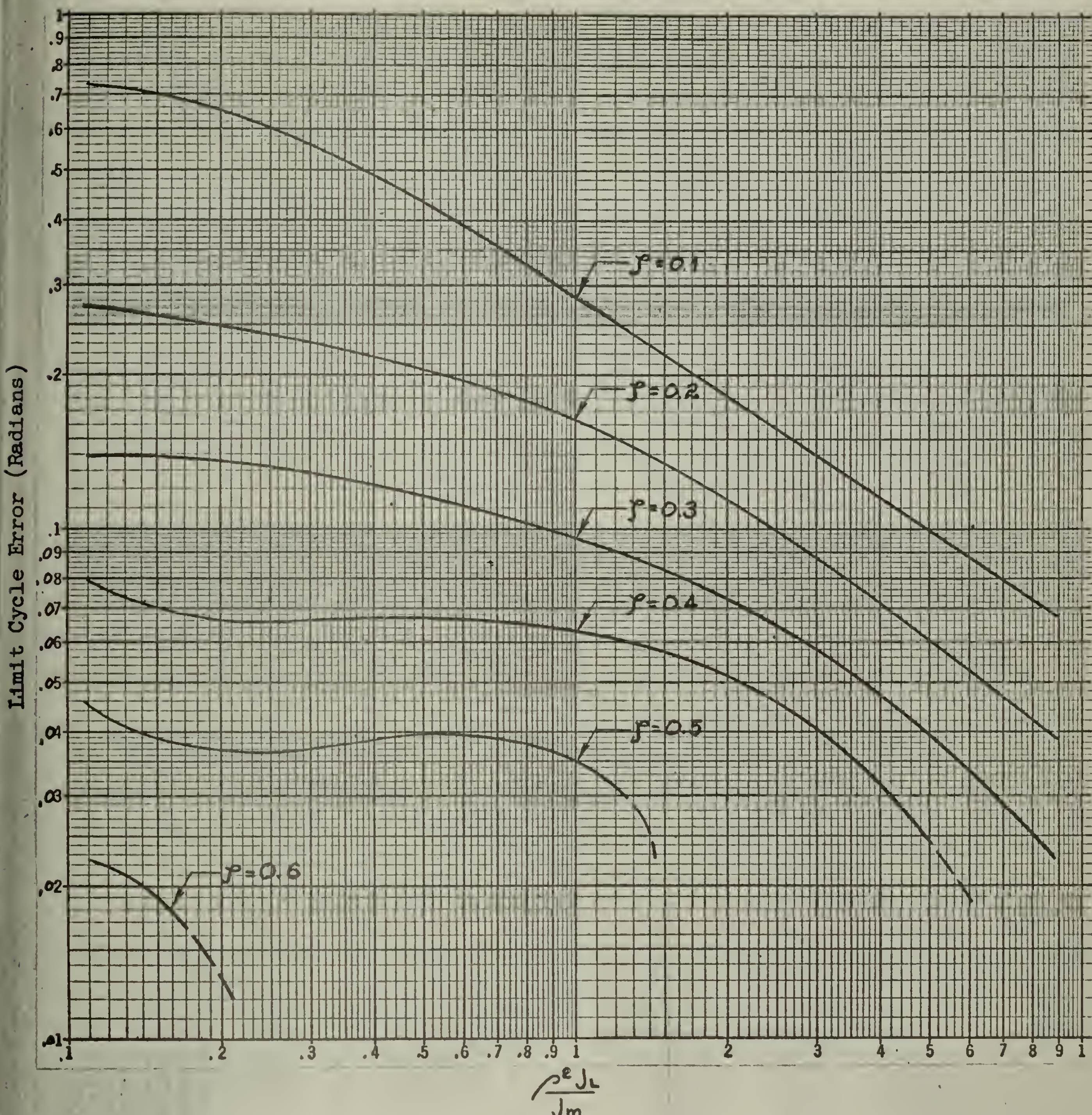

Fig. 19

Maximum Error of Limit Cycle from Unit Step Input

Limit Cycle Error (Radians) $\left(\frac{0.3}{\Delta}\right)$ for $\frac{\rho^2 J_L}{J_m}$ Variable

$$\frac{\rho^2 f_L}{F_T} = \frac{1}{\frac{f_m}{\rho^2 f_L} + 1} = 0.8$$

$$e = 0.8$$

No limit cycle exists for $\rho \geq 0.8$

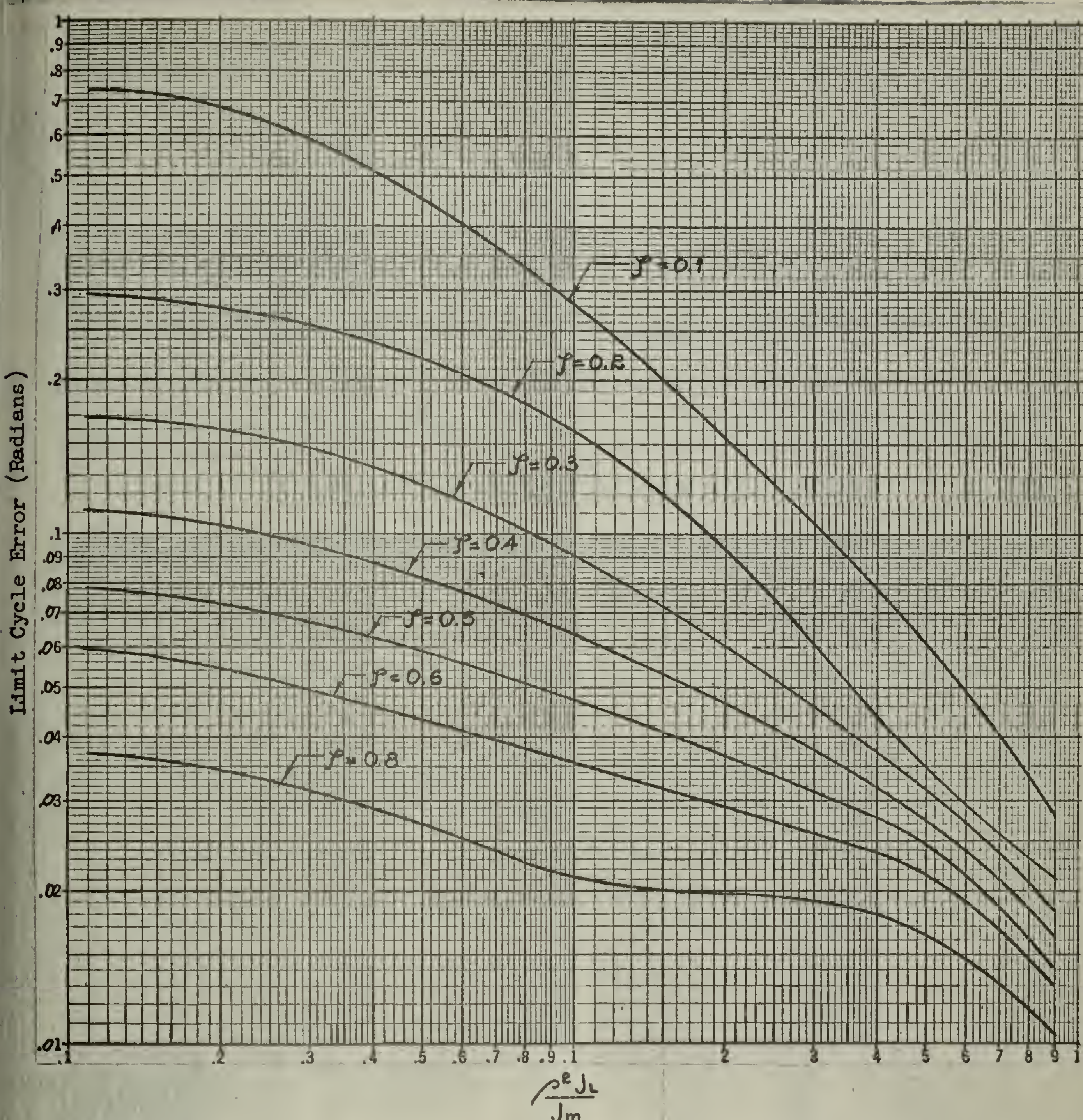

Fig. 20

Maximum Error of Limit Cycle from Unit Step Input

Limit Cycle Error (Radians) $\left(\frac{0.3}{\Delta}\right)$ for $\frac{\rho^2 J_L}{J_m}$ Variable

$$\frac{\rho^2 f_L}{F_T} = \frac{1}{\frac{f_m}{\rho^2 f_L} + 1} = 1.0$$

$$e = 0.8$$

No limit cycle exists for $\zeta \geq 1.0$

[illegible]

[illegible]

[illegible]

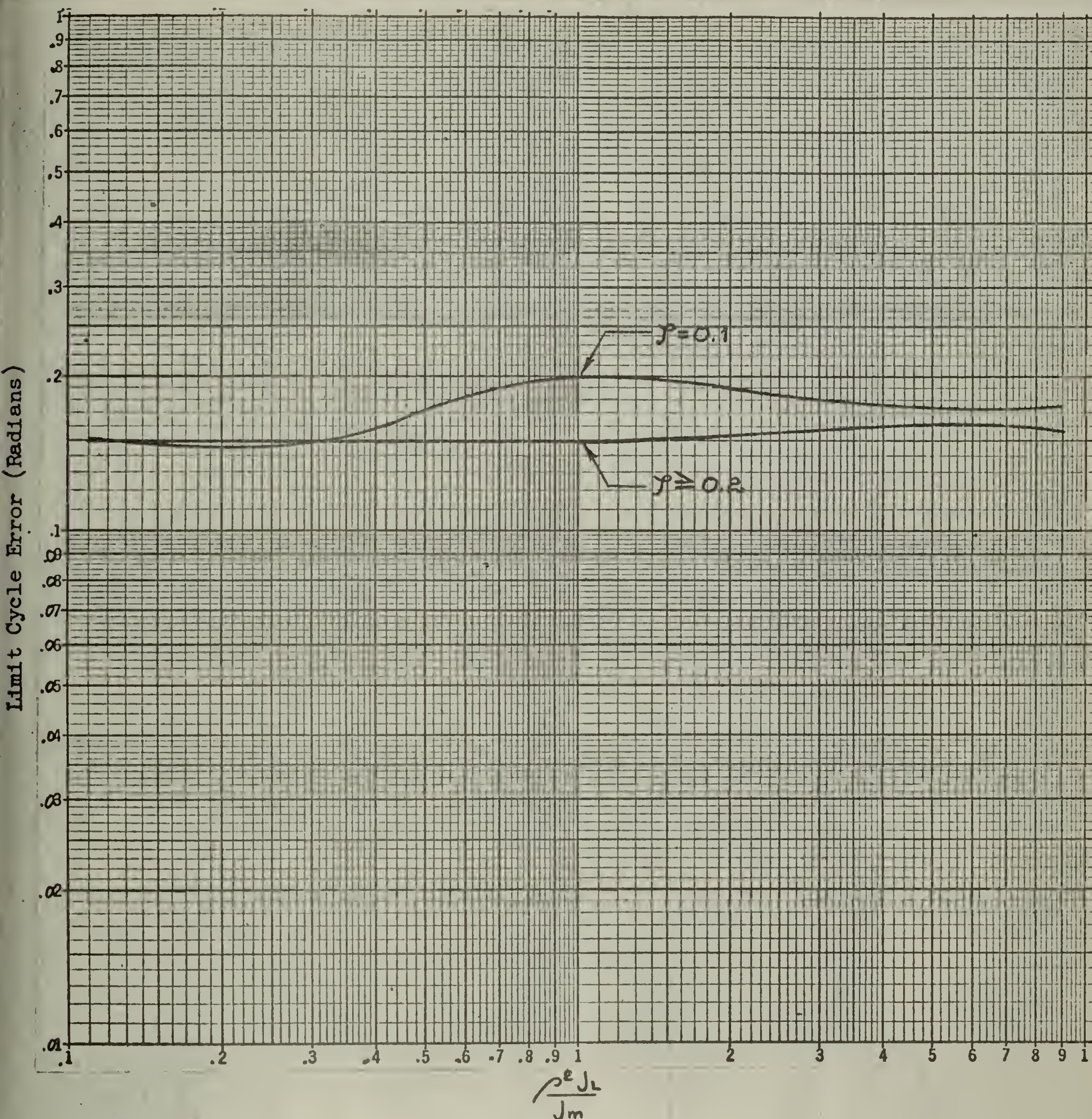

Fig. 21

Maximum Error of Limit Cycle from Unit Step Input

Limit Cycle Error (Radians) $\left(\frac{0.3}{\Delta}\right)$ for $\frac{\rho^2 J_L}{J_m}$ Variable

$$\frac{\rho^2 f_L}{F_T} = \frac{1}{\frac{f_m}{\rho^2 f_L} + 1} = 0$$

$$e = 1.0$$

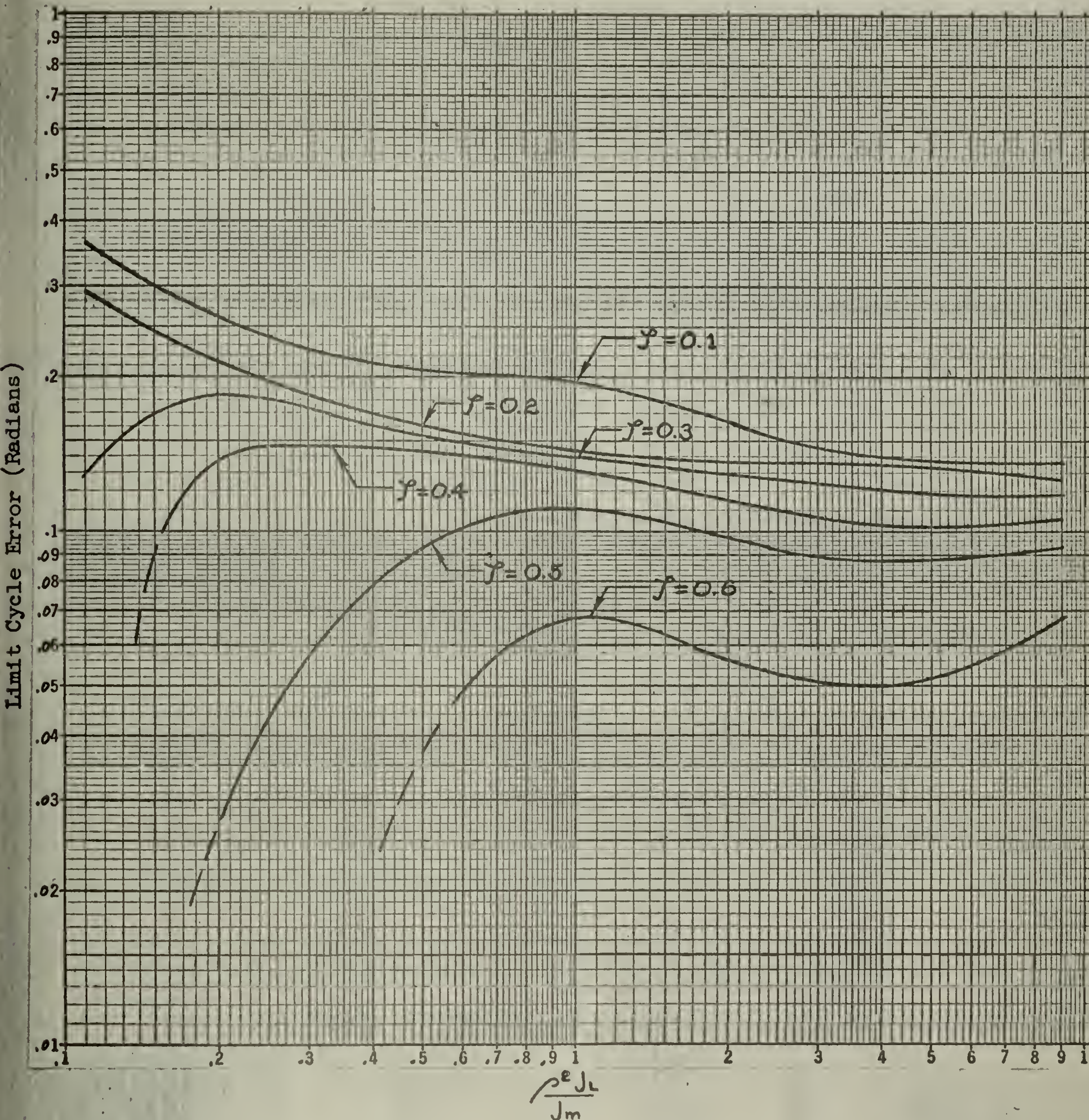

Fig. 22

Maximum Error of Limit Cycle from Unit Step Input

Limit Cycle Error (Radians) $\left(\frac{0.3}{\Delta}\right)$ for $\frac{\rho^2 J_L}{J_m}$ Variable

$$\frac{\rho^2 f_L}{F_T} = \frac{1}{\frac{f_m}{\rho^2 f_L} + 1} = 0.2$$

$$e = 1.0$$

No limit cycle exists for $\rho \geq 0.8$

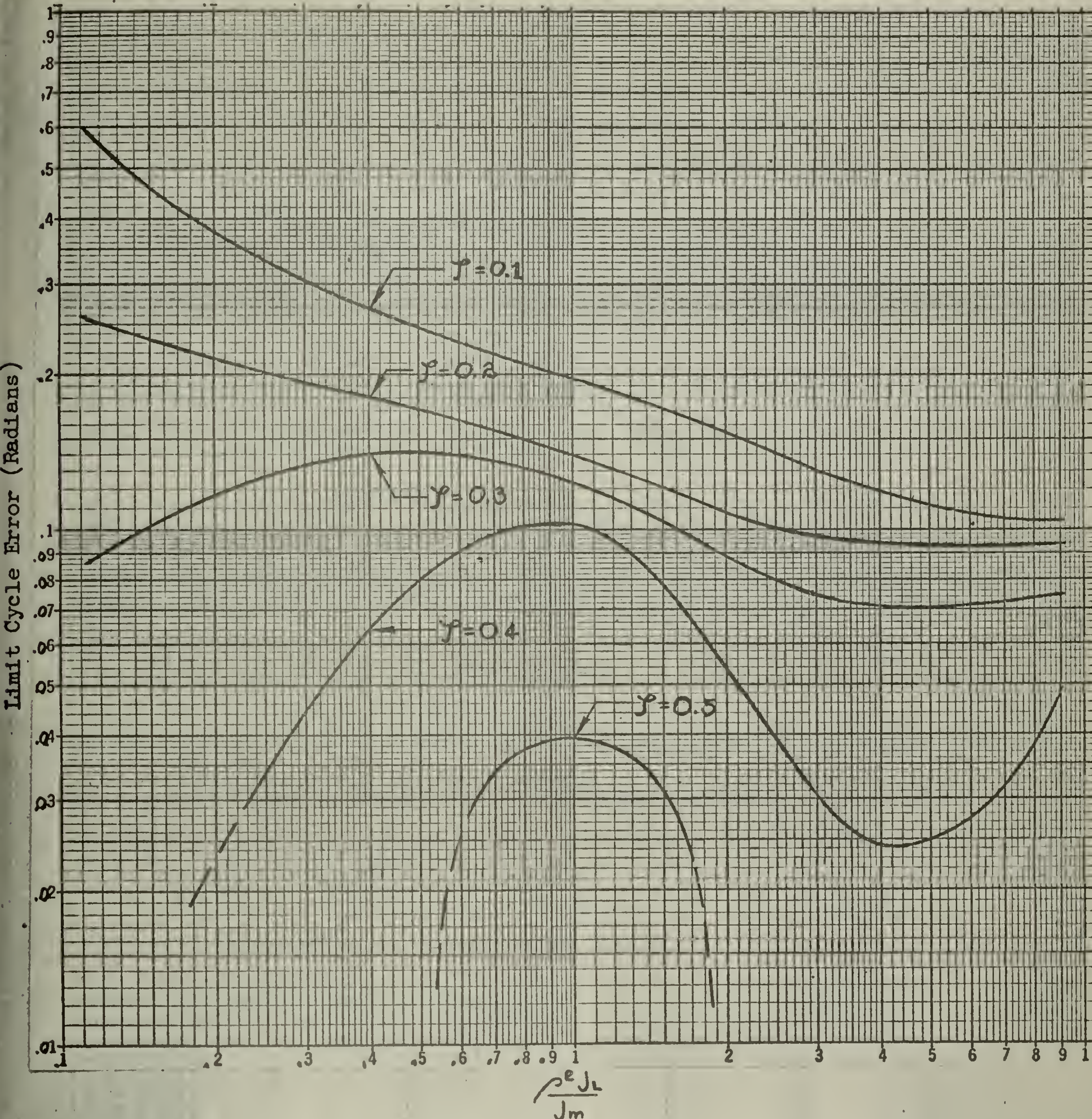

Fig. 23

Maximum Error of Limit Cycle from Unit Step Input

Limit Cycle Error (Radians) $\left(\frac{0.3}{\Delta}\right)$ for $\frac{\rho^2 J_L}{J_m}$ Variable

$$\frac{\rho^2 f_L}{F_T} = \frac{1}{\frac{f_m}{\rho^2 f_L} + 1} = 0.4$$

$$e = 1.0$$

No limit cycle exists for $\zeta \geq 0.6$

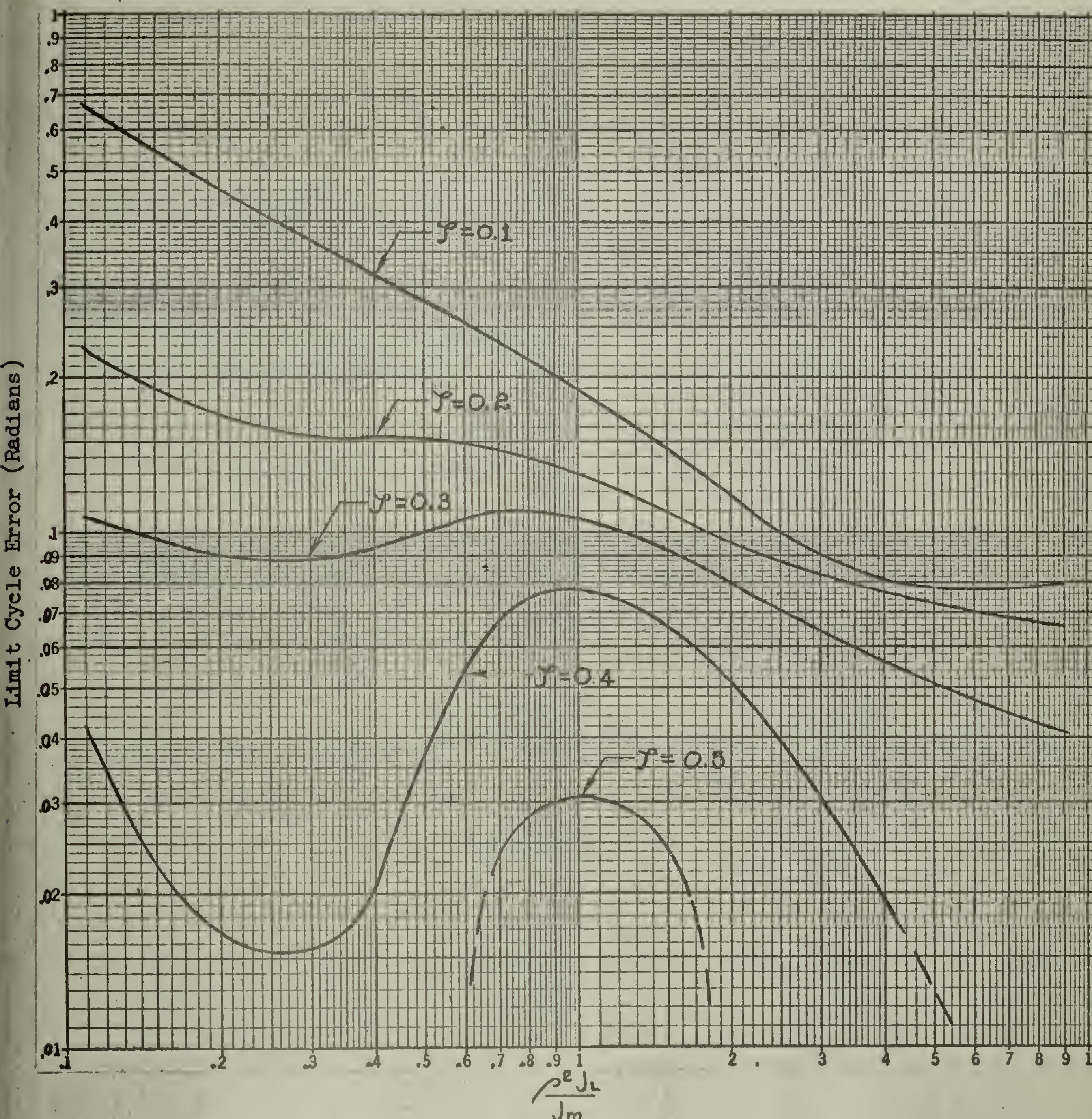

Fig. 24

Maximum Error of Limit Cycle from Unit Step Input

Limit Cycle Error (Radians) $\left(\frac{0.3}{\Delta}\right)$ for $\frac{\rho^2 J_L}{J_m}$ Variable

$$\frac{\rho^2 f_L}{F_T} = \frac{1}{\frac{f_m}{\rho^2 f_L} + 1} = 0.6$$

$e = 1.0$

No limit cycle exists for $\varsigma \geq 0.6$

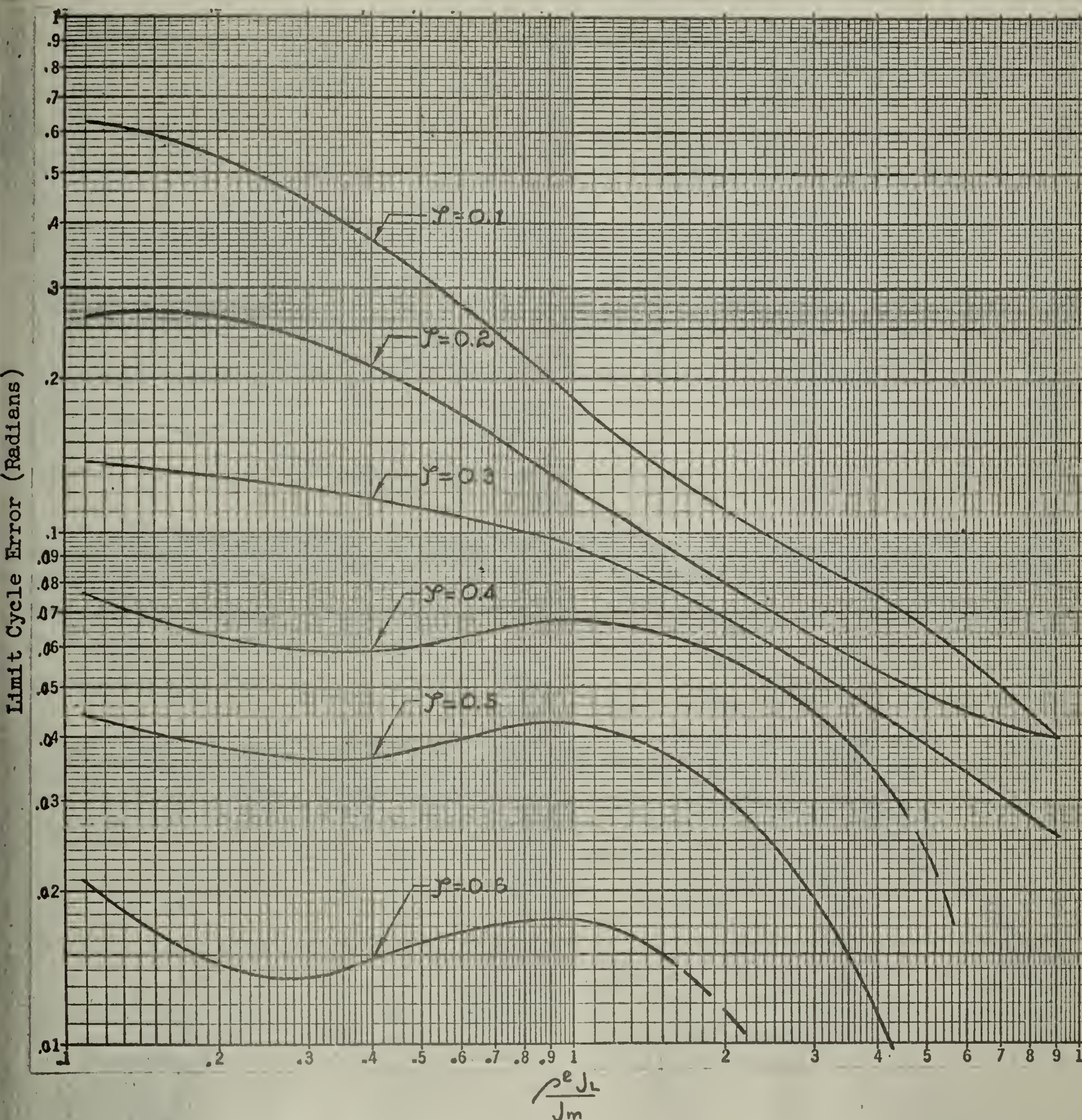

Fig. 25

Maximum Error of Limit Cycle from Unit Step Input

Limit Cycle Error (Radians) $\left(\frac{0.3}{\Delta}\right)$ for $\frac{\rho^2 J_L}{J_m}$ Variable

$$\frac{\rho^2 f_L}{F_T} = \frac{1}{\frac{f_m}{\rho^2 f_L} + 1} = 0.8$$

$$e = 1.0$$

No limit cycle exists for $\zeta \geq 0.8$

[illegible]

[illegible]

[illegible]

[illegible]

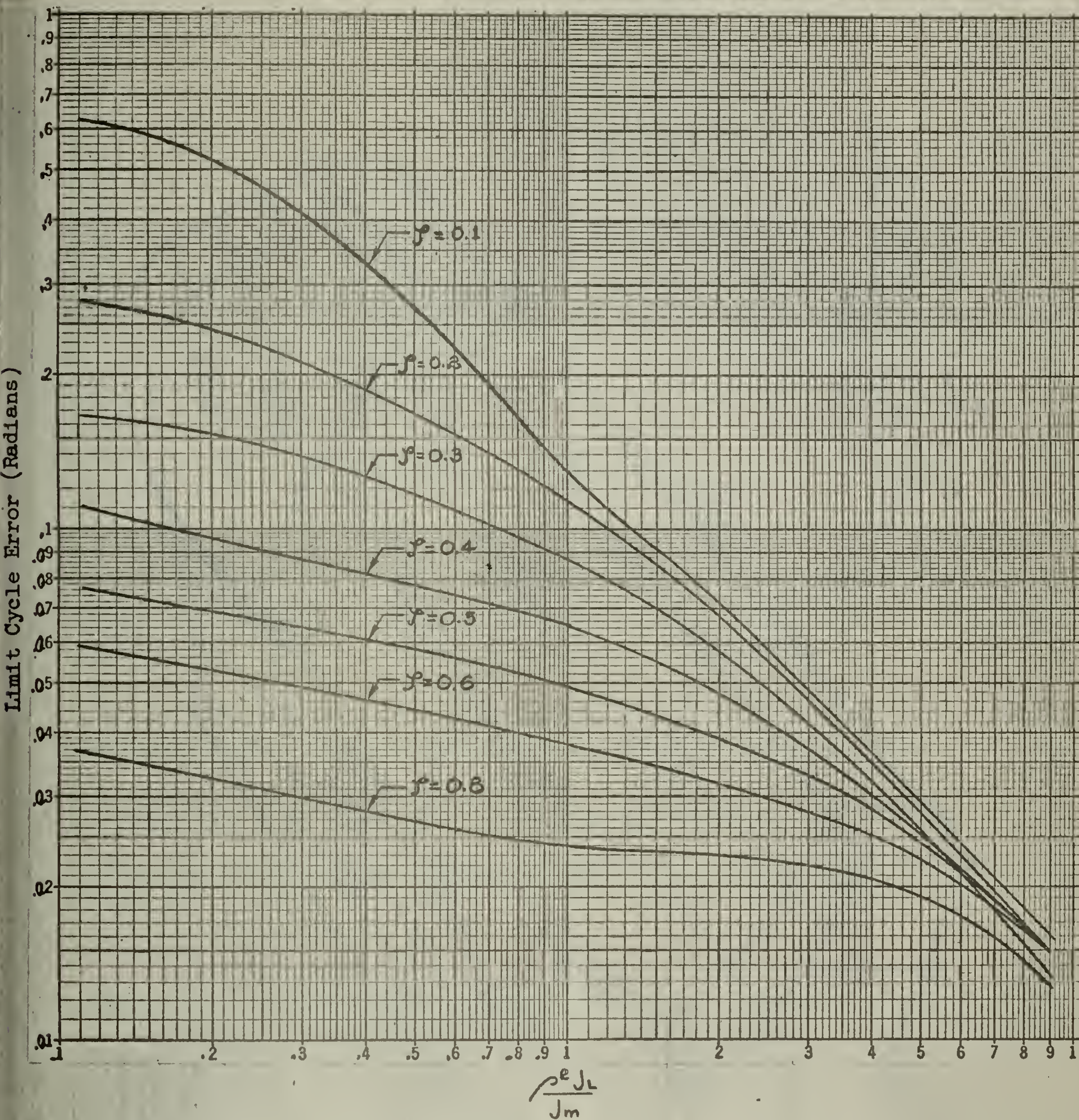

Fig. 26

Maximum Error of Limit Cycle from Unit Step Input

Limit Cycle Error (Radians) $\left(\frac{0.3}{\Delta}\right)$ for $\frac{\rho^2 J_L}{J_m}$ Variable

$$\frac{\rho^2 f_L}{F_T} = \frac{1}{\frac{f_m}{\rho^2 f_L} + 1} = 1.0$$

$e = 1.0$

No limit cycle exists for $\rho \geq 1.0$

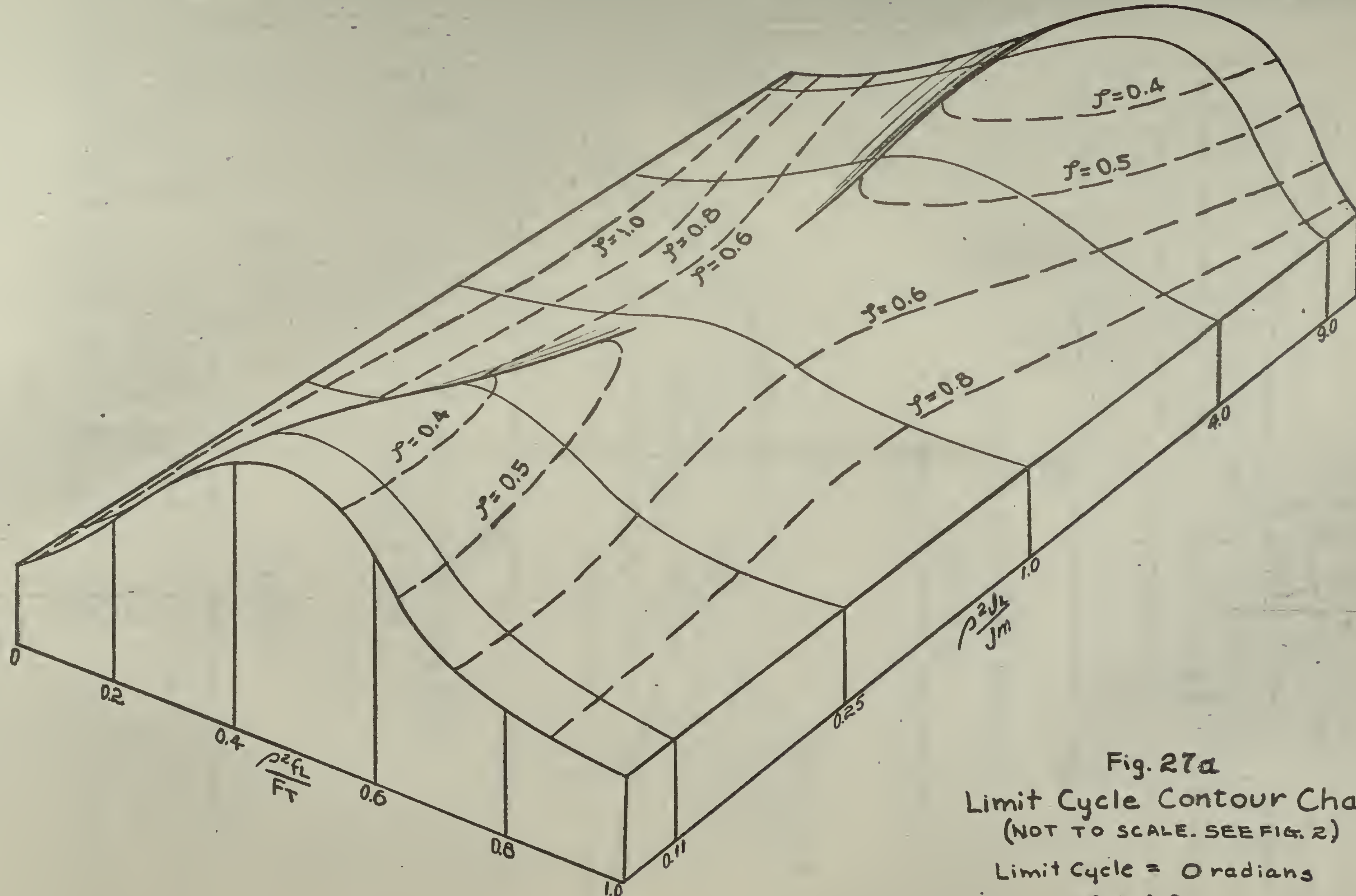

Fig. 27a
Limit Cycle Contour Chart
(NOT TO SCALE. SEE FIG. 2)
Limit Cycle = 0 radians
e = 1.0

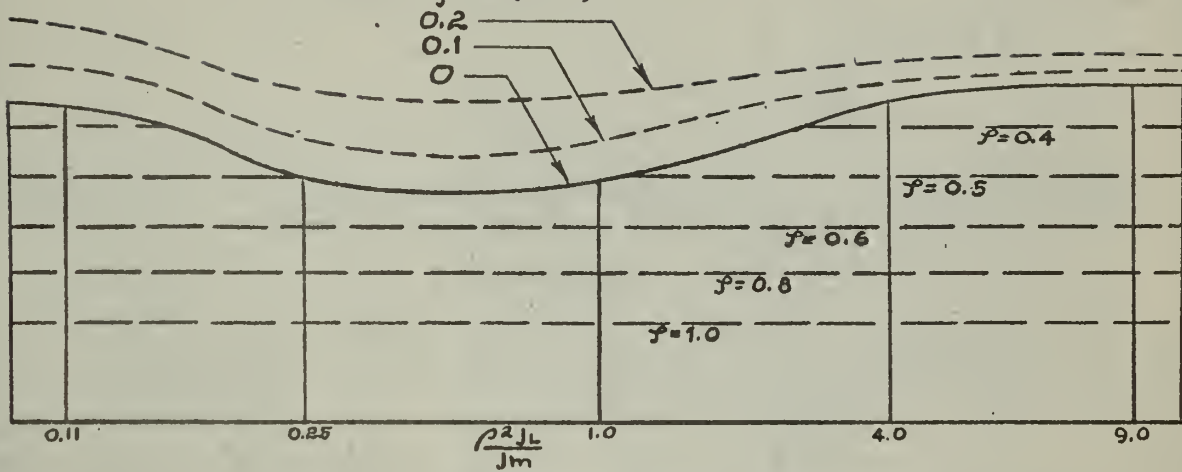

Constant $\frac{\rho^2 f_L}{F_T}$ Profile

$\frac{\rho^2 f_L}{F_T} = 0.6$

(NOT TO SCALE. SEE FIG. 24)

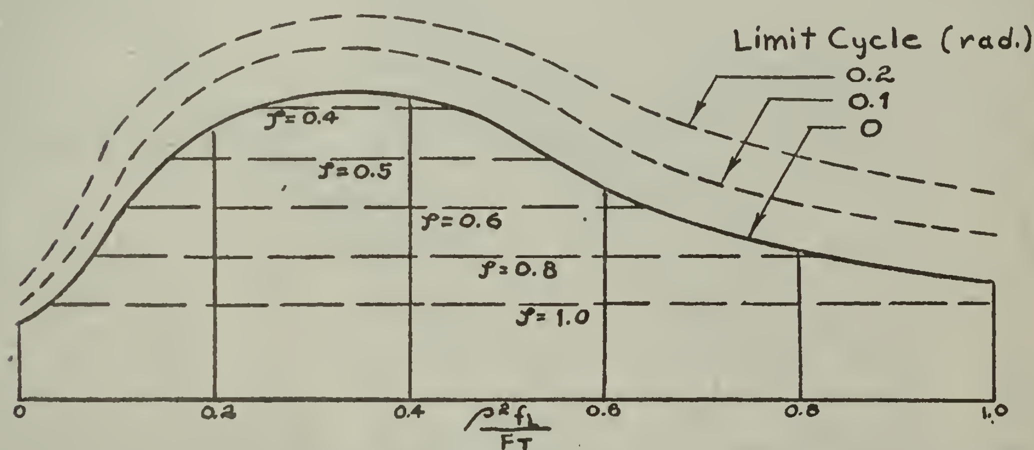

Constant $\frac{\rho^2 J_L}{J_m}$ Profile

$\frac{\rho^2 J_L}{J_m} = 0.11$

Fig. 27b

Limit Cycle Contour Chart
Profile Views

$e = 1.0$
$\Delta = 0.3$

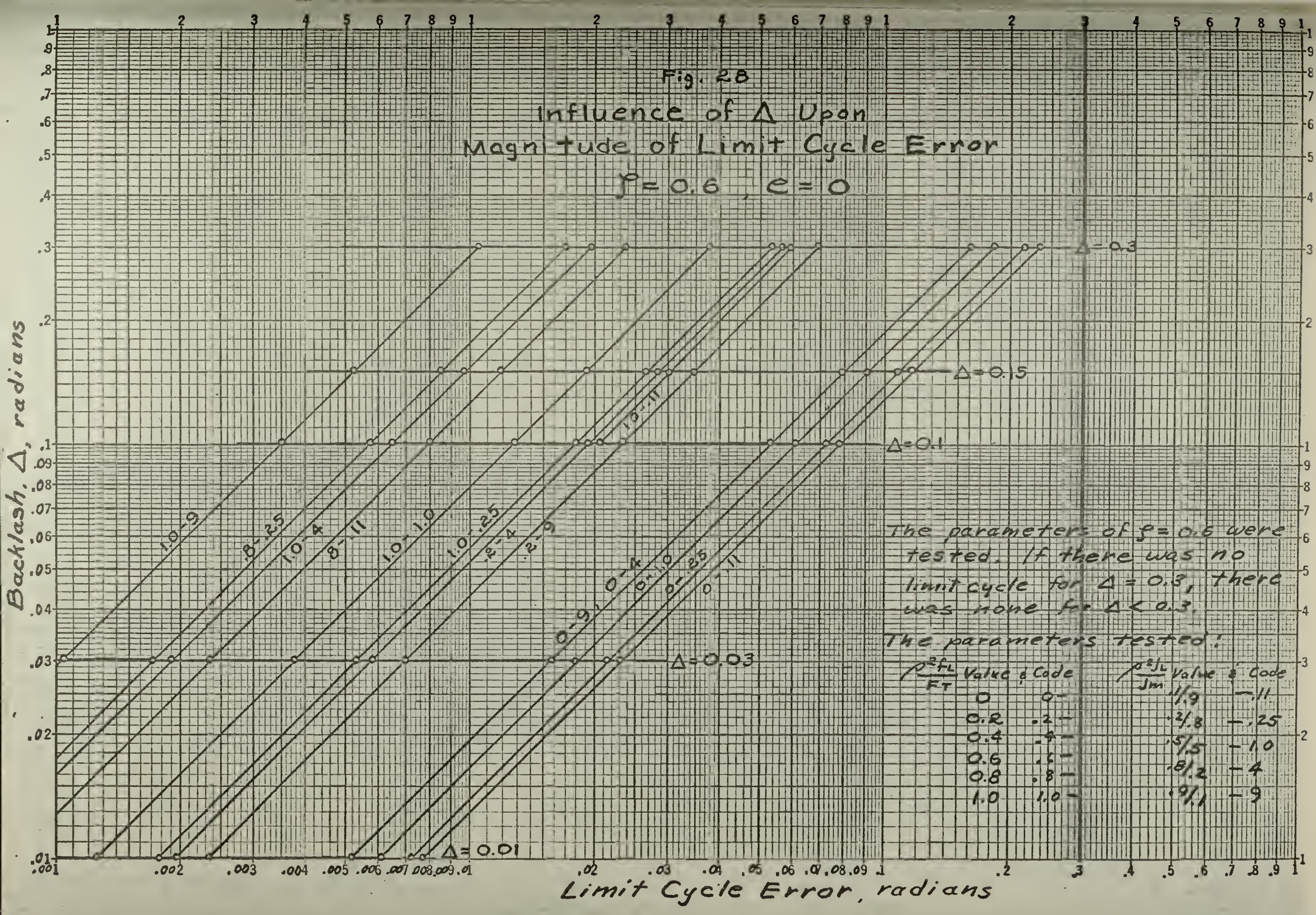

Fig. 28
Influence of Δ Upon Magnitude of Limit Cycle Error
ρ = 0.6 , e = 0
Δ = 0.3
Δ = 0.15
Δ = 0.1
Δ = 0.03
Δ = 0.01
The parameters of ρ = 0.6 were tested. If there was no limit cycle for Δ = 0.3, there was none for Δ < 0.3.
The parameters tested:
Value & Code
0 0
0.2 .2
0.4 .4
0.6 .6
0.8 .8
1.0 1.0
Value & Code
1/9 .11
2/8 .25
5/5 1.0
8/2 4
9/1 9
Backlash, Δ, radians
Limit Cycle Error, radians

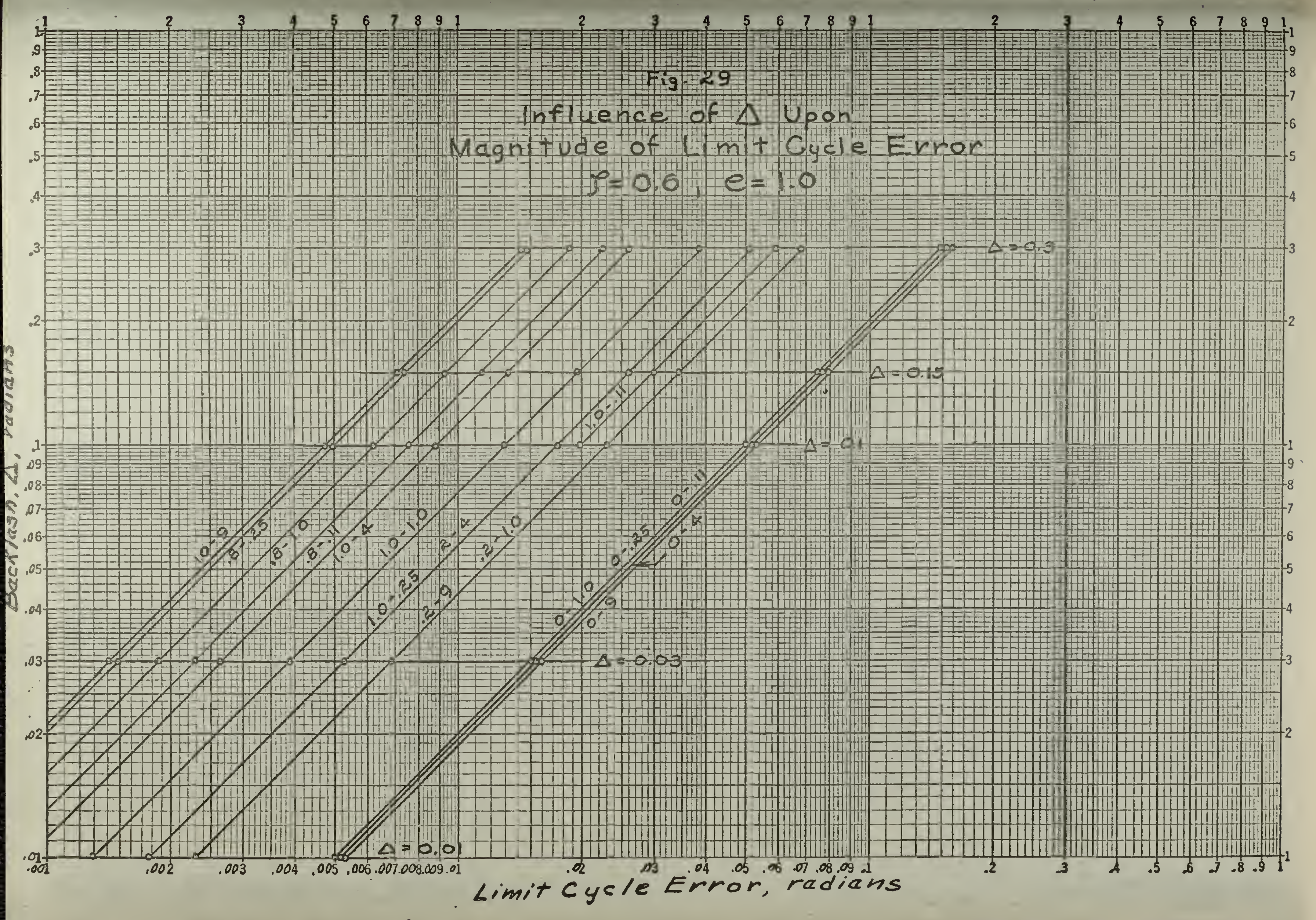

Fig. 29
Influence of Δ Upon
Magnitude of Limit Cycle Error
ζ = 0.6, e = 1.0
Δ = 0.3
Δ = 0.15
Δ = 0.1
Δ = 0.03
Δ = 0.01
1.0-.9
.8-.25
.8-1.0
.8-.11
1.0-.4
1.0-1.0
.2-.4
.2-1.0
1.0-.11
1.0-.25
.2-.9
0-.11
0-.25
0-.4
0-1.0
0-.9
Backlash, Δ, radians
Limit Cycle Error, radians

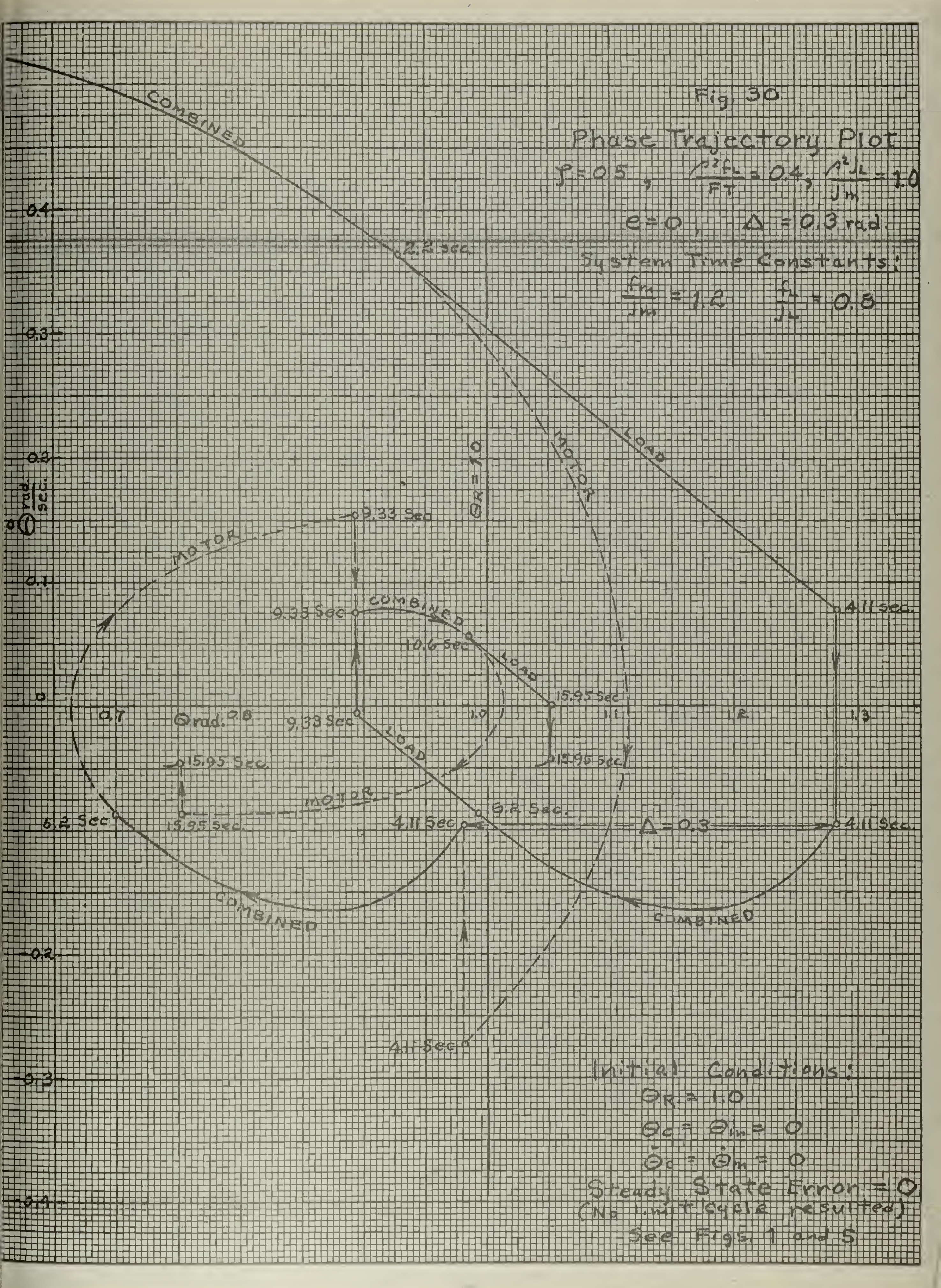

Fig. 30
Phase Trajectory Plot
$\zeta = 0.5$, $\frac{r^2 f_L}{F_T} = 0.4$, $\frac{r^2 J_L}{J_m} = 1.0$
$e = 0$, $\Delta = 0.3$ rad.
System Time Constants:
$\frac{f_m}{J_m} = 1.2$ $\frac{f_L}{J_L} = 0.8$
$\dot{\Theta}$ rad/sec.
Θ rad.
$\Theta_R = 1.0$
COMBINED
LOAD
MOTOR
2.2 sec.
9.33 Sec
10.6 Sec
15.95 Sec
4.11 Sec
6.2 Sec
8.4 Sec.
$\Delta = 0.3$
Initial Conditions:
$\Theta_R = 1.0$
$\Theta_c = \Theta_m = 0$
$\dot{\Theta}_c = \dot{\Theta}_m = 0$
Steady State Error = 0
(No Limit cycle resulted)
See Figs. 1 and 5

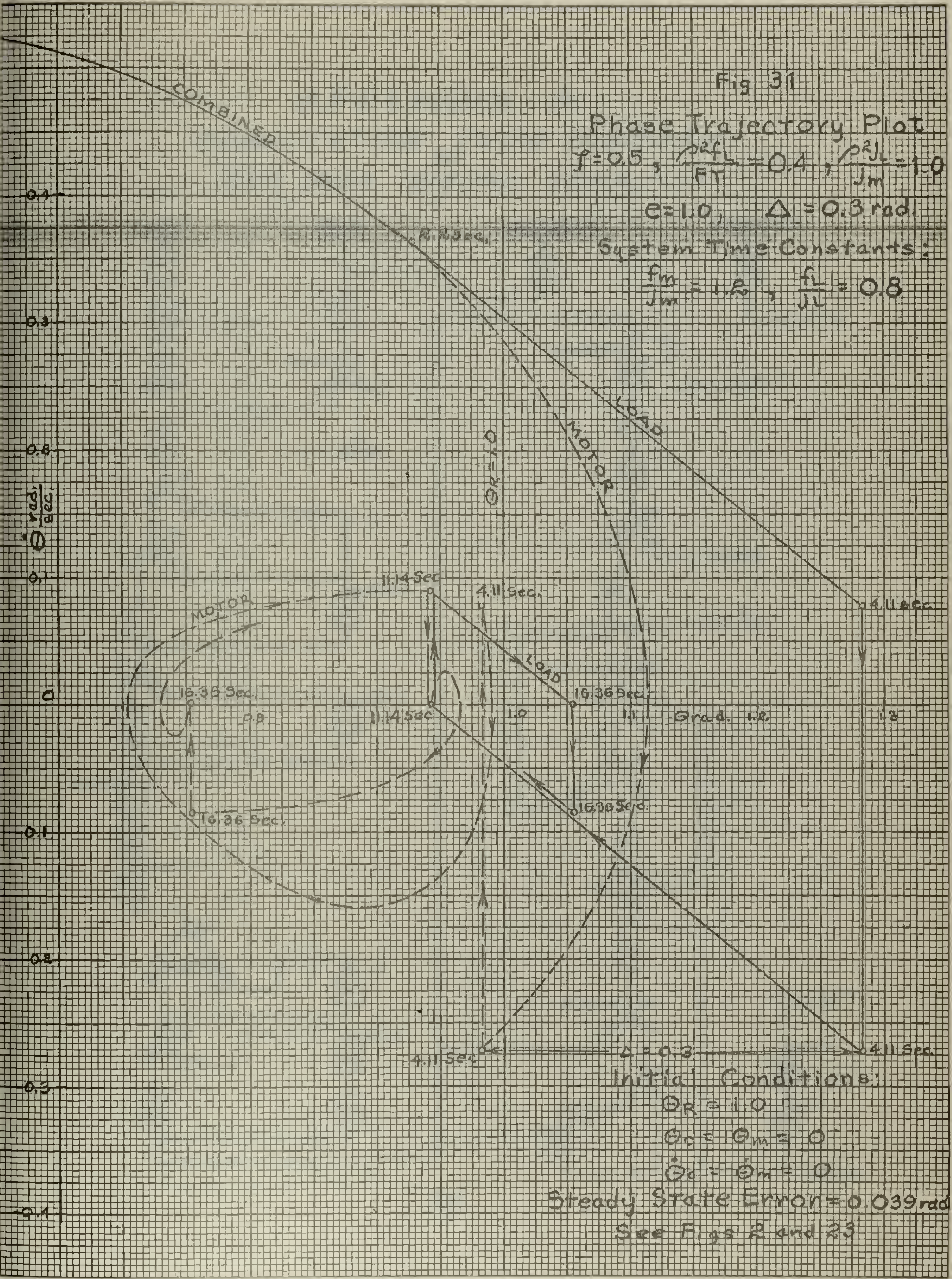

Fig 31
Phase Trajectory Plot
$\zeta = 0.5$, $\frac{\rho^2 f_L}{FT} = 0.4$, $\frac{\rho^2 J_L}{J_m} = 1.0$
$e = 1.0$, $\Delta = 0.3$ rad.
System Time Constants:
$\frac{f_m}{J_m} = 1.2$, $\frac{f_L}{J_L} = 0.8$
Initial Conditions:
$\theta_R = 1.0$
$\theta_c = \theta_m = 0$
$\dot{\theta}_c = \dot{\theta}_m = 0$
Steady State Error = 0.039 rad
See Figs 22 and 23
COMBINED
LOAD
MOTOR
$\theta_R = 1.0$
$\dot{\theta}$ rad/sec.
Grad.
2.83 Sec.
11.14 Sec
4.11 Sec.
16.36 Sec.
$\Delta = 0.3$

APPENDIX A

COMPUTATION FLOW DIAGRAM for CDC 1604 DIGITAL COMPUTER

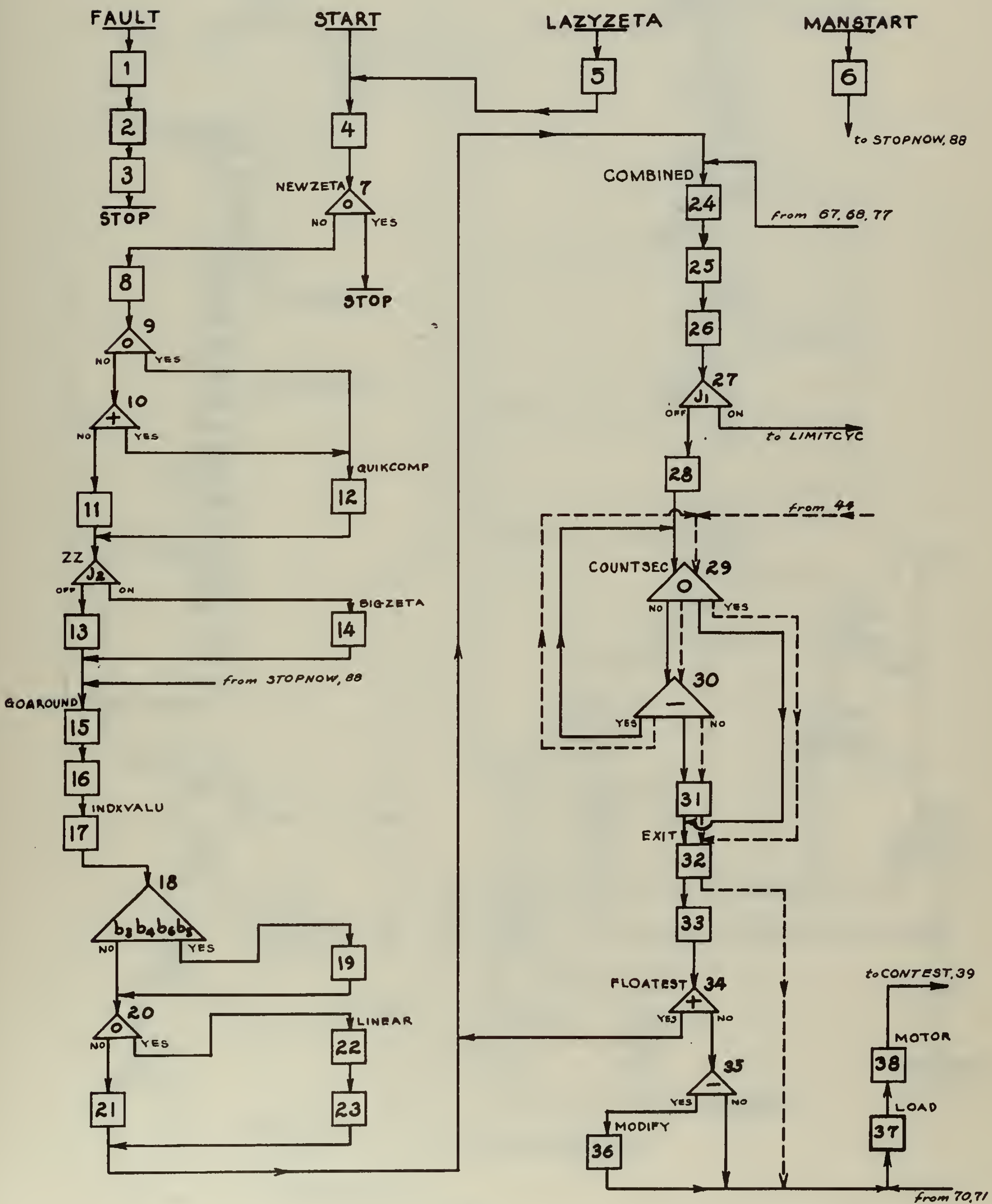

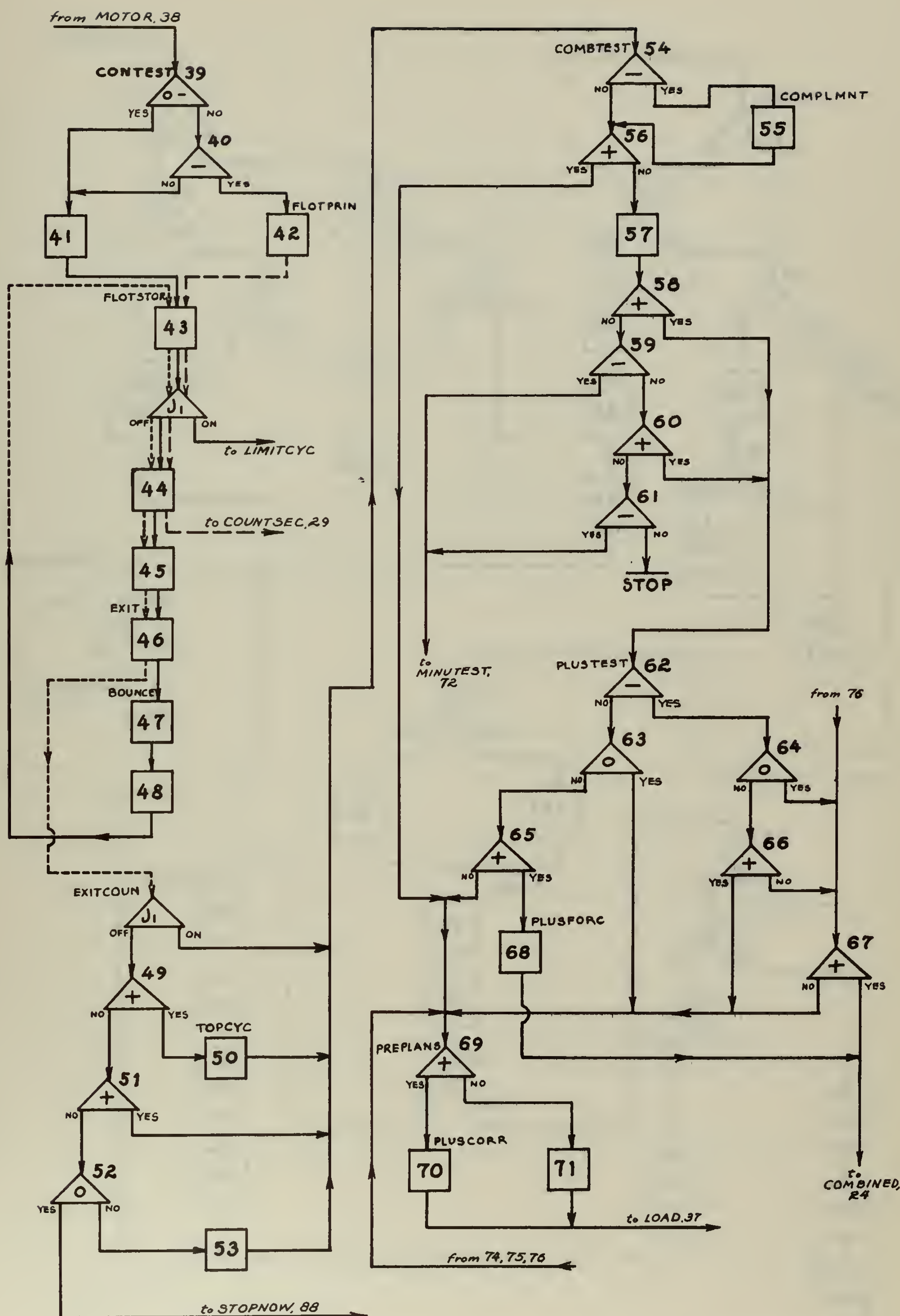

from MOTOR, 38
CONTEST 39
YES
NO
40
FLOTPRIN
41
42
FLOTSTOR
43
OFF
ON
to LIMITCYC
44
to COUNTSEC, 29
45
EXIT
46
BOUNCE
47
48
EXITCOUN
49
TOPCYC
50
51
52
53
to STOPNOW, 88
COMBTEST 54
COMPLMNT
55
56
57
58
59
60
61
STOP
to MINUTEST, 72
PLUSTEST 62
from 76
63
64
65
66
PLUSFORC
68
67
PREPLANS 69
PLUSCORR
70
71
to LOAD, 37
from 74, 75, 76
to COMBINED, 84

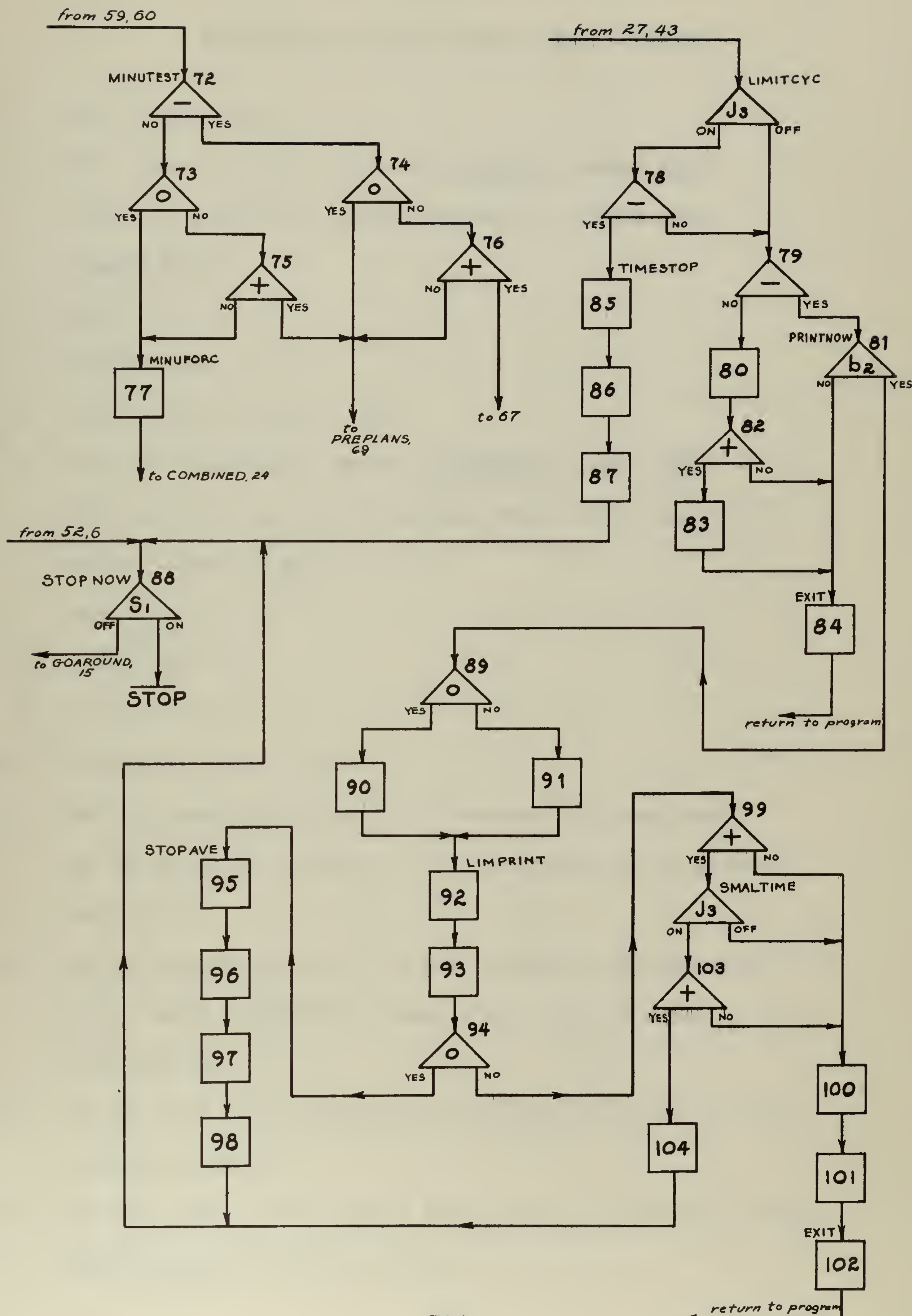

from 59, 60
MINUTEST 72
NO
YES
73
YES
NO
74
YES
NO
75
NO
YES
76
NO
YES
MINUFORC
77
to COMBINED, 24
to PREPLANS, 69
to 67
from 27, 43
LIMITCYC
J3
ON
OFF
78
YES
NO
TIMESTOP
85
86
87
79
NO
YES
PRINTNOW 81
b2
NO
YES
80
82
YES
NO
83
EXIT
84
return to program
from 52, 6
STOP NOW 88
S1
OFF
ON
to GOAROUND, 15
STOP
89
YES
NO
90
91
LIMPRINT
92
93
94
YES
NO
STOPAVE
95
96
97
98
99
YES
NO
SMALTIME
J3
ON
OFF
103
YES
NO
104
100
101
EXIT
102
return to program

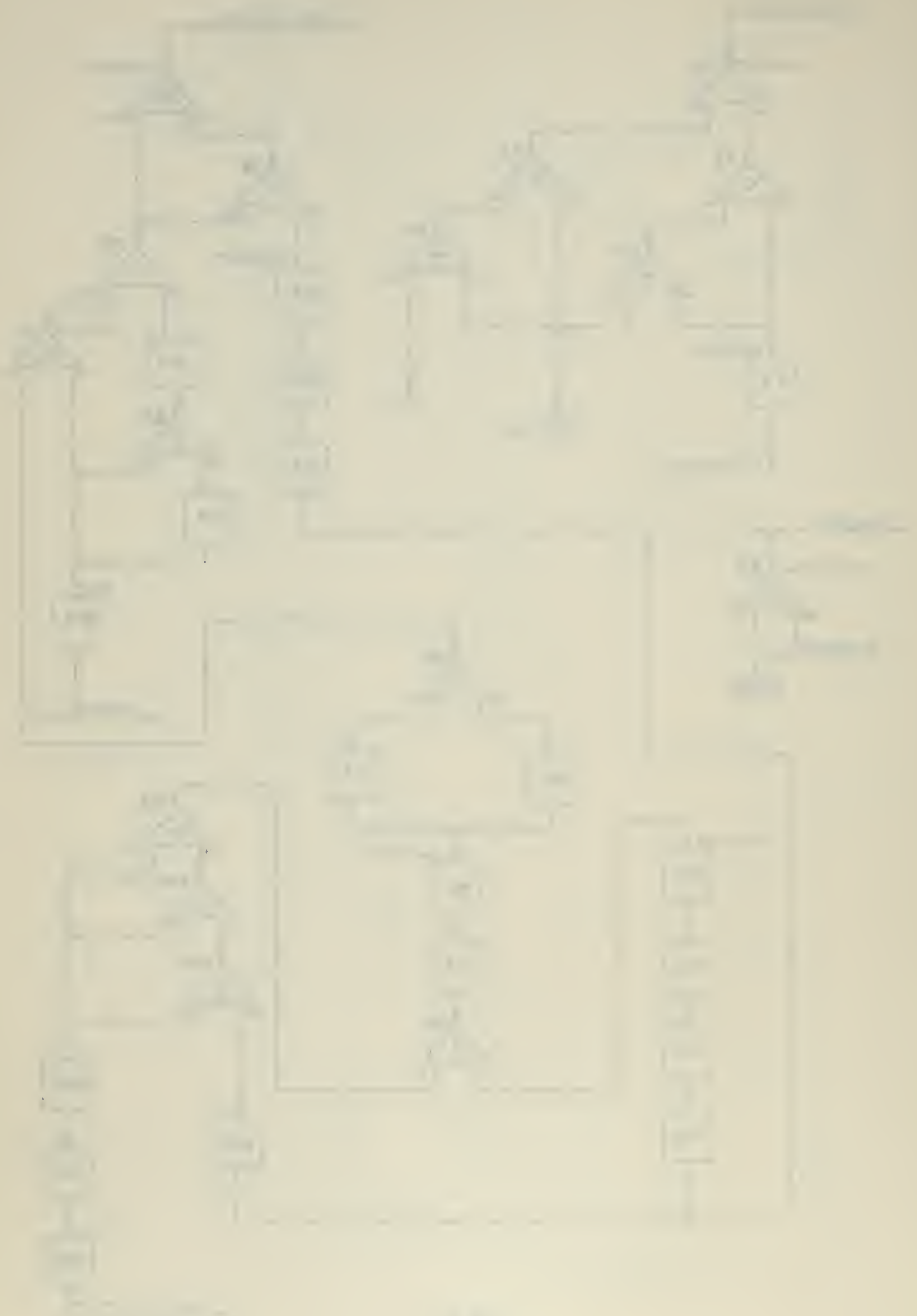

APPENDIX A (continued)

EXPLANATION OF FLOW DIAGRAM BLOCK SYMBOLS

1. Clear fault stop.

2. Print last overshoot stored in LIMITBUF (symbol 888).

   Print out position in phase trajectory of fault stop (symbol 666).

3. End of file.

4. Actuate fault stop.

5. Load zeta from Index 1 (b_1).

6. Print last overshoot stored on LIMITBUF (symbol 888).

   Print position in phase trajectory where it was manually stopped (symbol 1961).

7. Stop if Zeta = 0.

8. $2\zeta\omega_n = A$

9. Is zeta = 0.1?

10. Is zeta less than 0.1?

11. Set up computation time of 0.01 seconds for problem and set up for print at every 0.1 seconds when zeta is greater than 0.1.

12. Set up computation time of 0.004 seconds for problem and set up for print at every 0.1 seconds when zeta is equal to or less than 0.1.

13. Set up limit cycle print-out routine for 20 overshoots and average the last 8.

14. Set up number of limit cycle print-outs and averaging routine depending upon the size of zeta:

ρ	Overshoots	Start Averaging	Divide by *	Comp. Time
≥ 0.8	6	4	2.0	0.01
0.6	7	5	2.0	0.01
0.5	8	5	3.0	0.01
0.4	10	7	3.0	0.01
0.3	14	10	4.0	0.01
0.2	20	12	8.0	0.01
≤ 0.1	17	12	5.0	0.004

*The last row printed has this number printed on the far left if the problem has a normal solution. This number indicates how many overshoots were averaged. The average value has 1.0 subtracted from it and is printed in the far right of the same last row.

15. Page reject.

16. Clear buffers and set up for new problem.

17. Restitution, e, from Index 3 (b_3).

    Backlash, Δ, from Index 4 (b_4).

    J_m from Index 5 (b_5).

    $$\frac{J_T - J_m}{\rho^2} = J_L; \quad \frac{K}{J_m} = C; \quad \frac{J_m}{J_L}$$

    $\frac{f_L}{F_T}$ from Index 6 (b_6).

    $$(f_L/F_T)(2\rho\omega_n)(J_T) = f_L; \quad f_L/J_L = B$$

    $$\frac{f_L}{f_L/F_T} - \rho^2 f_L = f_m; \quad f_m/J_m = D$$

18. Have all values been cycled through?

19. Set STOPNOW after this run to stop absolutely.

20. Backlash, Δ , = 0?

21. Print consecutive number of this parameter run and all the parameters used:

$2\rho\omega_n = A$ $\quad J_m/J_L$ $\quad f_L/F_T$ $\quad e$ $\quad \Delta$ $\quad \rho$

J_m $\quad J_L$ $\quad J_m + \rho^2 J_L$ $\quad f_m$ $\quad f_L$ $\quad \rho^2$

K $\quad K/J_m = C$ $\quad f_m/J_m = D$ $\quad f_L/J_L = B$ $\quad \omega_n^2$ $\quad \rho$

22. Set program so always acts as combined system.

23. Print consecutive number of this parameter run and selected parameters for linear system:

$2\rho\omega_n = A$ $\quad J_m + \rho^2 J_L$ $\quad K$ $\quad \omega_n^2$ $\quad \rho$ $\quad \rho^2$

24. Solve the second order equation by Runge-Kutta-Gill numerical integration every 0.01 seconds problem time when zeta is greater than 0.1, otherwise every 0.004 seconds. Initial conditions are $\Theta_R = 1.0$, $\dot{\Theta}_c = \Theta_c = 0$ and $\ddot{\Theta}_c = 1.0$ or the previously computed point. Next point is computed by four iterations of:

$$\ddot{\Theta}_c = \omega_n^2 (\Theta_R - \Theta_c) - 2\rho\omega_n \dot{\Theta}_c$$

25. Set EXIT from print routine.

26. Load time, $\dot{\Theta}_c$ and Θ_c in print buffer.

27. Go to LIMITCYC to print only the overshoot. Otherwise print the phase trajectory points for each 0.1 seconds up to a maximum of 12 cycles.

28. Store 0 for $\dot{\Theta}_m$ and Θ_m

29. Is problem time 0.1 sec.?

30. Is problem time greater than 0.1 sec.?

31. Print the number of point computed, time, $\dot{\Theta}_c$ and Θ_c .

32. EXIT (automatically set for desired jump-out.)

33. Store time, $\ddot{\Theta}_c$, $\dot{\Theta}_c$ and Θ_c for motor and load initial conditions.

34. Is slope $N_L = N_S$?

$$\frac{(\Theta_R - \Theta_c)\,\omega_n^2}{\dot{\Theta}_c} - 2\zeta\omega_n + \frac{f_L}{J_L} = \text{positive value?}$$

35. Is $\dot{\Theta}_c$ negative?

36. Store $\dfrac{\Theta_c - \Delta}{\rho}$ in Θ_m

37. Solve $\ddot{\Theta}_c = -\left(f_L/J_L\right)\left(\dot{\Theta}_c\right)$ for $\dot{\Theta}_c$ and Θ_c

by Runge-Kutta-Gill.

38. Solve

$$\ddot{\Theta}_m = -\left(f_m/J_m\right)\left(\dot{\Theta}_m\right) + \left(K/J_m\right)\left(\Theta_R - \Theta_c\right)$$

for $\dot{\Theta}_m$ and Θ_m by Runge-Kutta-Gill

39. $\Theta_L - \rho\,\Theta_m \leq 0$?

40. $\Theta_L - \rho\,\Theta_m - \Delta$ = negative?

41. Set EXIT from print routine.

42. Set EXIT from print routine.

43. Load time, $\dot{\Theta}_c$ and Θ_c .

44. Load $\dot{\Theta}_m$ and Θ_m .

45. Print number of point computed and stored values.

46. EXIT (automatically set for desired jump-out).

47. Solve

$$\mathring{\Theta}_c' = \frac{J_m}{J_m + \rho^2 J_L}\left[\rho\,\mathring{\Theta}_m(1+e) + \dot{\Theta}_c\left(\rho^2\frac{J_L}{J_m} - e\right)\right]$$

$$\mathring{\Theta}_m' = \frac{\dot{\Theta}' - e(\rho\,\dot{\Theta}_m + \dot{\Theta}_c)}{\rho}$$

$$\ddot{\Theta}_m' = -\frac{f_m}{J_m}\mathring{\Theta}_m' + \frac{K}{J_m}(\Theta_R - \Theta_c)$$

48. Set EXIT from print routine.

49. Is $\mathring{\Theta}_c$ positive?

50. Set up to count one phase trajectory when $\mathring{\Theta}_c$ is negative.

51. Is $\Theta_c > 1.0$?

52. Have 12 cycles of phase trajectory been completed?

53. Arrange for no counting until $\dot{\Theta}_c$ is positive again.

54. Is $\rho\mathring{\Theta}_m - \mathring{\Theta}_c$ negative?

55. Set up $-(\rho\dot{\Theta}_m - \mathring{\Theta}_c)$.

56. Is $\rho\dot{\Theta}_m - \mathring{\Theta}_c$ greater than preselected ϵ ?

57. Set up combined system.

58. Is $\dot{\Theta}_c$ positive?

59. Is $\mathring{\Theta}_c$ negative?

60. Is $\Theta_c - 1$ positive?

61. Is $\Theta_c - 1$ negative?

62. Is $\Theta_c - 1$ negative?

63. $\Theta_c - \rho\Theta_m = 0$?

64. $\Theta_c - \rho\Theta_m = 0$?

65. Is $\Theta_c - \rho\Theta_m$ positive?

66. Is $\Theta_c - \rho\Theta_m$ positive?

67. Is Slope $N_L = N_S$?

$$\frac{(1-\theta_c)\,\omega_n^2}{\dot{\theta}_c} - 2\rho\omega_n + \frac{f_L}{J_L} = \text{positive value?}$$

68. Modify FLOATEST to keep system combined. Takes off modification when $\dot{\theta}_c$ is negative.

69. Is $\theta_c - \rho\,\theta_m$ positive?

70. Store $\dfrac{\theta_L - \Delta}{\rho}$ in θ_m.

71. Store $\dfrac{\theta_c}{\rho}$ in θ_m.

72. Is $\theta_c - 1$ negative?

73. $\theta_c - \rho\,\theta_m = 0$?

74. $\theta_c - \rho\,\theta_m = 0$?

75. Is $\theta_c - \rho\,\theta_m$ positive?

76. Is $\theta_c - \rho\,\theta_m$ positive?

77. Modify FLOATEST to keep system combined. Takes off modification when $\dot{\theta}_c$ is positive.

78. Have 1 1/2 minutes of real time elapsed since the last print-out?

79. Is $\theta_c < 1.0$?

80. Set up to print when in the fourth quadrant.

81. Check if in the fourth quadrant.

82. Is the new θ_c greater than the previous θ_c ?

83. Store the new time, $\dot{\theta}_c$ and θ_c .

84. EXIT (automatically set for desired jump-out).

85. Print the last overshoot stored in LIMITBUF (symbol 888)

86. Stop real time clock.

87. Print position in phase trajectory where it was stopped by the real time clock (symbol 999).

88. Return to beginning to start new problem if new parameters remain to be evaluated. Unconditional stop if all parameters have been evaluated.

89. Has the required number of overshoots been evaluated prior to starting the averaging routine?

90. Add the θ_c just evaluated to the previous sum for averaging.

91. Add one to the count prior to averaging.

92. Clear time clock.

93. Print time, $\dot{\theta}_c$ and θ_c .

94. Required number of total print-outs?

95. Clear buffers.

96. Obtain the average of θ_c .

97. Subtract 1.0.

98. Print the average of $\theta_c - 1.0$ and how many overshoots were utilized to obtain the average.

99. Is θ_c less than 1.005 radians?

100. Clear buffers.

101. Start real time clock.

102. <u>EXIT</u> (automatically set to desired jump-out).

103. Has 30 seconds of real time elapsed since the last print-out?

104. Print the position in the phase trajectory where it was stopped by the real time clock and θ_c being less than 1.005 radians (symbol <u>1005</u>).

Jump Switches:

J_1 - For LIMITCYC, allows the maximum overshoot print-out only. With J_1 down, a phase trajectory is printed for a maximum of 12 cycles.

J_2 - Set the number of print-outs depending on zeta. Change the number of overshoot values used to obtain the average value.

J_3 - Use the real time clock for an automatic recycle to a new parameter when have:

a. 1 1/2 minutes maximum after the last print-out.

b. 30 seconds maximum and θ_c is 1.005 radians or less.

Stop Switches:

S_1 - Stops at the end of this parameter run or stops at the end of the manual print-out.

APPENDIX B

COMPUTER PROGRAM

```
                                       ORG     00007
00007   74 0 00070   FAULT     EXF   0 00070
        75 0 40701             SLJ   0 FAULPRIN
                               ORG     40000
40000   74 0 00100   START     EXF   0 00100
        75 0 40004             SLJ   0 NEWZETA-1
40001   12 1 40623   LAZYZETA  LDA   1 ZETAINDX
        20 0 40425             STA   0 ZETA
40002   50 1 00000             ENI   1 0
        75 0 40000             SLJ   0 START
40003   75 0 40674   MANSTART  SLJ   0 MANUAL
        50 0 00000             ENI   0 0
40004   12 0 40565             LDA   0 NEWSTOP
        20 0 40563             STA   0 STOPNOW
40005   12 0 40425   NEWZETA   LDA   0 ZETA
        22 0 40564             AJP   0 STOPINDX
40006   32 0 40665             FMU   0 TWO
        32 0 40426             FMU   0 OMEGAN
40007   20 0 40404             STA   0 A
        12 0 40624             LDA   0 ZETAINDX+1
40010   31 0 40425             FSB   0 ZETA
        22 0 40433             AJP   0 QUIKCOMP
40011   22 2 40433             AJP   2 QUIKCOMP
        12 0 40402             LDA   0 POINT01
40012   20 0 40154             STA   0 TABLES+1
        20 0 40173             STA   0 TABLEL+1
40013   20 0 40207             STA   0 TABLEM+1
        12 0 40661             LDA   0 COUNT10
40014   20 0 40400             STA   0 TENTHSEC
        50 0 00000             ENI   0 0
40015   75 2 40437   ZZ        SLJ   2 BIGZETA
        50 0 00000             ENI   0 0
40016   12 0 40652             LDA   0 STOP20
        20 0 40616             STA   0 STOPZETA
40017   12 0 40662             LDA   0 COUNT12
        20 0 40617             STA   0 COUNTZET
40020   12 0 40672             LDA   0 EIGHT
        20 0 40620             STA   0 DIVIDE
40021   10 0 00010             ENA   0 10
        61 0 40562             SAL   0 STOPRINT
40022   75 4 71000   GOAROUND  SLJ   4 DECOF
        50 0 00000             ENI   0 0
40023   02 0 40427               02  0 FORZEROS
        04 0 00000               04  0 0
40024   12 0 40664             LDA   0 ONE
        20 0 40156             STA   0 UDOT
40025   10 0 00000             ENA   0 0
        20 0 00000             STA   0 0
40026   20 0 40162             STA   0 THETA
        20 0 40161             STA   0 THETADOT
40027   20 0 40157             STA   0 U
        20 0 40155             STA   0 T
40030   20 0 40377             STA   0 INDEX
        20 0 40615             STA   0 INDEXAVE
40031   20 0 40351             STA   0 PRINTBUF+3
        20 0 40352             STA   0 PRINTBUF+4
40032   20 0 40353             STA   0 PRINTBUF+5
        20 0 40614             STA   0 LIMINDEX
40033   20 0 40607             STA   0 LIMITBUF+2
        20 0 40610             STA   0 LIMITBUF+3
40034   20 0 40611             STA   0 LIMITBUF+4
        20 0 40612             STA   0 LIMITBUF+5
40035   20 0 40613             STA   0 LIMITBUF+6
        12 0 40621             LDA   0 PRINTSET
40036   20 0 40326             STA   0 OK2PRINT+1
        20 0 40335             STA   0 BOUNPRIN+4
40037   12 0 40622             LDA   0 NEWLIMPT
        20 0 40544             STA   0 LIMPRINT+1
40040   12 0 40253             LDA   0 FLOTDATA
        20 0 40071             STA   0 FLOATEST
40041   12 0 40254             LDA   0 FLOTDATA+1
        20 0 40072             STA   0 FLOATEST+1
40042   75 0 40452   NEWINPUT  SLJ   0 INDXVALU
        50 0 00000             ENI   0 00000
```

```
40043   12 0 40410             LDA   0 DELTA
        22 0 40500             AJP   0 LINEAR
40044   12 0 40513             LDA   0 NOSINK
        20 0 40071             STA   0 FLOATEST
40045   75 4 71000             SLJ   4 DECOF
        50 0 00000             ENI   0 0
40046   01 0 40404              01   0 A
        06 0 00001              06   0 1
40047   72 0 40046             RAO   0 *-1
        75 4 71000             SLJ   4 DECOF
40050   01 0 40412              01   0 MOINERT
        06 0 00000              06   0 0
40051   72 0 40510             RAO   0 LINEAR+10
        75 4 71000             SLJ   4 DECOF
40052   01 0 40420              01   0 KMOTCONS
        06 0 00000              06   0 0
40053   10 0 00000   COMBINED  ENA   0 0
        20 0 40160             STA   0 QX
40054   20 0 40163             STA   0 QY
        75 4 60200             SLJ   4 RUNGE
40055   00 0 40153               0   0 TABLES
        00 0 40164               0   0 DERIVES
40056   75 4 60201             SLJ   4 RUNGE+1
        50 0 00000             ENI   0 0
40057   75 0 40310             SLJ   0 COMBPRIN
        50 0 00000             ENI   0 0
40060   12 0 40155             LDA   0 T
        20 0 40174             STA   0 TL
40061   20 0 40210             STA   0 TM
        12 0 40156             LDA   0 UDOT
40062   20 0 40175             STA   0 VDOT
        33 0 40411             FDV   0 RHO
40063   20 0 40211             STA   0 WDOT
        12 0 40157             LDA   0 U
40064   20 0 40176             STA   0 V
        20 0 40200             STA   0 THETADL
40065   33 0 40411             FDV   0 RHO
        20 0 40212             STA   0 W
40066   20 0 40214             STA   0 THETADM
        12 0 40162             LDA   0 THETA
40067   20 0 40201             STA   0 THETAL
        33 0 40411             FDV   0 RHO
40070   20 0 40215             STA   0 THETAM
        50 0 00000             ENI   0 0
40071   13 0 40162   FLOATEST  LAC   0 THETA
        30 0 40664             FAD   0 ONE
40072   32 0 40424             FMU   0 OMEGANSQ
        33 0 40161             FDV   0 THETADOT
40073   31 0 40404             FSB   0 A
        30 0 40423             FAD   0 B
40074   22 2 40053             AJP   2 COMBINED
        12 0 40161             LDA   0 THETADOT
40075   22 3 40270             AJP   3 MODIFY
        50 0 00000             ENI   0 0
40076   10 0 00000   LOAD      ENA   0 0
        20 0 40177             STA   0 QL
40077   20 0 40202             STA   0 QLL
        20 0 40213             STA   0 QM
40100   20 0 40216             STA   0 QMM
        75 4 60200             SLJ   4 RUNGE
40101   00 0 40172               0   0 TABLEL
        00 0 40203               0   0 DERIVL
40102   75 4 60201             SLJ   4 RUNGE+1
        50 0 00000             ENI   0 0
40103   75 4 60200   MOTOR     SLJ   4 RUNGE
        50 0 00000             ENI   0 0
40104   00 0 40206               0   0 TABLEM
        00 0 40217               0   0 DERIVM
40105   75 4 60201             SLJ   4 RUNGE+1
        50 0 00000             ENI   0 0
40106   13 0 40215   CONTEST   LAC   0 THETAM
        32 0 40411             FMU   0 RHO
40107   30 0 40201             FAD   0 THETAL
        22 0 40112             AJP   0 BOUNCE
```

```
40110   22 3 40112             AJP   3 BOUNCE
        31 0 40410             FSB   0 DELTA
40111   22 3 40317             AJP   3 FLOTPRIN
        50 0 00000             ENI   0 0
40112   75 0 40331   BOUNCE    SLJ   0 BOUNPRIN
        50 0 00000             ENI   0 0
40113   12 0 40200             LDA   0 THETADL
        20 0 40212             STA   0 W
40114   12 0 40417             LDA   0 RHOSQ
        33 0 40405             FDV   0 INERTRAT
40115   31 0 40407             FSB   0 RESTITUT
        32 0 40200             FMU   0 THETADL
40116   20 0 40200             STA   0 THETADL
        12 0 40664             LDA   0 ONE
40117   30 0 40407             FAD   0 RESTITUT
        32 0 40411             FMU   0 RHO
40120   32 0 40214             FMU   0 THETADM
        30 0 40200             FAD   0 THETADL
40121   33 0 40414             FDV   0 TOTINERT
        32 0 40412             FMU   0 MOINERT
40122   20 0 40200             STA   0 THETADL
        20 0 40176             STA   0 V
40123   13 0 40176             LAC   0 V
        32 0 40423             FMU   0 B
40124   20 0 40175             STA   0 VDOT
        13 0 40214             LAC   0 THETADM
40125   32 0 40411             FMU   0 RHO
        30 0 40212             FAD   0 W
40126   32 0 40407             FMU   0 RESTITUT
        30 0 40200             FAD   0 THETADL
40127   33 0 40411             FDV   0 RHO
        20 0 40214             STA   0 THETADM
40130   20 0 40212             STA   0 W
        13 0 40212             LAC   0 W
40131   32 0 40422             FMU   0 D
        20 0 40211             STA   0 WDOT
40132   13 0 40201             LAC   0 THETAL
        30 0 40664             FAD   0 ONE
40133   32 0 40421             FMU   0 C
        30 0 40211             FAD   0 WDOT
40134   20 0 40211             STA   0 WDOT
        75 0 40332             SLJ   0 BOUNPRIN+1
40135   50 0 00000   COMBTEST  ENI   0 0
        12 0 40214             LDA   0 THETADM
40136   32 0 40411             FMU   0 RHO
        31 0 40200             FSB   0 THETADL
40137   22 3 40276             AJP   3 COMPLMNT
        50 0 00000             ENI   0 00000
40140   65 0 40403             THS   0 DIFFERNT
        75 0 40301             SLJ   0 PREPLANS
40141   12 0 40200             LDA   0 THETADL
        20 0 40161             STA   0 THETADOT
40142   20 0 40157             STA   0 U
        13 0 40157             LAC   0 U
40143   32 0 40404             FMU   0 A
        20 0 40156             STA   0 UDOT
40144   12 0 40201             LDA   0 THETAL
        20 0 40162             STA   0 THETA
40145   13 0 40162             LAC   0 THETA
        30 0 40664             FAD   0 ONE
40146   32 0 40424             FMU   0 OMEGANSQ
        30 0 40156             FAD   0 UDOT
40147   20 0 40156             STA   0 UDOT
        12 0 40174             LDA   0 TL
40150   20 0 40155             STA   0 T
        12 0 40200             LDA   0 THETADL
40151   22 2 40225             AJP   2 PLUSTEST
        22 3 40255             AJP   3 MINUTEST
40152   75 0 40273             SLJ   0 TESTZERO
        50 0 00000             ENI   0 0
40153   00 0 00000   TABLES    OCT     2
        00 0 00002
40154   17 7 15075             DEC     .01
        34 1 21727
```

```
40155   00 0 00000   T          DEC     0
        00 0 00000
40156   20 0 14000   UDOT       DEC     1.0
        00 0 00000
40157   00 0 00000   U          DEC     0
        00 0 00000
40160   00 0 00000   QX         DEC     0
        00 0 00000
40161   00 0 00000   THETADOT   DEC     0
        00 0 00000
40162   00 0 00000   THETA      DEC     0
        00 0 00000
40163   00 0 00000   QY         DEC     0
        00 0 00000
40164   13 0 40157   DERIVES    LAC   0 U
        32 0 40404              FMU   0 A
40165   20 0 40156              STA   0 UDOT
        13 0 40162              LAC   0 THETA
40166   30 0 40664              FAD   0 ONE
        32 0 40424              FMU   0 OMEGANSQ
40167   30 0 40156              FAD   0 UDOT
        20 0 40156              STA   0 UDOT
40170   12 0 40157              LDA   0 U
        20 0 40161              STA   0 THETADOT
40171   75 0 60202              SLJ   0 RUNGE+2
        50 0 00000              ENI   0 0
40172   00 0 00000   TABLEL     OCT     2
        00 0 00002
40173   17 7 15075              DEC     .01
        34 1 21727
40174   00 0 00000   TL         DEC     0
        00 0 00000
40175   00 0 00000   VDOT       DEC     0
        00 0 00000
40176   00 0 00000   V          DEC     0
        00 0 00000
40177   00 0 00000   QL         DEC     0
        00 0 00000
40200   00 0 00000   THETADL    DEC     0
        00 0 00000
40201   00 0 00000   THETAL     DEC     0
        00 0 00000
40202   00 0 00000   QLL        DEC     0
        00 0 00000
40203   13 0 40176   DERIVL     LAC   0 V
        32 0 40423              FMU   0 B
40204   20 0 40175              STA   0 VDOT
        12 0 40176              LDA   0 V
40205   20 0 40200              STA   0 THETADL
        75 0 60202              SLJ   0 RUNGE+2
40206   00 0 00000   TABLEM     OCT     2
        00 0 00002
40207   17 7 15075              DEC     .01
        34 1 21727
40210   00 0 00000   TM         DEC     0
        00 0 00000
40211   00 0 00000   WDOT       DEC     0
        00 0 00000
40212   00 0 00000   W          DEC     0
        00 0 00000
40213   00 0 00000   QM         DEC     0
        00 0 00000
40214   00 0 00000   THETADM    DEC     0
        00 0 00000
40215   00 0 00000   THETAM     DEC     0
        00 0 00000
40216   00 0 00000   QMM        DEC     0
        00 0 00000
40217   13 0 40201   DERIVM     LAC   0 THETAL
        32 0 40421              FMU   0 C
40220   20 0 40211              STA   0 WDOT
        13 0 40212              LAC   0 W
40221   32 0 40422              FMU   0 D
        30 0 40421              FAD   0 C
```

```
40222   30 0 40211            FAD  0 WDOT
        20 0 40211            STA  0 WDOT
40223   12 0 40212            LDA  0 W
        20 0 40214            STA  0 THETADM
40224   75 0 60202            SLJ  0 RUNGE+2
        50 0 00000            ENI  0 0
40225   12 0 40201  PLUSTEST  LDA  0 THETAL
        31 0 40664            FSB  0 ONE
40226   22 3 40232            AJP  3 PLUSTEST+5
        13 0 40215            LAC  0 THETAM
40227   32 0 40411            FMU  0 RHO
        30 0 40201            FAD  0 THETAL
40230   22 0 40301            AJP  0 PREPLANS
        22 2 40241            AJP  2 PLUSFORC
40231   75 0 40301            SLJ  0 PREPLANS
        50 0 00000            ENI  0 0
40232   13 0 40215            LAC  0 THETAM
        32 0 40411            FMU  0 RHO
40233   30 0 40201            FAD  0 THETAL
        22 0 40235            AJP  0 PLUSTEST+10
40234   22 2 40301            AJP  2 PREPLANS
        50 0 00000            ENI  0 0
40235   13 0 40162            LAC  0 THETA
        30 0 40664            FAD  0 ONE
40236   32 0 40424            FMU  0 OMEGANSQ
        33 0 40161            FDV  0 THETADOT
40237   31 0 40404            FSB  0 A
        30 0 40423            FAD  0 B
40240   22 2 40053            AJP  2 COMBINED
        75 0 40301            SLJ  0 PREPLANS
40241   12 0 40244  PLUSFORC  LDA  0 NUMB
        20 0 40071            STA  0 FLOATEST
40242   12 0 40245            LDA  0 NUMB+1
        20 0 40072            STA  0 FLOATEST+1
40243   75 0 40053            SLJ  0 COMBINED
        50 0 00000            ENI  0 0
40244   12 0 40161  NUMB      LDA  0 THETADOT
        22 2 40053            AJP  2 COMBINED
40245   75 0 40250            SLJ  0 RESTORET
        50 0 00000            ENI  0 0
40246   12 0 40161  DUMB      LDA  0 THETADOT
        22 3 40053            AJP  3 COMBINED
40247   75 0 40250            SLJ  0 RESTORET
        50 0 00000            ENI  0 0
40250   12 0 40253  RESTORET  LDA  0 FLOTDATA
        20 0 40071            STA  0 FLOATEST
40251   12 0 40254            LDA  0 FLOTDATA+1
        20 0 40072            STA  0 FLOATEST+1
40252   75 0 40053            SLJ  0 COMBINED
        50 0 00000            ENI  0 0
40253   13 0 40162  FLOTDATA  LAC  0 THETA
        30 0 40664            FAD  0 ONE
40254   32 0 40424            FMU  0 OMEGANSQ
        33 0 40161            FDV  0 THETADOT
40255   12 0 40201  MINUTEST  LDA  0 THETAL
        31 0 40664            FSB  0 ONE
40256   22 2 40262            AJP  2 MINUTEST+5
        13 0 40215            LAC  0 THETAM
40257   32 0 40411            FMU  0 RHO
        30 0 40201            FAD  0 THETAL
40260   22 0 40265            AJP  0 MINUFORC
        22 2 40301            AJP  2 PREPLANS
40261   75 0 40265            SLJ  0 MINUFORC
        50 0 00000            ENI  0 0
40262   13 0 40215            LAC  0 THETAM
        32 0 40411            FMU  0 RHO
40263   30 0 40201            FAD  0 THETAL
        22 0 40301            AJP  0 PREPLANS
40264   22 2 40235            AJP  2 PLUSTEST+10
        75 0 40301            SLJ  0 PREPLANS
40265   12 0 40246  MINUFORC  LDA  0 DUMB
        20 0 40071            STA  0 FLOATEST
40266   12 0 40247            LDA  0 DUMB+1
        20 0 40072            STA  0 FLOATEST+1
```

```
40267   75 0 40053             SLJ  0 COMBINED
        50 0 00000             ENI  0 0
40270   12 0 40162   MODIFY    LDA  0 THETA
        31 0 40410             FSB  0 DELTA
40271   33 0 40411             FDV  0 RHO
        20 0 40215             STA  0 THETAM
40272   75 0 40076             SLJ  0 LOAD
        50 0 00000             ENI  0 0
40273   12 0 40201   TESTZERO  LDA  0 THETAL
        31 0 40664             FSB  0 ONE
40274   22 2 40225             AJP  2 PLUSTEST
        22 3 40255             AJP  3 MINUTEST
40275   76 0 00000             SLS  0 0
        50 0 00000             ENI  0 0
40276   20 0 40300   COMPLMNT  STA  0 COMPLMNT+2
        13 0 40300             LAC  0 COMPLMNT+2
40277   75 0 40140             SLJ  0 COMBTEST+3
        50 0 00000             ENI  0 0
40300   00 0 00000             BSS    1
        00 0 00000
40301   13 0 40215   PREPLANS  LAC  0 THETAM
        32 0 40411             FMU  0 RHO
40302   30 0 40201             FAD  0 THETAL
        22 2 40305             AJP  2 PLUSCORR
40303   12 0 40201             LDA  0 THETAL
        33 0 40411             FDV  0 RHO
40304   20 0 40215             STA  0 THETAM
        75 0 40076             SLJ  0 LOAD
40305   12 0 40201   PLUSCORR  LDA  0 THETAL
        31 0 40410             FSB  0 DELTA
40306   33 0 40411             FDV  0 RHO
        20 0 40215             STA  0 THETAM
40307   75 0 40076             SLJ  0 LOAD
        50 0 00000             ENI  0 0
40310   12 0 40354   COMBPRIN  LDA  0 COMBEXIT
        20 0 40360             STA  0 EXIT
40311   12 0 40155             LDA  0 T
        20 0 40346             STA  0 PRINTBUF
40312   12 0 40157             LDA  0 U
        20 0 40347             STA  0 PRINTBUF+1
40313   12 0 40162             LDA  0 THETA
        20 0 40350             STA  0 PRINTBUF+2
40314   75 1 40522             SLJ  1 LIMITCYC
        10 0 00000             ENA  0 0
40315   20 0 40351             STA  0 PRINTBUF+3
        20 0 40352             STA  0 PRINTBUF+4
40316   75 0 40321             SLJ  0 COUNTSEC
        50 0 00000             ENI  0 0
40317   12 0 40355   FLOTPRIN  LDA  0 FLOTEXIT
        20 0 40360             STA  0 EXIT
40320   75 4 40337             SLJ  4 FLOTSTOR
        50 0 00000             ENI  0 0
40321   72 0 40377   COUNTSEC  RAO  0 INDEX
        12 0 40377             LDA  0 INDEX
40322   15 0 40400             SUB  0 TENTHSEC
        22 0 40325             AJP  0 OK2PRINT
40323   22 2 40322             AJP  2 COUNTSEC+1
        14 0 40400             ADD  0 TENTHSEC
40324   20 0 40377             STA  0 INDEX
        75 0 40360             SLJ  0 EXIT
40325   75 4 71000   OK2PRINT  SLJ  4 DECOF
        50 0 00000             ENI  0 0
40326   00 0 40346              00  0 PRINTBUF
        06 0 00001              06  0 1
40327   72 0 40326             RAO  0 /-1
        10 0 00000             ENA  0 0
40330   20 0 40377             STA  0 INDEX
        75 0 40360             SLJ  0 EXIT
40331   12 0 40356   BOUNPRIN  LDA  0 BOUNEXIT
        75 0 40333             SLJ  0 BOUNPRIN+2
40332   12 0 40357             LDA  0 BOUNEXIT+1
        50 0 00000             ENI  0 0
40333   20 0 40360             STA  0 EXIT
        75 4 40337             SLJ  4 FLOTSTOR
```

```
40334     75 4 71000              SLJ  4 DECOF
          50 0 00000              ENI  0 0
40335     00 0 40346               00  0 PRINTBUF
          06 0 00001               06  0 1
40336     75 0 40360              SLJ  0 EXIT
          50 0 00000              ENI  0 0
40337     75 0 00000    FLOTSTOR  SLJ  0 0
          12 0 40174              LDA  0 TL
40340     20 0 40346              STA  0 PRINTBUF
          12 0 40176              LDA  0 V
40341     20 0 40347              STA  0 PRINTBUF+1
          12 0 40201              LDA  0 THETAL
40342     20 0 40350              STA  0 PRINTBUF+2
          75 1 40522              SLJ  1 LIMITCYC
40343     12 0 40212              LDA  0 W
          20 0 40351              STA  0 PRINTBUF+3
40344     12 0 40215              LDA  0 THETAM
          20 0 40352              STA  0 PRINTBUF+4
40345     75 0 40337              SLJ  0 FLOTSTOR
          50 0 00000              ENI  0 0
40346     00 0 00000    PRINTBUF  BSS    6
          00 0 00000
40354     75 0 40060    COMBEXIT  SLJ  0 COMBINED+5
          50 0 00000              ENI  0 0
40355     75 0 40076    FLOTEXIT  SLJ  0 LOAD
          50 0 00000              ENI  0 0
40356     75 0 40113    BOUNEXIT  SLJ  0 BOUNCE+1
          50 0 00000              ENI  0 0
40357     75 0 40361              SLJ  0 EXITCOUN
          50 0 00000              ENI  0 0
40360     00 0 00000    EXIT      BSS    1
          00 0 00000
40361     75 1 40135    EXITCOUN  SLJ  1 COMBTEST
          72 0 40377              RAO  0 INDEX
40362     72 0 40335              RAO  0 BOUNPRIN+4
          12 0 40347              LDA  0 PRINTBUF+1
40363     22 2 40372              AJP  2 TOPCYC
          12 0 40350              LDA  0 PRINTBUF+2
40364     31 0 40664              FSB  0 ONE
          22 2 40135              AJP  2 COMBTEST
40365     72 0 40615              RAO  0 INDEXAVE
          12 0 40615              LDA  0 INDEXAVE
40366     15 0 40662              SUB  0 COUNT12
          22 0 40563              AJP  0 STOPNOW
40367     14 0 40662              ADD  0 COUNT12
          20 0 40615              STA  0 INDEXAVE
40370     12 0 40375              LDA  0 NEGAJUMP
          20 0 40364              STA  0 EXITCOUN+3
40371     75 0 40135              SLJ  0 COMBTEST
          50 0 00000              ENI  0 00000
40372     12 0 40350    TOPCYC    LDA  0 PRINTBUF+2
          31 0 40664              FSB  0 ONE
40373     22 3 40135              AJP  3 COMBTEST
          12 0 40376              LDA  0 NEWLOWER
40374     20 0 40364              STA  0 EXITCOUN+3
          75 0 40135              SLJ  0 COMBTEST
40375     75 0 40135    NEGAJUMP  SLJ  0 COMBTEST
          50 0 00000              ENI  0 0
40376     31 0 40664    NEWLOWER  FSB  0 ONE
          22 2 40135              AJP  2 COMBTEST
40377     00 0 00000    INDEX     OCT    0
          00 0 00000
40400     00 0 00000    TENTHSEC  OCT    12
          00 0 00012
40401     17 7 04061    POINT004  DEC    0.004
          11 5 64570
40402     17 7 15075    POINT01   DEC    0.01
          34 1 21727
40403     17 3 74000    DIFFERNT  OCT    1737400000000000
          00 0 00000
40404     20 0 06314    A         DEC    .8
          63 1 46314
40405     20 0 14000    INERTRAT  DEC    1.0
          00 0 00000
```

```
40406   00 0 00000   FLFTPRIN BSS     1
        00 0 00000
40407   00 0 00000   RESTITUT DEC     0
        00 0 00000
40410   17 7 64631   DELTA    DEC     .3
        46 3 14631
40411   20 0 14000   RHO      DEC     1.0
        00 0 00000
40412   20 0 04000   MOINERT  DEC     .5
        00 0 00000
40413   00 0 00000   JLOADVAL BSS     1
        00 0 00000
40414   20 0 14000   TOTINERT DEC     1.0
        00 0 00000
40415   00 0 00000   FMOTOR   BSS     1
        00 0 00000
40416   00 0 00000   FLOAD    BSS     1
        00 0 00000
40417   20 0 14000   RHOSQ    DEC     1.0
        00 0 00000
40420   20 0 14000   KMOTCONS DEC     1.0
        00 0 00000
40421   20 0 24000   C        DEC     2.0
        00 0 00000
40422   17 7 66314   D        DEC     .4
        63 1 46314
40423   17 7 15075   B        DEC     .01
        34 1 21727
40424   20 0 14000   OMEGANSQ DEC     1.0
        00 0 00000
40425   00 0 00000   ZETA     BSS     1
        00 0 00000
40426   20 0 14000   OMEGAN   DEC     1.0
        00 0 00000
40427   00 0 00000   FORZEROS BSS     4
        00 0 00000
                     RUNGE    EQU     60200
                     DECOF    EQU     71000
40433   12 0 40401   QUIKCOMP LDA   0 POINT004
        20 0 40154            STA   0 TABLES+1
40434   20 0 40173            STA   0 TABLEL+1
        20 0 40207            STA   0 TABLEM+1
40435   12 0 40654            LDA   0 STOP25
        20 0 40400            STA   0 TENTHSEC
40436   75 0 40015            SLJ   0 ZZ
        50 0 00000            ENI   0 0
40437   50 1 00000   BIGZETA  ENI   1 0
        50 0 00000            ENI   0 0
40440   12 0 40425            LDA   0 ZETA
        31 1 40636            FSB   1 POINT8
40441   22 2 40444            AJP   2 ZETAPLUS
        22 0 40444            AJP   0 ZETAPLUS
40442   54 1 00006            ISK   1 6
        75 0 40440            SLJ   0 /-2
40443   50 1 00006            ENI   1 6
        50 0 00000            ENI   0 0
40444   12 1 40645   ZETAPLUS LDA   1 STOP6
        20 0 40616            STA   0 STOPZETA
40445   12 1 40655            LDA   1 COUNT4
        20 0 40617            STA   0 COUNTZET
40446   12 1 40665            LDA   1 TWO
        20 0 40620            STA   0 DIVIDE
40447   12 1 40645            LDA   1 STOP6
        15 1 40655            SUB   1 COUNT4
40450   61 0 40562            SAL   0 STOPRINT
        50 1 00000            ENI   1 0
40451   75 0 40022            SLJ   0 GOAROUND
        50 0 00000            ENI   0 0
40452   12 3 40706   INDXVALU LDA   3 RESTVALU
        20 0 40407            STA   0 RESTITUT
40453   12 4 40726            LDA   4 DELTAVAL
        20 0 40410            STA   0 DELTA
40454   12 5 40747            LDA   5 JMOTVALU
        20 0 40412            STA   0 MOINERT
```

```
40455     12 0 40414               LDA   0 TOTINERT
          31 0 40412               FSB   0 MOINERT
40456     33 0 40417               FDV   0 RHOSQ
          20 0 40413               STA   0 JLOADVAL
40457     12 0 40420               LDA   0 KMOTCONS
          33 0 40412               FDV   0 MOINERT
40460     20 0 40421               STA   0 C
          12 0 40412               LDA   0 MOINERT
40461     33 0 40413               FDV   0 JLOADVAL
          20 0 40405               STA   0 INERTRAT
40462     12 6 40774               LDA   6 FLFTRATO
          20 0 40406               STA   0 FLFTPRIN
40463     32 0 40404               FMU   0 A
          32 0 40414               FMU   0 TOTINERT
40464     20 0 40416               STA   0 FLOAD
          33 0 40413               FDV   0 JLOADVAL
40465     20 0 40423               STA   0 B
          12 0 40416               LDA   0 FLOAD
40466     32 0 40417               FMU   0 RHOSQ
          20 0 40415               STA   0 FMOTOR
40467     12 0 40404               LDA   0 A
          32 0 40414               FMU   0 TOTINERT
40470     31 0 40415               FSB   0 FMOTOR
          20 0 40415               STA   0 FMOTOR
40471     33 0 40412               FDV   0 MOINERT
          20 0 40422               STA   0 D
40472     54 3 00001               ISK   3 1
          75 0 40043               SLJ   0 NEWINPUT+1
40473     54 4 00000               ISK   4 0
          75 0 40043               SLJ   0 NEWINPUT+1
40474     54 6 00005               ISK   6 5
          75 0 40043               SLJ   0 NEWINPUT+1
40475     54 5 00004               ISK   5 4
          75 0 40043               SLJ   0 NEWINPUT+1
40476     12 0 40564               LDA   0 STOPINDX
          20 0 40563               STA   0 STOPNOW
40477     75 0 40043               SLJ   0 NEWINPUT+1
          50 0 00000               ENI   0 0
40500     12 0 40512   LINEAR      LDA   0 NOFLOAT
          20 0 40071               STA   0 FLOATEST
40501     12 0 40404               LDA   0 A
          20 0 40514               STA   0 PRINDELT
40502     12 0 40414               LDA   0 TOTINERT
          20 0 40515               STA   0 PRINDELT+1
40503     12 0 40420               LDA   0 KMOTCONS
          20 0 40516               STA   0 PRINDELT+2
40504     12 0 40424               LDA   0 OMEGANSQ
          20 0 40517               STA   0 PRINDELT+3
40505     12 0 40411               LDA   0 RHO
          20 0 40520               STA   0 PRINDELT+4
40506     12 0 40417               LDA   0 RHOSQ
          20 0 40521               STA   0 PRINDELT+5
40507     72 0 40510               RAO   0 /+1
          75 4 71000               SLJ   4 DECOF
40510     01 0 40514                 01  0 PRINDELT
          06 0 00000                 06  0 0
40511     72 0 40046               RAO   0 NEWINPUT+4
          75 0 40053               SLJ   0 COMBINED
40512     75 0 40053   NOFLOAT     SLJ   0 COMBINED
          50 0 00000               ENI   0 0
40513     13 0 40162   NOSINK      LAC   0 THETA
          30 0 40664               FAD   0 ONE
40514     00 0 00000   PRINDELT    BSS     6
          00 0 00000
40522     75 3 40523   LIMITCYC    SLJ   3 /+1
          75 0 40525               SLJ   0 /+3
40523     50 0 00000               ENI   0 0
          12 0 00000               LDA   0 0
40524     65 0 40603               THS   0 TIME90SC
          75 0 40566               SLJ   0 TIMESTOP
40525     12 0 40350               LDA   0 PRINTBUF+2
          31 0 40664               FSB   0 ONE
40526     22 3 40534               AJP   3 PRINTNOW
          50 2 77775               ENI   2 77775
```

```
40527   12 0 40607             LDA  0 LIMITBUF+2
        31 0 40350             FSB  0 PRINTBUF+2
40530   22 2 40360             AJP  2 EXIT
        12 0 40346             LDA  0 PRINTBUF
40531   20 0 40605             STA  0 LIMITBUF
        12 0 40347             LDA  0 PRINTBUF+1
40532   20 0 40606             STA  0 LIMITBUF+1
        12 0 40350             LDA  0 PRINTBUF+2
40533   20 0 40607             STA  0 LIMITBUF+2
        75 0 40360             SLJ  0 EXIT
40534   54 2 77775   PRINTNOW  ISK  2 77775
        75 0 40360             SLJ  0 EXIT
40535   12 0 40615             LDA  0 INDEXAVE
        15 0 40617             SUB  0 COUNTZET
40536   22 0 40541             AJP  0 /+3
        14 0 40617             ADD  0 COUNTZET
40537   20 0 40615             STA  0 INDEXAVE
        72 0 40615             RAO  0 INDEXAVE
40540   75 0 40543             SLJ  0 LIMPRINT
        50 0 00000             ENI  0 0
40541   12 0 40607             LDA  0 LIMITBUF+2
        30 0 40613             FAD  0 LIMITBUF+6
40542   20 0 40613             STA  0 LIMITBUF+6
        50 0 00000             ENI  0 0
40543   74 0 02000   LIMPRINT  EXF  0 02000
        75 4 71000             SLJ  4 DECOF
40544   01 0 40605              01  0 LIMITBUF
        06 0 00001              06  0 1
40545   72 0 40544             RAO  0 /-1
        72 0 40614             RAO  0 LIMINDEX
40546   12 0 40614             LDA  0 LIMINDEX
        15 0 40616             SUB  0 STOPZETA
40547   22 0 40555             AJP  0 STOPAVE
        14 0 40616             ADD  0 STOPZETA
40550   20 0 40614             STA  0 LIMINDEX
        12 0 40604             LDA  0 TOOSMALL
40551   31 0 40607             FSB  0 LIMITBUF+2
        22 2 40573             AJP  2 SMALTIME
40552   10 0 00000             ENA  0 0
        20 0 40607             STA  0 LIMITBUF+2
40553   20 0 00000             STA  0 0
        74 0 01000             EXF  0 01000
40554   75 0 40360             SLJ  0 EXIT
        50 0 00000             ENI  0 0
40555   10 0 00000   STOPAVE   ENA  0 0
        20 0 40605             STA  0 LIMITBUF
40556   20 0 40606             STA  0 LIMITBUF+1
        20 0 40607             STA  0 LIMITBUF+2
40557   12 0 40613             LDA  0 LIMITBUF+6
        33 0 40620             FDV  0 DIVIDE
40560   31 0 40664             FSB  0 ONE
        20 0 40610             STA  0 LIMITBUF+3
40561   75 4 71000             SLJ  4 DECOF
        50 0 00000             ENI  0 0
40562   01 0 40605   STOPRINT   01  0 LIMITBUF
        06 0 00000              06  0 0
40563   76 1 40022   STOPNOW   SLS  1 GOAROUND
        50 0 00000             ENI  0 0
40564   76 0 40000   STOPINDX  SLS  0 START
        50 0 00000             ENI  0 0
40565   76 1 40022   NEWSTOP   SLS  1 GOAROUND
        50 0 00000             ENI  0 0
40566   50 2 00000   TIMESTOP  ENI  2 0
        75 4 71000             SLJ  4 DECOF
40567   01 0 40605              01  0 LIMITBUF
        04 0 01570              04  0 1570
40570   74 0 02000             EXF  0 02000
        75 4 71000             SLJ  4 DECOF
40571   01 0 40346              01  0 PRINTBUF
        04 0 01747              04  0 1747
40572   75 0 40563             SLJ  0 STOPNOW
        50 0 00000             ENI  0 0
40573   75 3 40574   SMALTIME  SLJ  3 /+1
        75 0 40552             SLJ  0 LIMPRINT+7
```

```
40574      50 0 00000                    ENI     0 0
           12 0 00000                    LDA     0 0
40575      65 0 40602                    THS     0 TIME30SC
           75 0 40577                    SLJ     0 /+2
40576      75 0 40552                    SLJ     0 LIMPRINT+7
           50 0 00000                    ENI     0 0
40577      75 4 71000                    SLJ     4 DECOF
           50 0 00000                    ENI     0 0
40600      01 0 40346                     01     0 PRINTBUF
           04 0 01755                     04     0 1755
40601      75 0 40563                    SLJ     0 STOPNOW
           50 0 00000                    ENI     0 0
40602      00 0 00000        TIME30SC    OCT       3410
           00 0 03410
40603      00 0 00000        TIME90SC    OCT       12430
           00 0 12430
40604      20 0 14012        TOOSMALL    DEC       1.005
           17 2 70243
40605      00 0 00000        LIMITBUF    BSS       7
           00 0 00000
40614      00 0 00000        LIMINDEX    BSS       1
           00 0 00000
40615      00 0 00000        INDEXAVE    BSS       1
           00 0 00000
40616      00 0 00000        STOPZETA    BSS       1
           00 0 00000
40617      00 0 00000        COUNTZET    BSS       1
           00 0 00000
40620      00 0 00000        DIVIDE      BSS       1
           00 0 00000
40621      00 0 40346        PRINTSET     00     0 PRINTBUF
           06 0 00001                     06     0 1
40622      01 0 40605        NEWLIMPT     01     0 LIMITBUF
           06 0 00001                     06     0 1
40623      17 7 36314        ZETAINDX    DEC       0.05
           63 1 46314
40624      17 7 46314                    DEC       0.1
           63 1 46314
40625      17 7 56314                    DEC       0.2
           63 1 46314
40626      17 7 64631                    DEC       0.3
           46 3 14631
40627      17 7 66314                    DEC       0.4
           63 1 46314
40630      20 0 04000                    DEC       0.5
           00 0 00000
40631      20 0 04631                    DEC       0.6
           46 3 14631
40632      20 0 05463                    DEC       0.7
           14 6 31463
40633      20 0 06314                    DEC       0.8
           63 1 46314
40634      20 0 07146                    DEC       0.9
           31 4 63146
40635      20 0 14000                    DEC       1.0
           00 0 00000
40636      20 0 06314        POINT8      DEC       .8
           63 1 46314
40637      20 0 04631        POINT6      DEC       .6
           46 3 14631
40640      20 0 04000        POINT5      DEC       .5
           00 0 00000
40641      17 7 66314        POINT4      DEC       .4
           63 1 46314
40642      17 7 64631        POINT3      DEC       .3
           46 3 14631
40643      17 7 56314        POINT2      DEC       0.2
           63 1 46314
40644      17 7 46314        POINT1      DEC       0.1
           63 1 46314
40645      00 0 00000        STOP6       OCT       6
           00 0 00006
40646      00 0 00000        STOP7       OCT       7
           00 0 00007
```

```
40647     00 0 00000     STOP8     OCT      10
          00 0 00010
40650     00 0 00000     STOP10    OCT      12
          00 0 00012
40651     00 0 00000     STOP14    OCT      16
          00 0 00016
40652     00 0 00000     STOP20    OCT      24
          00 0 00024
40653     00 0 00000     STOP17    OCT      21
          00 0 00021
40654     00 0 00000     STOP25    OCT      31
          00 0 00031
40655     00 0 00000     COUNT4    OCT      4
          00 0 00004
40656     00 0 00000     COUNT5    OCT      5
          00 0 00005
40657     00 0 00000               OCT      5
          00 0 00005
40660     00 0 00000     COUNT7    OCT      7
          00 0 00007
40661     00 0 00000     COUNT10   OCT      12
          00 0 00012
40662     00 0 00000     COUNT12   OCT      14
          00 0 00014
40663     00 0 00000               OCT      14
          00 0 00014
40664     20 0 14000     ONE       DEC      1.0
          00 0 00000
40665     20 0 24000     TWO       DEC      2.0
          00 0 00000
40666     20 0 24000               DEC      2.0
          00 0 00000
40667     20 0 26000     THREE     DEC      3.0
          00 0 00000
40670     20 0 26000               DEC      3.0
          00 0 00000
40671     20 0 34000     FOUR      DEC      4.0
          00 0 00000
40672     20 0 44000     EIGHT     DEC      8.0
          00 0 00000
40673     20 0 35000     FIVE      DEC      5.0
          00 0 00000
40674     50 1 00000     MANUAL    ENI    1 0
          75 4 71000               SLJ    4 DECOF
40675     01 0 40605                01    0 LIMITBUF
          04 0 01570                04    0 1570
40676     50 2 00000               ENI    2 0
          75 4 71000               SLJ    4 DECOF
40677     01 0 40346                01    0 PRINTBUF
          04 0 03651                04    0 3651
40700     75 0 40563               SLJ    0 STOPNOW
          50 0 00000               ENI    0 0
40701     50 1 00000     FAULPRIN  ENI    1 0
          75 4 71000               SLJ    4 DECOF
40702     01 0 40605                01    0 LIMITBUF
          04 0 01570                04    0 1570
40703     50 2 00000               ENI    2 0
          75 4 71000               SLJ    4 DECOF
40704     01 0 40346                01    0 PRINTBUF
          04 0 01232                04    0 1232
40705     74 0 42003               EXF    0 42003
          76 0 40000               SLS    0 START
40706     20 0 14000     RESTVALU  DEC      1.0
          00 0 00000
40707     00 0 00000               DEC      0
          00 0 00000
40710     20 0 04631               DEC      0.6
          46 3 14631
40711     20 0 06314               DEC      0.8
          63 1 46314
40712     00 0 00000               BSS      14
          00 0 00000
40726     17 7 64631     DELTAVAL  DEC      .3
          46 3 14631
```

```
40727     17 7 46314              DEC    .1
          63 1 46314
40730     17 7 27534              DEC    .03
          12 1 72702
40731     17 7 15075              DEC    0.01
          34 1 21727
40732     17 7 05075              DEC    0.005
          34 1 21727
40733     00 0 00000              BSS    14
          00 0 00000
40747     17 7 46314    JMOTVALU  DEC    .1
          63 1 46314
40750     17 7 56314              DEC    .2
          63 1 46314
40751     20 0 04000              DEC    .5
          00 0 00000
40752     20 0 06314              DEC    .8
          63 1 46314
40753     20 0 07146              DEC    .9
          31 4 63146
40754     00 0 00000              BSS    20
          00 0 00000
40774     00 0 00000    FLFTRATO  DEC    0
          00 0 00000
40775     17 7 56314              DEC    .2
          63 1 46314
40776     17 7 66314              DEC    .4
          63 1 46314
40777     20 0 04631              DEC    .6
          46 3 14631
41000     20 0 06314              DEC    .8
          63 1 46314
41001     20 0 14000              DEC    1.0
          00 0 00000
41002     17 7 35075              DEC    0.04
          34 1 21727
41003     17 7 46314              DEC    0.1
          63 1 46314
41004     20 0 07146              DEC    0.9
          31 4 63146
41005     00 0 00000              BSS    20
          00 0 00000
                                  END
```

Solution number 3					
$2\zeta\omega_n$ 99999999	$\frac{J_m}{J_L}$ 99999999	$\frac{f_L}{f_T}$ 79999999	e 99999999	Δ 29999999	ρ 99999999
J_m 49999999	J_L 49999999	$J_m+\rho^2 J_L$ 99999999	f_m 20000000	f_L 79999999	ρ^2 99999999
K 99999999	$\frac{K}{J_m}$ 19999999 1	$\frac{f_m}{J_m}$ 40000000	$\frac{f_L}{J_L}$ 15999999 1	ω_n^2 99999999	ζ 49999999

Point number	t		$\dot{\theta}_c$		θ_c		$\dot{\theta}_m$		θ_m	
1	10000000		95004083-	1	48334152-	2				
2	19999999		18006400		18669244-	1				
3	29999999		25531729		40519239-	1				
4	40000000		32098164		69412993-	1				
5	50000000		37734520		10440547					
6	59999999		42475713		14458358					
7	69999999		46361850		18907183					
8	79999999		49437347		23703703					
9	89999999		51750106		28769225					
10	99999999		53350719		34029984					
11	10999999	1	54291737		39417381					
12	11999999	1	54626982		44868139					
13	12999999	1	54410913		50324400					
14	14000000	1	53698048		55733762					
15	15000000	1	52542443		61049253					
16	16000000	1	50997217		66229265					
17	17000000	1	49114140		71237437					
18	18000000	1	46943268		76042502					
19	19000000	1	44532629		80618101					
20	20000000	1	41927962		84942563					
21	21000000	1	39172497		88998670					
22	22000000	1	36306785		92773391					
23	23000000	1	33368563		96257613					
24	24000000	1	30392671		99445851					
25	25000000	1	27410989		10233595	1				
26	26000000	1	24452419		10492882	1				
27	27000000	1	21542892		10722807	1				
28	28000000	1	18705407		10923980	1				
29	29000000	1	15989086		11097264	1	15926240		11097173	1
30	30000000	1	13625000		11245019	1	12991268		11241908	1
31	31000000	1	11610459		11370928	1	99052498-	1	11356496	1
32	32000000	1	98937811-	1	11478221	1	67134562-	1	11439661	1
33	33000000	1	84309241-	1	11569649	1	34535657-	1	11490539	1
34	34000000	1	71843596-	1	11647559	1	15682165-	2	11508610	1
35	35000000	1	61221074-	1	11713950	1	-31509827-	1	11493639	1
36	36000000	1	52169158-	1	11770525	1	-64486655-	1	11445624	1
37	37000000	1	44455624-	1	11818734	1	-97189429-	1	11364757	1
38	38000000	1	37882584-	1	11859816	1	-12947823		11251384	1
39	39000000	1	32281408-	1	11894823	1	-16124091		11105976	1
40	40000000	1	27508401-	1	11924654	1	-19238868		10929107	1
41	41000000	1	23441113-	1	11950075	1	-22285244		10721427	1
42	42000000	1	19975199-	1	11971737	1	-25257956		10483648	1
43	43000000	1	17021742-	1	11990196	1	-28153122		10216527	1
44	44000000	1	14504971-	1	12005926	1	-30968015		99208537	
45	45000000	1	12360321-	1	12019330	1	-33700866		95974404	
46	46000000	1	10532771-	1	12030752	1	-36350703		92471132	
Contact 1	46600000	1	95686438-	2	12036778	1	-37900604		90243442	
number 1	46600000	1	-37900604		12036778	1	95686438-	2	90243442	
47	47000000	1	-35550956		11889925	1	-60605683-	2	90374327	
48	48000000	1	-30294526		11561398	1	-39333994-	1	90140801	
49	49000000	1	-25815292		11281446	1	-65385515-	1	89611697	
50	50000000	1	-21998341		11042886	1	-85373205-	1	88853284	
51	51000000	1	-18745749		10839599	1	-10028037		87921151	
52	52000000	1	-15974074		10666370	1	-11094153		86861815	
53	53000000	1	-13612208		10518753	1	-11806455		85714102	

APPENDIX C

PHASE TRAJECTORY PRINT OUT
(Numbers indicated in tenths followed by power of 10)

Solution number	1	$2\zeta\omega_n$ 79999999		J_m/J_L 11111111		f_L/f_T 39999999		e 99999999	Δ 29999999	ρ 99999999
		J_m 99999999-	1	J_L 89999999		$J_m+\rho^2 J_L$ 99999999		f_m 47999999	f_L 31999999	ρ^2 99999999
		K 99999999		K/J_m 99999999	1	f_m/J_m 47999999	1	f_L/J_L 35555555	ω_n^2 99999999	ζ 39999999
number of maximum	1	t 33800000	1	$\dot{\theta}_c$ 52456182-	1	θ_c 13396964	1			
	2	11230000	2	38509278-	1	11053498	1			
	3	21289999	2	12863485-	1	10697107	1			
	4	32499999	2	79971808-	2	10583527	1			
	5	44279999	2	65238396-	2	10542905	1			
	6	56369999	2	59130680-	2	10524201	1			
	7	68649998	2	55271237-	2	10511522	1			
	8	81049998	2	53208045-	2	10504778	1			
	9	93519998	2	51991503-	2	10500457	1			
	10	10602999	3	51279129-	2	10498432	1			
	3	number of maximums averaged						50122288- 1	average positive error in Limit cycle	

APPENDIX D 1

TYPICAL PRINT OUT ILLUSTRATING LIMIT CYCLE
(Numbers indicated in tenths followed by power of 10)

2	$2\zeta\omega_n$ 79999999		J_m/J_L 11111111		f_L/F_T 59999999		e 99999999	Δ 29999999	ρ 99999999
	J_m 99999999-	1	J_L 89999999		$J_m+\rho^2 J_L$ 99999999		f_m 32000000	f_L 47999999	ρ^2 99999999
	K 99999999		K/J_m 99999999	1	f_m/J_m 32000000	1	f_L/J_L 53333333	ω_n^2 99999999	ζ 39999999
number of maximum 1	t 35400000	1	$\dot{\theta}_c$ 17098208-	1	θ_c 13104190	1			
2	11580000	2	17034145-	1	10721242	1			
3	23279999	2	18292628-	2	10323347	1			
4	38859999	2	35712402-	3	10200613	1			
5	58729999	2	72447348-	4	10138780	1			
6	83939998	2	11243587-	4	10098946	1			
7	11619999	3	10685365-	5	10071240	1			
8	15810000	3	47854719-	7	10051391	1			
9	21077001	3	29068282-	8	10037079	1			
1005	215160011794	3			-167815371770 -	2	999996862854		

1005 indicates θ_c max. less than 1005 and 30 sec. of real time has elapsed since the last maximum was recorded (low velocity).

The time velocity, and position of the last computed point is printed.

APPENDIX D 2

TYPICAL PRINT OUT ILLUSTRATING NO LIMIT CYCLE
(Numbers indicated in tenths followed by power of 10)